

**THE IMPACT OF TWO SPATIAL STRATEGIES ON
ENTORHINAL AND HIPPOCAMPAL INVOLVEMENT
IN VISUAL PATH INTEGRATION**

A Dissertation
Presented to
The Academic Faculty

by

Jimmy Y. Zhong

In Partial Fulfillment
of the Requirements for the Degree
Doctor of Philosophy (PhD) in the
School of Psychology

Georgia Institute of Technology
August 2019

COPYRIGHT © 2019 BY J. Y. ZHONG

**THE IMPACT OF TWO SPATIAL STRATEGIES ON
ENTORHINAL AND HIPPOCAMPAL INVOLVEMENT
IN VISUAL PATH INTEGRATION**

Approved by:

Dr. Scott D. Moffat, Advisor/Chair
School of Psychology
Georgia Institute of Technology

Dr. Christopher K. Hertzog
School of Psychology
Georgia Institute of Technology

Dr. Mark E. Wheeler
School of Psychology
Georgia Institute of Technology

Dr. Paul M. Verhaeghen
School of Psychology
Georgia Institute of Technology

Dr. Roberta L. Klatzky
Department of Psychology
Carnegie Mellon University

Date Approved: 30th April 2019

In memory of my maternal grandfather and all his sacrifices

ACKNOWLEDGEMENTS

Completing this dissertation is *no mean feat* and I am obliged to express my *heartfelt gratitude* to the following figures. First, I thank my advisor and Dissertation Chair, Dr. Scott Moffat, for his expert guidance on experimental design, hyper-vigilant scrutiny of my writings, and generous financial support, without which the successful completion of this project, and many others, shall not be possible. Second and equally important, I thank my friend and ex-roommate, Albith Delgado (GT Class of 2016, MS, Ivan Allen College), for teaching me programming in the Unity engine, crucial skills that allowed me to *survive* to this day.

I also thank my dissertation committee members, for all their positive feedback and encouragement. In no order of merit, I thank Dr. Roberta Klatzky, for highlighting the pertinence of strategy-related catch trials; Dr. Mark Wheeler, for introducing me to the within-trial model and for fMRI analysis and AFNI's "tent" function; Dr. Chris Hertzog, for his numerous works on memory and metacognition, which inspired the design of the strategy effectiveness survey in this study; and Dr. Paul Verhaeghen, for reminding me of the crucial importance of testing participants with a separate set of trials during fMRI scanning.

In addition, I thank Dr. Vishwadeep Ahluwalia (Research Scientist at CABI), for establishing the fMRI scanning sequence based on the best possible settings available for acquiring signals from the hippocampal formation. I further thank him, together with Nytavia Wallace (Radiologist and fMRI Technologist at CABI) and Kathryn Harbin (GT

Class of 2018, School of Biological Sciences), for advice and assistance with participant recruitment and fMRI data collection.

Finally, I thank my mother for much needed emotional and financial support, and for *continuously updating* me about the *necessity of fighting for a better tomorrow*.

TABLE OF CONTENTS

	Page
ACKNOWLEDGEMENTS	iv
LIST OF TABLES	x
LIST OF FIGURES	xi
SUMMARY	xiii
 <u>CHAPTER</u>	
1 CHAPTER 1 INTRODUCTION	1
1.1 Extant Neuroimaging Studies on Visual Path Integration in Humans	4
1.2 Role of the Hippocampus in Path Integration: Contentious Findings	10
1.3 Taking a Closer Look at the Contentious Findings over Hippocampal Involvement in Human Path Integration	13
1.4 Identifying the Functional Roles of the Hippocampus and Entorhinal Cortex through differential Path integration Strategy Use	19
1.4.1 Implications	22
1.5 Study Overview and Hypotheses	24
1.5.1 Experiment 1	24
1.5.2 Experiment 2	26
2 CHAPTER 2 METHODS	29
2.1 Participants	29
2.2 Online Surveys	32
2.3 Experimental Stimuli (for both Experiments 1 & 2)	32
2.3.1 Data Recording	39
2.4 Procedure	42
2.4.1 Experiment 1: Strategy Learning and Behavioral Testing	42

2.4.1.1	Joystick Control Practice and Test	42
2.4.1.2	Strategy Manipulation and Physical Practice	44
2.4.1.3	Path Integration Practice Task	47
2.4.1.4	Post-practice Survey	50
2.4.1.5	Path Integration Test Session	50
2.4.1.6	Post-test Survey	54
3	CHAPTER 3 EXPERIMENT 1 RESULTS	55
3.1	Covariate Selection	56
3.2	Mixed-model ANOVAs / ANCOVAs	59
3.2.1	Within-subjects Main Effects and Interactions	59
3.2.2	Between-group Main Effects and Interactions	60
3.2.2.1	Mean Errors and Response Time	60
3.2.2.2	Random Errors	61
3.2.2.3	Post-hoc Analyses of Strategy x Sex Interactions	64
3.2.2.4	Catch Trial Performance Difference between Male and Female Configural Updaters	65
4	CHAPTER 4 EXPERIMENT 1 DISCUSSION	69
5	CHAPTER 5 EXPERIMENT 2 METHODS	74
5.1	Participants	74
5.2	Experimental Design	76
5.3	Procedure	77
5.3.1	Pre-scan Practice in a Mock fMRI Scanner	77
5.3.2	fMRI Scanning Session	79
5.3.2.1	Image Acquisition	79
5	CHAPTER 6 RESULTS: EXPERIMENT 2	81
6.1	Behavioral Data Analysis	81

6.1.1 Covariate Selection	82
6.1.2 Main Effects of Strategy Group and Path Category	82
6.1.3 Sex Differences in Performance among Configural Updaters	83
6.1.4 Strategy Group Differences in Performance among Female Participants	84
6.2 fMRI Data Analysis	86
6.2.1 Preprocessing of Single-subject Data	86
6.2.2 Group-level Random Effects Analysis	88
6.2.2.1 Whole-brain Analysis	88
6.2.2.2 Region-of-interest Analysis	89
6.2.3 Whole-brain and ROI-based Activations and Deactivations in Configural and Continuous Updaters	90
6.2.3.1 Phase-specific Activations and Deactivations (Non-contrast-related)	90
6.2.3.2 Phase-specific Activations (Contrast-related)	92
6.2.3.3 Between-group Comparisons of Whole-brain and ROI-based Activations (Non-contrast-related)	93
6.2.3.4 Between-group Comparisons of Whole-brain and ROI-based Activations (Contrast-related)	93
6.2.4 Brain-behavior Correlations	98
6 CHAPTER 7 EXPERIMENT 2 DISCUSSION	104
7 CHAPTER 8 SUMMARY OF MAJOR FINDINGS	112
8 CHAPTER 9 GENERAL DISCUSSION	114
APPENDIX A: Computer Experience Questionnaire	119
APPENDIX B: Spatial Anxiety Scale	120
APPENDIX C: Sample Practice Paths drawn by a Configural Updater	121
APPENDIX D: Effectiveness of Strategy Use Scale	122

LIST OF TABLES

	Page
Table 1: Descriptive statistics of the demographic and survey/pretest variables of participants receiving continuous updating and configural updating strategy instructions	31
Table 2: Outbound and homebound path parameters for in-lab behavioral testing	36
Table 3: Outbound and homebound path parameters for testing in the MRI scanner	37
Table 4: Partial correlations between mean error measures, mean response time, and survey/pretest measures after controlling for sex and strategy group effects	58
Table 5: Partial correlations between random error and survey/pretest measures after controlling for sex and strategy group effects	58
Table 6: Main, interaction, and covariate effects derived from the group variables of strategy and sex in terms of four mean error measures and mean response time	62
Table 7: Main, interaction, and covariate effects derived from the group variables of strategy and sex in terms of four random error measures	63
Table 8: Post-hoc independent <i>t</i> test statistics comparing female configural updaters with female continuous updaters and male configural updaters	66
Table 9: Descriptive statistics of the demographic and survey/pretest variables of continuous and configural updaters who underwent fMRI scanning	75
Table 10: Significant within-subjects effects derived from outbound path category in terms of mean navigational errors	85
Table 11: Brain activations / deactivations in configural and continuous updaters during each navigational phase	94
Table 12 : Positive brain-behavior correlations during the homebound phases of simple and complex paths	100
Table 13: Negative brain-behavior correlations during the homebound phases of simple and complex paths	101

LIST OF FIGURES

	Page
Figure 1: Real-world triangle completion (Loomis et al., 1993, 1999)	4
Figure 2: Visual path integration in featureless virtual plain (Wolbers et al., 2007)	6
Figure 3: Visual path integration in a virtual tunnel (Gramann et al., 2005)	7
Figure 4: Visual path integration in featureless virtual plain (Arnold et al., 2014)	15
Figure 5: Three types of path integration error variables (Wiener et al., 2011)	22
Figure 6: Virtual environment and blueprints of two separate sets of outbound paths for in-lab behavioral testing and fMRI scanning	38
Figure 7: Schematic showing the computation of the navigational error variables	41
Figure 8: A scene from the Unreal virtual arena used for general joystick practice	43
Figure 9: Scenes from the Unity virtual maze used for testing joystick control	43
Figure 10: Scenes from the in-lab practice task	49
Figure 11: On-screen messages from the catch trials in each strategy group	53
Figure 12: Significant two-way interactions between sex and strategy group in terms of distance- and direction-related mean errors	67
Figure 13: Significant two-way interactions between sex and strategy group in terms of distance- and direction-related random errors	68
Figure 14: Regions of phase-specific, non-contrast-related activations and deactivations in configural and continuous updaters during the outbound and homebound phases	95
Figure 15: Magnified coronal view of activation in the left entorhinal cortex among continuous updaters derived from the contrast of activations between simple and complex homebound phases [complex > simple]	96
Figure 16: Marginally significant clusters of activation in the left hippocampus in configural and continuous updaters derived from the contrast of activations between simple and complex homebound phases [complex > simple]	97

Figure 17: Brain-behavior correlations observed from all participants, configural updaters, and continuous updaters in the simple homebound phase	102
Figure 18: Brain-behavior correlations observed from all participants, configural updaters, and continuous updaters in the complex homebound phase	103

SUMMARY

Previous neuroimaging and neuropsychological studies showed inconsistent findings concerning the involvement of the hippocampal formation in path integration, and the current study aimed to clarify this ambiguity. Specifically, this study investigated the extent to which the hippocampus proper, the entorhinal cortex, and neocortical regions were activated based on the implementation of *continuous* and *configural* updating strategies (one per participant) when performing a virtual path completion task. While *configural* updating required *allocentric* encoding of the outbound path's shape, *continuous* updating required constant tracking of *egocentric* movements with reference to a point of origin.

Findings from in-lab behavioral testing (Experiment 1) showed that neither strategy elicited more accurate path integration performance than the other — and did *not* support previous findings showing that *configural* updating elicited higher performance accuracy when compared with *continuous* updating (He & McNamara, 2018; Wiener, Berthoz, & Wolbers, 2011). Despite these null effects, strategy use was found to be moderated by the sex of the participant: male *configural* updaters outperformed female *configural* updaters on almost all types of path integration errors, and female *continuous* updaters outperformed female *configural* updaters in terms of distance error measures. Arguably, the former findings reflected unique challenges on the part of female *configural* updaters with *allocentric* perspective-taking in the absence of *idiothetic* self-motion cues while the latter findings reflected better spatial processing among female participants from an *egocentric* perspective concomitant with *continuous* updating

strategy use than from an allocentric perspective concomitant with configural updating strategy use.

In Experiment 2, a subsample of the participants who completed Experiment 1 performed a new set of path integration trials in the fMRI scanner. The activation patterns of each strategy group were examined and compared based on whole-brain and region-of-interest (ROI) analyses, the latter of which encompassed the hippocampus and entorhinal cortex. A within-trial ROI analysis of activation patterns showed that continuous updaters exhibited significant activation in the left entorhinal cortex based on a contrast of activations derived from simple and complex paths [complex > simple] during the homebound phase. Marginally significant activations in the left hippocampus in both strategy groups were also found based on ROI analysis and the same type of descriptive contrast. In each strategy group, within-trial analysis at the whole-brain level further showed significant non-contrast-related patterns of activations (in the left parietal cortex) and deactivations (in the right medial prefrontal cortex and right lateral temporal lobe) during the homebound phase of simple paths. In addition, brain-behavior correlations associated individual differences in visual path integration with non-contrast-related functional activity changes in the occipito-parietal and inferior frontal regions, but not in the hippocampus or the entorhinal cortex.

Taken together, these fMRI findings suggest that extrahippocampal attentional and perceptual processes facilitated visual path integration, and that the entorhinal cortex and hippocampus may be more involved in detecting switches in homing decisions or responses between paths of varying complexity than in monitoring performance changes over a single category of paths.

CHAPTER 1

INTRODUCTION

When navigating our everyday environments, we rely not just on visible objects or landmarks but also on self-motion cues in the form of internal/idiothetic (i.e., vestibular and proprioceptive) and/or external/allothetic (i.e., visual and acoustic flow) cues to track our current course of travel and compute moment-to-moment changes in position and orientation. The process of estimating distance and directional changes relative to a starting position and integrating such displacements with self-motion cues to compute and update a homing vector is termed *path integration* (also known as *dead reckoning*) [see, e.g., Gallistel, 1990; Mittelstaedt & Mittelstaedt, 1980, 1982; Müller & Wehner, 1988; for reviews, see Etienne & Jeffry, 2004; Loomis, Klatzky, Golledge, & Philbeck, 1999; Loomis, Klatzky, & Golledge, 2001; Srinivasan, 2015].

Path integration was first postulated to apply to humans by Darwin (1873), who documented the remarkable feat of how North Siberian natives charted a course of return after meandering through featureless icy plains. Subsequent empirical studies showed that this homing ability existed in a wide variety of animals, including insects (e.g., honey bees, Saharan desert ants), spiders, birds (e.g., pigeons, geese), and mammals (e.g., golden hamsters, gerbils, dogs, humans) [Gallistel, 1990; Mittelstaedt & Mittelstaedt, 1980, 1982; see Etienne & Jeffery, 2004, Srinivasan, 2015, for reviews of path integration in non-human animals; see Loomis et al., 1999, 2001, for reviews of path integration in humans]. To date, research on path integration has continued to attract the attention of spatial cognition researchers in view of the possibilities it offers for greater

insights into the basic processes/mechanisms that are involved in spatial perception and cognitive mapping (see, e.g., Burgess, 2014; Hafting, Fyhn, Molden, Moser, & Moser, 2005; Moser, Kropff, & Moser, 2008).

The traditional behavioral paradigm used for studying path integration in humans is the path- or triangle-completion task (see, e.g., Klatzky et al., 1990; Loomis et al., 1993; Fukusima, Loomis, & Da Silva, 1997; Philbeck, Klatzky, Behrmann, Loomis, & Goodridge, 2001; Sholl, 1989). The path completion task, originally developed by Klatzky et al. (1990), requires a participant, donning blindfolds and headphones, to walk two or more straight segments with one or more turns in between under the guidance of the experimenter, and to walk back (or point back) to the origin on his/her initiative at the end of the outbound journey. Triangle completion is the popular derivative of this path completion protocol and refers to participants' attempts at returning to the origin (or pointing toward it) after traversing two straight segments with one turn (i.e., the whole trajectory forms a triangle) [Klatzky, Loomis, Beall, Chance, & Golledge, 1998; Loomis et al., 1993; Philbeck et al., 2001; Sholl, 1989]. Importantly, the donning of blindfolds and headphones throughout the task blocked out visual and auditory cues that could facilitate the updating of positional estimates and obliged the participant to attend to idiothetic cues from vestibular and proprioceptive systems (e.g., efferent motor commands, kinesthetic feedback from the musculature, acceleratory signals from the vestibular system) for an *online* updating of the perceived home or target location. With regard to homing responses, participants have been found to commit systematic errors that are contingent on path parameters. Such errors refer to overestimating short homing distances and small directional turns, as well as underestimating longer homing distances

and larger directional turns (Fujita, Klatzky, Loomis, & Golledge, 1993; Loomis et al., 1993) [see Fig. 1]. These regular patterns of errors have been found in numerous path/triangle completion studies conducted in both real-world (e.g., Klatzky et al., 1990; Loomis et al., 1993; Sholl, 1989; Philbeck et al., 2001; Wiener, Berthoz, & Wolbers, 2011) and virtual reality settings (e.g., Adamo, Briceño, Sindone, Alexander, & Moffat, 2012; Arnold, Burles, Bray, Levy, & Iaria, 2014; Gramann, Müller, Eick, & Schönebeck, 2005; Harris & Wolbers, 2012; Klatzky et al., 1998; Mahmood, Adamo, Briceno, & Moffat, 2009; Wolbers, Wiener, Mallot, and Büchel, 2007).

The classical *configural encoding model* (Fujita et al., 1993) attempted to explain these systematic errors of return as arising out of difficulties in generating a configural mental representation of the outbound path, and *not* when participants executed their homeward responses. An alternative mathematical model — the *leaky path integration model* (Lappe & Frenz, 2009; Lappe, Jenkin, & Harris, 2007; Lappe, Stiels, Frenz, & Loomis, 2011) — proposes that the representation of distance is affected by two parameters: a *leak rate* and a *gain rate*. The leak rate reflects the extent to which an integrated distance estimate decays over the length of locomotion whereas the gain rate describes the amount of distance that is added to the integrated distance estimate with each single step. When combined, these two parameters can explain the underestimation and overestimation of travel distances when combined with relevant distance or positional values (see Lappe et al., 2007). Notably, the leak rate tends to become progressively larger with longer distances away from home, leading to the underestimation of return distance during triangle completion (Harris & Wolbers, 2012).

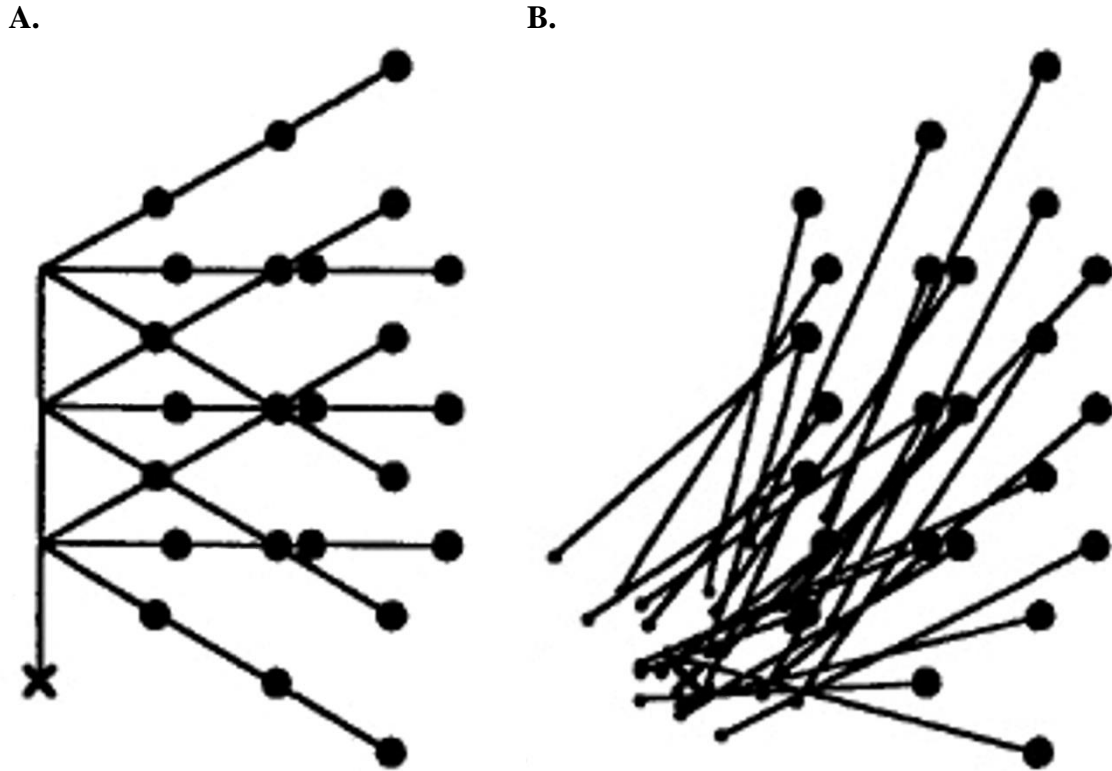


Fig. 1. (A) Depictions of the triangular paths used by Loomis et al. (1993). “X” represents the origin of travel and the large dots (A, B) represent the termini of the two-legged outbound paths, each being 2, 4, or 6 m. The turn varied between 60, 90, and 120 degrees. (B) Average performance of Loomis et al.’s (1993) participants. Small dots represent the centroids of the stopping points of 37 participants. Most of those centroids did *not* coincide with the origin of travel, indicating the existence of systematic errors. [Adapted from figure 5.3 of Loomis et al. (1999). Reproduced with permission.]

1,1 Extant Neuroimaging Studies on Visual Path Integration in Humans

Over the past decade, there have been a series of neuroimaging studies that investigated the neural correlates of human path integration through virtual reality forms of the triangle completion task (for fMRI studies, see Arnold et al., 2014; Wolbers, Wiener, Mallot, & Büchel, 2007; for EEG studies, see Chiu et al., 2012; Lin, Chiu, & Gramann 2015; Gramann, Müller, Schönebeck, & Debus, 2006; Gramann et al., 2010; Plank, Müller, Onton, Makeig, & Gramann, 2010). Unlike the behavioral studies on

human path integration that excluded the availability of visual cues, participants performing virtual triangle completion in neuroimaging experiments receive full exposure to visual cues in the form of optic flow at the cost of having no proprioceptive or kinesthetic feedback due to the testing constraints of neuroimaging experiments that prevent locomotion. Consequently, participants performing triangle completion in virtual environments focus primarily on the integration of optic flow information when computing their homing responses at the end of outbound paths. Therefore, the performance of path integration in virtual reality has been termed *visual path integration* (Gramann et al., 2005).

The common feature of all these virtual triangle completion tasks was the presentation of open plains (Arnold et al., 2014; Wolbers et al., 2007) [see Fig. 2] or passageways (Chiu et al., 2012; Lin et al., 2015; Gramann et al., 2006, 2010; Plank et al., 2010) [see Fig. 3] that were devoid of any salient landmark or object cues. In such virtual environments, the perception of optic flow was rendered through experimentally controlled translations and rotations. In a typical path integration trial, the participants experienced animated / passive motion either along the outbound path of the triangular trajectory (two straight segments with a turn in between, Chiu et al., 2012; Lin et al., 2015; Gramann et al., 2006, 2010; Plank et al., 2010; Wolbers et al., 2007) or along the entire three legs/segments of the triangular trajectory (Arnold et al., 2014). The homing responses generally involve: (i) pointing back to the starting position by deflecting the joystick (Wolbers et al., 2007), (ii) pressing buttons (e.g., mouse buttons) to adjust 3D homing arrows (Chiu et al., 2012; Lin et al., 2015; Gramann et al., 2006, 2010; Plank et al., 2010), or (iii) pressing buttons to indicate whether or not they have successfully

returned to their starting position (Arnold et al., 2014). As for fMRI-based control trials, they varied across studies from animations of travels (pre-configured by the experimenter) along one straight path (i.e., a forward translation, Arnold et al., 2014; Gramann et al., 2006, 2010; Plank et al., 2010) or along winding paths with turns that differed from the turns in the test trials (see Gramann et al., 2006, 2010; Lin et al., 2015; Wolbers, 2007).

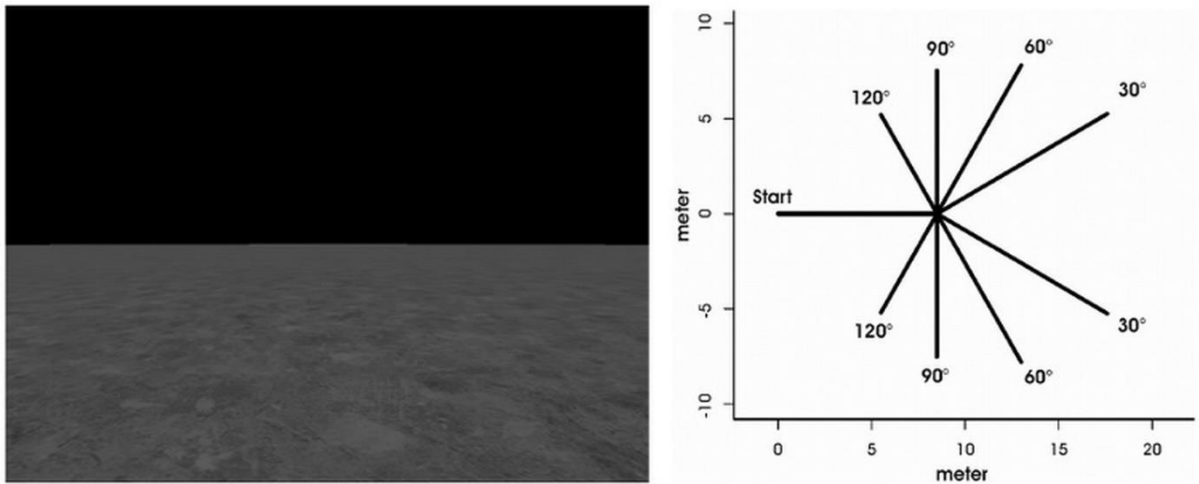


Fig. 2. A ground-level view of the featureless virtual plain used by Wolbers et al. (2007) and a schematic diagram of the outbound paths with turns that varied systematically in increments of 30° from 30° to 120° in both clockwise and anticlockwise directions. Each of the eight outbound paths were presented five times. The second segment after the turn was varied in length to keep the animation within a suitable temporal range for functional scanning. The participants pointed back to the perceived starting position at the end of travel along each outbound path. [Adapted from figure 1 of Wolbers et al. (2007). Reproduced in compliance with the terms of Creative Commons Attribution License supported by *The Journal of Neuroscience* and the *Society for Neuroscience*.]

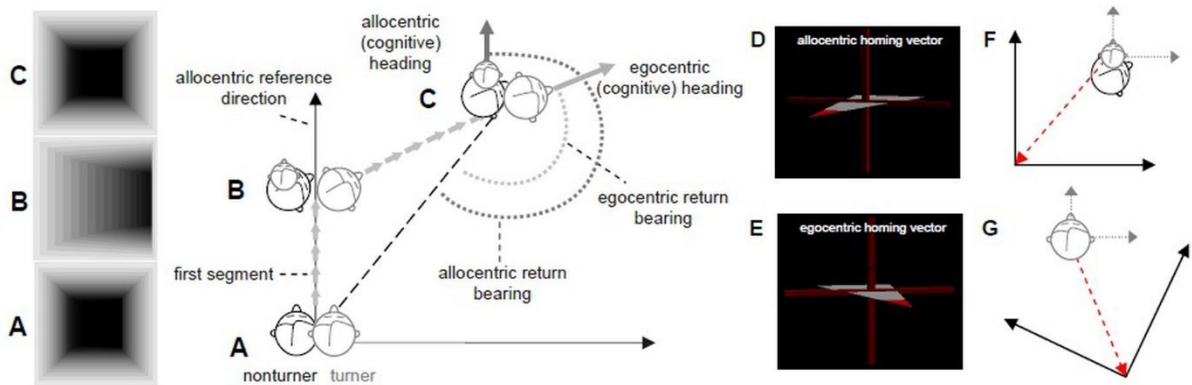


Fig. 3. The virtual tunnel task used by Gramann and colleagues showing: (A - C) the first-person scenes during a typical tunnel passage along a straight segment along with a schema of the allocentric and egocentric return bearings, and (D, E) the two types of homing vectors that can be specified based on adjusting the 3D homing arrows at the end of the tunnel passageway. Panels F and G show the schematics of the mental representations of the allocentric and egocentric homing vectors. [Retrieved from: <http://sccn.ucsd.edu/~klaus/images/Description%20Strategy.pdf>; Reproduced with permission.]

*To download an animation of a sample virtual tunnel trial with allocentric and egocentric homing vectors at the end, please access: http://sccn.ucsd.edu/~klaus/download/tunnel_cat.mpg)

Distinct types of data analyses were applied to the respective neuroimaging studies. In the first fMRI study on visual path integration, Wolbers et al. (2007) contrasted functional activity between path integration and control conditions, and parametric modulation of brain activity in selected regions by variation in the accuracy of homeward pointing responses. The analysis of the functional contrast maps revealed activations in the precuneus, subdivisions of the intraparietal sulcus, posterior middle temporal gyrus, and superior frontal gyrus. Parametric analysis further revealed negative correlations between pointing errors and activations in the right hippocampus and bilateral medial prefrontal cortex (BA9) during encoding of the outbound paths across subjects.

As for the EEG studies on visual path integration, the modes of analyses involved:

(i) EEG current density reconstruction (Gramann et al., 2006), and (ii) EEG independent

component analysis (ICA) – a spatio-temporal filtering method that separates the far-field EEG potentials arising from synchronized cellular assemblies into spatially fixed but temporally separated processes (Chiu et al., 2012; Lin et al., 2015; Gramann et al., 2010; Plank et al., 2010; for details of ICA, see Makeig, Bell, Jung, & Sejnowski, 1996; Onton & Makeig, 2006; Onton, Westerfield, Townsend, & Makeig, 2006). Based on these EEG analysis techniques, a common set of brain regions was observed to be activated during virtual triangle completion across these studies; namely, the precuneus (BA 7), the retrosplenial cortex (RSC) [BA 29/30], and the middle frontal cortex/gyrus (BA 6, BA 9). The precuneus was demonstrated to be more highly activated [as assessed through EEG source density and alpha desynchronization (i.e., decreased oscillation of the alpha frequency band, 8 – 13 Hz)] *before* and *during* the turning phase(s) of the outbound path among participants who preferred an egocentric/body-centered frame of reference for estimating their positional changes (“Turners”, see Fig. 3G) in comparison to participants who strongly preferred an allocentric/environment-centered frame of reference for estimating their positional changes (“Non-turners”, see Fig. 3F) [Chiu et al., 2012; Gramann et al., 2006; Lin et al., 2015; Plank et al., 2010]. These findings implicated the precuneus as a key site for attending to optic flow and integrating it with egocentric positional estimates. Conversely, when Non-turners were compared with Turners, higher alpha desynchronization in the right precuneus / posterior parietal cortex has also been observed during the turning phase of an outbound route (Lin et al., 2015; Gramann et al., 2010). This suggests that the right precuneus / posterior parietal cortex could also be involved in directing information about egocentric directional changes to the construction of an allocentric representation of the outbound path (Lin et al., 2015).

Similarly, alpha desynchronization in the RSC has been shown to be higher in Non-Turners than in Turners *before* and *after* the turning phase, and alpha power increases in the RSC have been shown to be comparatively higher in Turners during the turning phase (Lin et al., 2015). Critically, Lin et al. (2015) showed that RSC event-related spectral perturbations (ERSPs) [i.e., power frequencies of brain waves] during separate path integration phases covaried differently with the pointing errors committed by Non-Turners. Specifically, Non-Turners' pointing errors covaried negatively with the ERSPs recorded before and after the turn but positively with the ERSPs recorded during the turn. Based on these findings, Lin et al. (2015) proposed that the RSC was involved in two types of cognitive processes: (i) the integration of ego-motion information with allocentric reference frames (e.g., boundaries of the virtual environment) during forward translations (before and after the turn), and (ii) the computation and tracking of allocentric headings during turns. The second part of their proposal was supported by more recent findings showing that the RSC was selectively involved in processing rotational changes during virtual motion (Chrastil, Sherrill, Hasselmo, & Stern, 2016).

Unlike the precuneus and RSC whose activations are influenced by the type of spatial reference frame that one prefers, activation in the middle frontal cortex (BA 6 and/or BA 9) has consistently been found to occur during the turning phase of the outbound path *irrespective* of the preferred perspective or reference frame [in the form of EEG current density, see Gramann et al., 2006; in the form of theta band synchronizations (4 – 8 Hz ERSPs), see Chiu et al., 2012; Gramann et al., 2010; Lin et al., 2015; Plank et al., 2010]. These findings implicated an essential role of the middle frontal cortex in monitoring changes in virtual motion (Gramann et al., 2010; Plank et al.,

2010). This interpretation aligns with Wolbers et al.'s (2007) view that the medial prefrontal cortex is crucially involved in maintaining spatial information in working memory for the subsequent computation of homing responses.

1.2 Role of the Hippocampus in Path Integration: Contentious Findings

The hippocampus is a major component of the medial temporal lobe that has been regarded as functionally involved in spatial navigation, particularly in the formation of cognitive maps (O'Keefe & Nadel, 1978), as well as in the strategic control of attention and memory processing (Anderson, Morris, Amaral, Bliss, & O'Keefe, 2007). Behavioral neuroscience studies on the foraging behavior of rats have generally linked the hippocampus to path integration (see, e.g., McNaughton et al., 1996; Whishaw, McKenna, & Maaswinkel, 1997; Wiener, Korshuno, Garcia, & Berthoz, 1995). Notably, Whishaw et al. (1997) argued that one of the specialized functions of the hippocampus pertains to coding for idiothetic information (i.e., efferent signals to the musculature, afferent proprioception from the muscles and joints) and channeling such information toward the optimal processing of allothetic information (i.e., visual, auditory, olfactory cues) [see also Whishaw & Tomie, 1996]. Specifically, the relevance of the hippocampus for path integration was demonstrated by random and inaccurate homing responses of rats with fornix-fimbria lesions (Whishaw & Gorny, 1999; Whishaw, Hines, & Wallace, 2001; Whishaw & Maaswinkel, 1998; Whishaw & Tomie, 1996). Unlike the control rats (with intact hippocampus) who found their way back to home locations under both light and dark (or blindfolded) conditions, fornix-fimbria lesioned rats returned home

successfully only when allothetic cues were available (e.g., in a lighted room with visual cues). More specifically, the fornix-fimbria lesioned rats became disoriented or took suboptimal return paths when restricted to idiothetic cues (Whishaw & Gorny, 1999; Whishaw et al., 2001), and perseverated in returning, under both light and dark conditions, to a refuge location that was used during training (Whishaw & Maaswinkel, 1998; Whishaw & Tomie, 1996). Overall, these findings gave the earliest support for the pertinence of the hippocampus for path integration; ostensibly, lesions to the fornix-fimbria fibers impaired spatial learning that was attuned to idiothetic signals from the vestibular and proprioceptive systems.

In humans, Wolbers et al. (2007) demonstrated that pointing errors from the path integration trials correlated negatively with activation in the right hippocampus on a trial-by-trial basis (i.e., better pointing performance was associated with higher hippocampal activation across trials). This negative correlation was unaffected by overall performance levels and applied to both good and poor path integrators. This finding was interpreted to suggest that the hippocampus was involved in integrating distance and direction signals for updating the coordinates of the starting position during spatial displacements. Region-of-interest (ROI) analyses performed by Chrastil et al. (2016) focusing on the hippocampus supported this interpretation by showing that bilateral activation in the anterior hippocampus (in the same areas as those found by Wolbers et al., 2007) was positively correlated with the amount of translations and rotations that were accurately encoded during virtual motion episodes.

Furthermore, several neuropsychological studies showed that epileptic patients with right hippocampal resections demonstrated deficiencies in path integration with

regard to estimating (i) the distances from the starting position during blindfolded walking (Philbeck, Behrmann, Levy, Potoicchio, & Caputy, 2004) and (ii) the angle-of-return (i.e., homing direction/vector) during triangle completion (Worsley et al., 2001). In addition, recent research on wayfinding (i.e., goal-directed navigation to places that are beyond the sensory horizon, see Golledge 1999; see also Wolbers & Wiener, 2014, for a review) in virtual environments implicated that the hippocampus was involved in a dynamic/continuous tracking of distances to a goal as perceived from the egocentric/first-person perspective (Howard et al., 2014; Sherrill et al., 2013), and that hippocampal activity was influenced by top-down signals from the medial frontal cortex when navigating to a previously observed target under the availability of salient optic flow information (Sherrill et al., 2015), as well as when making flexible navigational decisions at common hallways/intersections (Brown, Ross, Toyne, & Stern, 2012). Altogether, these findings support the notion that the hippocampus is a key component for path integration and spatial navigation in general.

Despite these positive findings, there have been several notable studies that argued against the pertinence of the hippocampus for path integration (Alyan & McNaughton, 1999; Arnold et al., 2014; Kim, Sapiurka, Clark, & Squire, 2013; Shrager, Kirwan, & Squire, 2008). Alyan & McNaughton (1999) showed that hippocampectomized rats with lesions in the dorsal and ventral regions of the hippocampus could perform a path integration task as well as healthy control rats. Likewise, neuropsychological studies involving human subjects showed that memory-impaired/amnesic patients with lesions in the hippocampus and adjacent regions in the medial temporal lobe (MTL) performed as well as healthy control subjects in a

blindfolded return-to-origin task (Kim et al., 2013), and in a pointing-back-to-the-start task at the end of an outbound path (Shrager et al., 2008). Moreover, a fMRI study by Arnold et al. (2014) that required participants to estimate return/homebound path distances during virtual triangle completion showcased activations across a wide range of brain areas that excluded the hippocampus. The authors attributed the lack of hippocampal involvement to the possibility that the hippocampus may be more relevant for tracking the starting position prior to return rather than tracking the entire triangular route, and that hippocampal activation may be more influenced by directional estimates than distance estimates. Regardless of the reason for the absence of hippocampal involvement in path integration, these studies all suggested that the hippocampus is *not essential* for determining homing responses, and that extrahippocampal areas and neural circuits involved in cognitive control, spatial attention, and working memory (see Arnold et al., 2014, for details) are more likely to constitute a neural system that supports path integration.

1.3 Taking a Closer Look at the Contentious Findings over Hippocampal Involvement in Human Path Integration

Due to these contentious findings over the involvement of the hippocampus in human path integration, differences in methodology, primarily in terms of experimental design and subject characteristics, must be considered. Starting with Arnold et al.'s (2014) study, their participants experienced animated motion along all three legs of a triangular path and were instructed to decide whether the return path's distance was more

(or less) than its actual distance based on one of two button presses. Unlike the traditional triangle completion task which involved either walking or pointing back to the origin, each of which generated precise and continuous measures of accuracy, this task consisted of a binary decision of the return path distance being matched (or mismatched) with their estimated return distance (see Fig. 4). This makes it hard to infer whether or not the judgment of the return vector relates to an updating of the starting position relative to changes in position and orientation along the outbound path (the first two legs/segments). This spatial updating mechanism, characteristic of path integration, was originally proposed by Wolbers et al. (2007) to represent the function of the right hippocampus; and it is likely that the transformation of the original triangle completion paradigm into a task wherein the participant had *no control* over the trajectory of the return path diminished the amount of cognitive effort directed toward the spatial updating of the starting position, eventually culminating in the absence of hippocampal activation. Moreover, it is unknown if Arnold et al.'s (2014) participants applied a time- or pace counting strategy that facilitated their estimations of the return length. Unlike some other studies, which implemented steps to deter the use of such an analytical, non-spatial strategy (see, e.g., Klatzky et al., 1990; Philbeck et al., 2004), Arnold et al. (2014) did not carry out such control procedures, and hence it is unclear whether the wide-ranging activations they observed in the frontoparietal network (comprising the medial frontal gyrus, anterior cingulate cortex, caudate nucleus, supramarginal gyrus, angular gyrus, superior parietal lobule, and right precuneus) reflected the operation of strategies or working memory processes that are non-inherently associated with visual path integration.

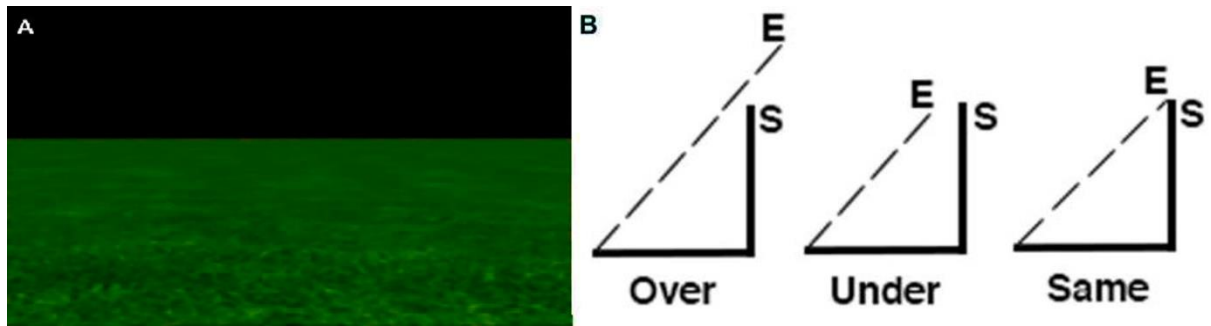


Fig. 4. (A) A first-person view of the featureless virtual plain implemented by Arnold et al. (2014) for triangle completion. (B) The participants performed estimations (E) of the return distance to the start (S) based on three categories of triangular paths reflecting an overshoot, undershoot, and matching of the estimated end-point in relation to the starting position. The participants pressed one of two buttons indicating whether the animated return path's distance matched (or mismatched; either overshoot or undershoot) their estimated return distance [Adapted from figure 1 of Arnold et al. (2014). Reproduced in compliance with the terms of Creative Commons Attribution License supported by Frontiers Media SA.].

In the two neuropsychological studies that called into question the involvement of the hippocampus in path integration (Kim et al., 2013; Shrager et al., 2008), memory-impaired patients and healthy control subjects were tested under blindfolded condition using path integration tasks that required walking back to the starting position after a self-directed search of target objects (i.e., tiles on the floor) [Kim et al., 2013], and pointing back to the starting position after traversing outbound paths with one and two turns (Shrager et al., 2008). In view of non-significant group differences in performance, the authors of both studies stressed the importance of working memory for carrying out the essential spatial computations during path integration and proposed that the MTL may be more involved in converting information from spatial perception into long-term memory than in processing information directed to path integration *per se*.

However, a more detailed examination of the patient profiles revealed a caveat. Although all the patients experienced considerable degrees of hippocampal volume loss that reflected an almost complete loss of hippocampal neurons (as stipulated by Kim et al., 2013), *not everyone* experienced lesions to the adjacent entorhinal cortex or

subiculum. The entorhinal cortex is a vital subregion of the hippocampal formation that was found to contain grid cells with hexagonally arranged firing fields that topographically map onto the geometric surface of the environment in both rats (Fyhn, Molden, Witter, Moser, & Moser, 2004; Hafting et al., 2005; Moser et al., 2008) and humans (Doeller, Barry, & Burgess, 2010; Jacobs et al., 2013). Crucially, these grid-like firing patterns were proposed to be coincident with an *online computation* of positional and directional estimates during events involving path integration (Chen, He, Kelly, Fiete, & McNamara, 2015), wayfinding (Howard et al., 2014; Spiers & Maguire, 2007) and spatial orientation (Chadwick, Jolly, Amos, Hassabis, & Spiers, 2015). Compared with severely amnesic patients that have more than 90% reductions in hippocampal and parahippocampal volumes [two in Shrager et al.'s (2008) study and one in Kim et al.'s (2013) study], three moderately amnesic patients in Shrager et al.'s (2008) study had bilateral hippocampal volume reductions of 46%, 48%, and 49%, respectively, while four moderately amnesic patients in Kim et al.'s (2013) study had bilateral hippocampal volume reductions of 35%, 46%, 48%, and 49%.¹ It is vital to note that all moderately amnesic patients in both studies did *not* have large bilateral reduction in the volume of the parahippocampal gyrus (which includes the entorhinal cortex in its rostral region; the patients had between 5% to 17% reduction in the parahippocampal gyrus in comparison to the control mean). Therefore, it is very likely that large parts of the entorhinal cortex in these patients remained intact, and that might have enabled them to generate relatively

¹ Interestingly, hippocampectomized rats that demonstrated comparable levels of path integration performance as healthy control rats also did *not* experience extensive damage to their hippocampus, with sparing of the dentate gyrus and the CA3 (Alyan & McNaughton, 1999).

accurate directional (Shrager et al., 2008) and Euclidean distance-to-goal estimates (Kim et al., 2013). More importantly, Shrager et al. (2008) encouraged their participants to actively maintain the outbound path in mind during each trial – a strategy-inducing procedure that was not attempted in any previous studies on path integration (see, e.g., Klatzky et al., 1990, 1998; Loomis et al., 1993, 1998; Philbeck et al., 2001). This led to two severely amnesic patients (with an average bilateral volume reduction in the hippocampus and parahippocampus that exceeded 90%) and four control participants reporting attempts to continuously track their position and update it relative to the starting position as they moved. The two severely amnesic patients performed as well as the four control subjects when pointing back to their starting positions immediately at the end of outbound travel. However, these two patients performed significantly poorer than the control subjects after a period of distraction; this suggested the presence of deficits in the retrieval of path integration-related spatial information that relied on the integrity of the MTL.

On the other hand, neuropsychological studies which supported the involvement of the hippocampus in human path integration (Philbeck et al., 2004; Worsley et al., 2001) recruited epileptic patients that experienced resections of the entire entorhinal cortex and amygdala, and approximately half (Philbeck et al., 2004) to two-thirds (Worsley et al., 2001) of the hippocampus. Apart from the removal of brain areas that exceeded the extent of lesioned sites in the memory-impaired patients of Shrager et al. (2008) and Kim et al. (2013), Philbeck et al. (2004) and Worsley et al. (2001) also recruited relatively more patients that counterbalanced the number of control subjects. Worsley et al. (2001) tested 33 patients (16 with right temporal lobectomy; 17 with left

temporal lobectomy) versus 16 control participants while Philbeck et al. (2004) tested 18 patients (10 with right temporal lobectomy; eight with left temporal lobectomy) versus 10 control participants. In general, the findings showed that epileptic patients with right temporal lobectomy were the poorest performers in the path integration tasks. Specifically, Philbeck et al. (2004) showed that right temporal lobectomy patients overshot the target location — marked by a cone placed five meters away from the starting position — to a significantly larger extent than both left temporal lobectomy patients and control participants when they had to walk blindfolded to it. Similarly, in a triangle completion task, Worsley et al. (2001) showed that right temporal lobectomy patients overshot the required return distance and overturned the required angle-of-return in magnitudes larger than both left temporal lobectomy patients and control participants. Importantly, unlike Shrager et al.'s (2008) protocol, no instructions were given to the patients about keeping the outbound path in mind as they walked. Overall, in view that both studies (i) tested patients with resections of both the hippocampus and the entorhinal cortex, (ii) ensured a balanced ratio of patients and controls, and (iii) avoided the induction of specific strategies, one could argue that these findings offer a more convincing picture of MTL's functional role in path integration.

1.4 Identifying the Functional Roles of the Hippocampus and Entorhinal Cortex through Differential Path Integration Strategy Use

The extant literature provides evidence both supporting and negating the relevance of the hippocampus for human path integration — and raises the question of whether or not activation in the hippocampus and the adjacent entorhinal cortex could be induced using different path integration strategies. Based on a real-world triangle completion task, Wiener et al. (2011) proposed two kinds of path integration strategies: (i) a *configural updating strategy* focusing on encoding the shape of the outbound path and computing homeward responses based on the encoded mental image; and (ii) a *continuous updating strategy* focusing on keeping track of the start position at all times along the outbound path (i.e., moment-to-moment updating) in order to maintain a constantly updated homing vector. Wiener et al. (2011) theorized that these two strategies largely differed in terms of the timing of home vector computation. While continuous updating refers to an *online* process whereby the homing vector is computed continuously during navigation to the exclusion of a need for visualizing the shape of the outbound path, configural updating refers to an *offline* process whereby the homing vector is computed at the end of the outbound path based on an encoded representation of the path.

To assess the impact of these two forms of spatial updating on real-world path integration, Wiener et al. (2011) instructed their participants to apply these two strategies *in sequence* over two counterbalanced blocks of outbound paths — that is, the same group of participants were tested in the use of both strategies. The differences in homing performance arising from the use of these two strategies were exhibited in terms of head

orientation and corresponding path integration errors. When the participants applied configural updating, they showed little head movements when traversing both segments of the outbound path. By contrast, when they applied continuous updating, they were strongly biased to turning their heads in the direction of the starting position as they walked along the second segment of the outbound path after the turn. Regardless of the length of the outbound path, the participants took longer time in attempting to return to the perceived starting position when they applied configural updating than when they applied continuous updating. However, path length mattered with regard to distance and angular measures. After traversing longer outbound paths (mean length = 15.3 m, mean turning angle = 148°), the participants committed lower magnitudes of direction errors, distance errors, and homing errors (see Fig. 5, for an illustration of such errors) when they applied configural updating than when they applied continuous updating. The differences in the commission of errors between the two strategy conditions were comparatively smaller after traversals on shorter outbound paths (mean length = 8.3 m, mean turning angle = 101°). Overall, these findings showed that the implementation of two different path integration strategies generated contrasting patterns of path integration performance.

Recently, a virtual reality study by He and McNamara (2018) incorporated physical translations (i.e. updating of scenes in headmounted display with each forward leg movement) and extended the differential application of these two strategies to judgments of relative directions (JRDs) between virtual objects arranged in a geometrically regular layout. Configural strategy users were instructed to visualize the shape of a path that bypassed three virtual posts whereas continuous strategy users were instructed to update

their position and orientation continuously with respect to a red virtual post appearing close to the starting position. Results showed that configural strategy users committed significantly *fewer* errors when their heading directions at the time of pointing were aligned with the reference directions/axes of the object array (e.g., North) than when their heading directions were misaligned with such reference directions. This behavioral pattern did not apply to the continuous strategy users, who demonstrated comparable levels of pointing errors regardless of whether or not their heading directions were aligned with any reference direction of concern. These findings suggested that configural strategy users selected allocentric reference frames to encode the configuration of objects and prioritized the retrieval of spatial information organized along the directions of reference axes. By contrast, continuous strategy users' responses suggested that they were inattentive to the layout geometry of the virtual objects and that they referred to egocentric cues or reference frames when making their pointing responses.

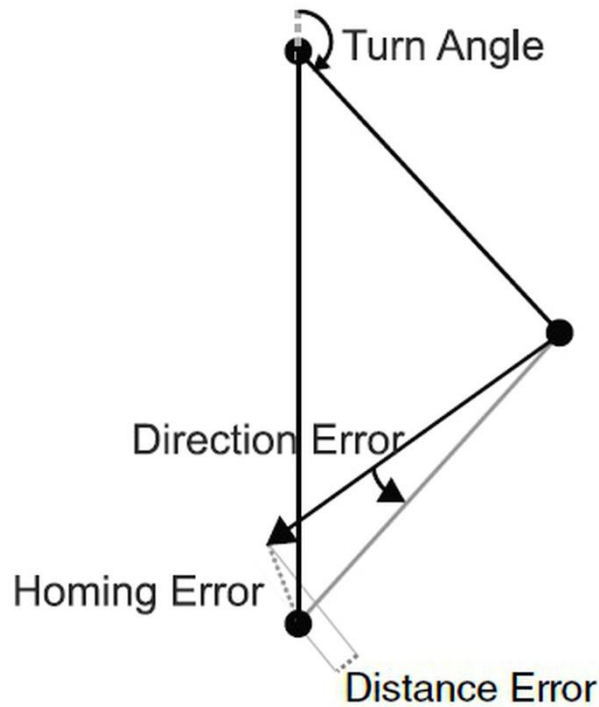


Fig. 5. The three error variables used by Wiener et al. (2011) in their real-world triangle completion task: (i) *direction error* — the difference between the expected and actual angle-of-return; (ii) *distance error*— the difference between the expected and actual linear distance/path of travel; and (iii) *homing error* — the Euclidean distance between the starting and stopping position. [Adapted from figure 1 of Wiener et al. (2011). Reproduced with permission.]

1.4.1 Implications

In retrospect, by comparing Wiener et al.’s findings with the neuropsychological studies conducted by Shrager et al. (2008) and Kim et al. (2013), it seems possible that the amnesic patients might have preserved the ability to implement some form of spatial strategy resembling Wiener et al.’s (2011) continuous updating strategy. This possibility is supported by previous studies (as aforementioned) that implicated the involvement of extrahippocampal regions like the middle frontal cortex/gyrus and the precuneus / posterior parietal cortex in a dynamic updating of the homing vector when traversing virtual outbound paths (Chiu et al., 2012; Gramann et al., 2006; Plank et al., 2010).

Moreover, in view that the moderately amnesic patients (Kim et al., 2013; Shrager et al., 2008) had largely intact entorhinal cortices, the entorhinal cortex might be another region that is involved in continuous updating. This is supported by previous studies implicating that the entorhinal cortex is involved in the online computation of: (i) Euclidean distances toward distal locations (Howard et al., 2014; Spiers & Maguire, 2007), (ii) linear/path distances toward a point of origin (Jacob et al., 2017), and (iii) intended geocentric directions to target objects (Chadwick et al., 2015). Most probably, these online vector computations are dependent on the spatially stable firing patterns of entorhinal grid cells (Fyhn et al., 2004; Jacobs et al., 2013; Gil et al., 2018; Hafting et al., 2005; Stangl et al., 2018). With firing fields that represent the vertices of tessellating triangles arranged in a hexagonal lattice, a common spatial metric with the same scale and orientation is maintained across the geometric surfaces of different environments (Hafting et al., 2005; McNaughton, Battaglia, Jensen, Moser, & Moser, 2006). This uniform distribution of firing fields of grid cells can be conceived as neuronal nodes in a mapping of topographical space to mediate the continuous/dynamic updating of positional or locational changes (McNaughton, Battaglia, Jensen, Moser, & Moser, 2006). Importantly, the multi peaked firing pattern exhibited by grid cells does *not* need reciprocal inputs from the hippocampus to maintain the number of firing peaks and the size/scale of the firing field, implicating that spatial information about self-movements can be expressed primarily by the entorhinal cortex (Fyhn et al., 2004). This might explain why Shrager et al.'s (2008) amnesic patients (with largely intact entorhinal cortices) can perform as well as the control subjects despite experiencing hippocampal atrophy.

On the other hand, the resection of the medial temporal lobes in the epileptic patients (Philbeck et al., 2004; Worsley et al., 2001) might have abolished or complicated the use of a path integration strategy resembling Wiener et al.'s (2011) configural updating strategy. This could be seen from the finding of Shrager et al.'s (2008) amnesic patients being unable to conduct homeward pointing as well as the controls after a period of distraction (see Experiment 5, Shrager et al., 2008), which implicated certain deficits in forming or accessing offline representations of the outbound paths (e.g., an aerial view of the traversed path).

1.5 Study Overview and Hypotheses

In view of these implications and the absence of any neuroimaging study to date showing how individual differences in path integration strategy use could influence the levels of activity in the hippocampal formation and extrahippocampal regions, the current study aimed to investigate the extent to which continuous and configural updating strategy use would engage the hippocampal formation, as well as navigationally relevant extrahippocampal regions.

1.5.1 Experiment 1

The current study aimed to apply functional magnetic resonance imaging (fMRI) to record and compare the patterns of neural activations in two groups of participants who implemented the continuous and configural updating strategies as set forth by Wiener et al. (2011). To ensure that the participants received adequate task exposure before

undergoing MRI scanning, they began by performing visual path integration in a desert-like virtual environment devoid of landmarks in the experimental lab. Throughout the experiment, the participants were randomly assigned to use either the continuous updating strategy or the configural updating strategy. Subjective variables that could influence visual path integration performance (e.g., computer experience, inherent navigation strategy preferences, spatial anxiety) were assessed using surveys and analyzed for potential inclusion as covariates when comparing the performance between the two strategy groups (see Methods and Results, for details).

When performing the path integration task, the two groups of strategy users experienced two types of outbound paths in equal proportions: (i) *simple paths* with one turn each, and (ii) *complex paths* with two turns each (see Methods, for details). The differences between configural and continuous updaters in homing performance were analyzed as a function of these two types of outbound paths.

With reference to Wiener et al.'s (2011) findings which showed that a speed-accuracy tradeoff was induced by configural updating strategy use, it was hypothesized that the configural updating strategy users would demonstrate lower magnitudes of direction and distance errors, but longer homing latency (i.e., time spent on the homebound journey), than continuous updating strategy users overall. It was also hypothesized that path integration accuracy (in terms of absolute values) will decline among the configural updating strategy users with increases in outbound path complexity across three levels, from simple paths (comprising of one turn each) to complex paths (comprising of two turns each). This hypothesis pays heed to previous studies which showed that the configural encoding of distance and turn values tend to become less

precise (or more effortful) with increases in the number of turns and segments (Fujita et al., 1993; Harris & Wolbers, 2012; Klatzky et al., 1990; Loomis et al., 1999).

By contrast, the continuous updating strategy users were not expected to demonstrate any significant changes in path integration accuracy (in terms of both absolute and signed values) with increasing path complexity. This adheres to Loomis et al.'s (1999) notion that a moment-to-moment updating of spatial displacements from the starting position should lead to the commission of distance or direction errors of relatively equal proportions across outbound paths of varying complexity. Specifically, Loomis et al. (1999) postulated that continuous spatial updating would be affected by consistent errors in the encoding of outbound distance or turn values, which vary by a constant factor/ratio with each footstep or turn, irrespective of outbound path complexity.

1.5.2 Experiment 2

In the fMRI experiment, the same group of participants who completed the first experiment will perform the visual path integration task (with a new set of trials) based on an event-related design that seek to differentiate between the cognitive processes involved in the outbound and homebound phases of the path integration trials (see Methods, for details).

In view that the entorhinal cortex comprises grid cells (Doeller et al., 2010; Jacobs et al., 2013), whose activity potentially contribute to the online computation of variation in distances (Hafting et al., 2005; Gil et al., 2018; Jacob et al., 2017; McNaughton et al., 2006; Stangl et al., 2018) and heading directions (Gil et al., 2018; Stangl et al., 2018), it was first hypothesized that continuous updating strategy use would engage the entorhinal

cortex during the homebound phase when homing vectors need to be dynamically computed.

Next, it was hypothesized that continuous updating strategy use would engage the hippocampus *contingent* on the recruitment of the entorhinal cortex. This is because the entorhinal cortex is directly adjacent to the hippocampus and inputs highly processed multisensory information (from the neocortex) to the hippocampus through the perforant pathway (Witter et al., 2000; see also Canto, Wouterlood, & Witter, 2008, for a review). The perforant pathway has been shown to contribute to the proper functioning of spatial working memory (Vago & Kesner, 2008) and long-term spatial memory consolidation (Remondes & Schuman, 2004). Critically, afferent signals from the dorsolateral and ventromedial bands of the entorhinal cortex converging on the dorsal and ventral layers of the hippocampus have been suggested to mediate the functional differences between these two hippocampal subregions (Steffenach, Witter, Moser, & Moser, 2005). These suggestions align well with recent proposals that the formation and modulation of hippocampal place cell activity may be engendered by efferent spatial signals from the entorhinal grid and border cells (see Grieves & Jeffry, 2017; Moser, Rowland, & Moser, 2015; Savelli, Yoganarasimha, & Knierim, 2008; Solstad, Boccara, & Kropff, Moser, & Moser, 2008).

As for configural updating strategy users, it was hypothesized that they would engage the hippocampus during the homebound phase. This hypothesis was made with reference to previous findings (as aforementioned) which implicated that patients with hippocampal atrophy (Study 5, Shrager et al., 2008) and right MTL resection (Philbeck et al., 2004; Worsley et al., 2001) experienced difficulties with the processing of distance

and direction information. Based on the observation that Shrager et al.'s (2008) patients failed to perform as well as the controls after a period of distraction (Study 5, Shrager et al., 2008), it is possible that the implementation of an imagery strategy akin to the configural updating strategy – which the patients most probably had a deficit in – was involved in an *offline retrieval* of the outbound path. Conceptually, this possibility is tied to the classical cognitive map theory (O'Keefe & Nadel, 1978), which proposed the hippocampus as the neural substrate for storing an allocentric spatial representation of the environment, as well as to numerous empirical findings that posited a pivotal role of the hippocampus in cognitive mapping and spatial memory formation (e.g., Bohbot, Iaria, & Petrides, 2004; Iaria, Petrides, Guariglia, Ptito, & Petrides, 2007; Harris & Wolbers, 2014; Schinazi, Nardi, Newcombe, Shipley, & Epstein, 2013; Spiers & Maguire, 2006; Whishaw & Tomie, 1996).

CHAPTER 2

EXPERIMENT 1

METHODS

2.1 Participants

50 participants [22 females; M (SD) age = 20.53 (3.44); age range: 18 – 38] were recruited from Georgia Tech and the wider academic community in Atlanta, GA. All were right-handed, had intact vision, and neither had any neurological or psychiatric disorders nor MRI contraindications. Before coming to the lab, they were surveyed using the Qualtrics survey tool (licensed by GT for campus use; accessible at: <https://webmasters.gatech.edu/handbook/forms-and-surveys>) regarding their physical and health conditions, computer experience, and levels of spatial anxiety when navigating their everyday environments (see section below, for specifics about the questionnaires administered online).

In the lab, the experimenter assessed the participants' handedness (Edinburgh handedness questionnaire, Oldfield, 1971), visual acuity (Snellen Eye Chart), and sensitivity to both color (Ishihara Color Plates Test) and contrast (Mars Letter Contrast Sensitivity Test). Table 1 shows the demographic details and survey/pretest measures from all participants separated into two strategy groups based on the instructions they received. Ratings from self-report items were summed to provide summated scale scores for spatial anxiety and computer experience, respectively. Total strategy effectiveness concerned the

sum of two ratings obtained from both in-lab practice and test sessions. The two groups did not differ significantly on any of these measures ($ps > .05$).

Table 1

Descriptive Statistics of the Demographic and Survey/Pretest Variables of Participants receiving Continuous Updating and Configural Updating Strategy Instructions

Survey/Pretest variable	Continuous Updaters ($n = 24$)			Configural Updaters ($n = 26$)			Difference (Continuous – Configural)	
	$M (SD)$	$Min.$	$Max.$	$M (SD)$	$Min.$	$Max.$	$M (SE)$	95% CI
Age	21.25 (4.53)	18	38	21.27 (3.65)	18	30	-0.02 (1.16)	[-2.35, 2.31]
Sex (% females)	46	-	-	42	-	-	-	-
Spatial anxiety	20.13 (6.50)	9	33	19.35 (6.44)	9	29	0.78 (1.83)	[-2.90, 4.46]
Computer experience	15.12 (3.38)	9	21	15.97 (3.27)	10	21	-0.84 (0.94)	[-2.73, 1.05]
Ishihara color blindness	13.69 (1.53)	6.5	14	12.92 (2.94)	4	14	0.76 (0.67)	[-0.58, 2.11]
Mars contrast sensitivity	1.86 (0.05)	1.8	1.92	1.85 (0.05)	1.8	1.92	0.01(0.01)	[-0.02, 0.03]
Joystick speed test (s)	66.96 (5.24)	59	78	66.96 (6.51)	57	87	-.003 (1.68)	[-3.38, 3.38]
Total strategy effectiveness	12.50 (3.88)	3	20	12.65 (2.38)	7	18	-.15 (0.90)	[-1.97, 1.66]

2.2 Online Surveys

In the online Qualtrics survey, in addition to health-related screening questions confirming participants' eligibility for the fMRI experiment, the participants completed: (i) a three-item *Computer Experience Questionnaire (CEQ)* [Moffat, Hampson, & Hatzipantelis, 1998], and (ii) an eight-item *Spatial Anxiety Scale* (Lawton, 1994).

For the CEQ, the participants rated their frequencies of computer usage and computer/video game-play on a seven-point Likert scale from “1” (*I have never played computer games*) to “7” (*almost everyday*) [see Appendix A, for items]. For the *Spatial Anxiety Scale* (Lawton, 1994), the participants rated the amount of anxiety they felt when returning to a familiar place, searching for unfamiliar places, and finding shortcuts (see Appendix B, for items). A five-point Likert scale was used, ranging from “1” (*not anxious*) to “5” (*very anxious*).

Summated scale scores (i.e., sums of ratings from items constituting a scale/subscale) from each of the three questionnaires were computed and analyzed for consideration as covariates when comparing the path integration performance of the two strategy groups (see Results, for details).

2.3 Experimental Stimuli (for both Experiments 1 & 2)

The game engine, Unity Pro v5.0.2 (Unity Technologies, Inc., San Francisco, CA, USA), was used to create and animate a desktop virtual environment from the first-person

perspective at an eye height of 1.7 m.² The virtual environment featured a desert with a starry night sky (see Fig. 6A). An optimal presentation of optic flow information during virtual movements was intended through changes in the uniformity of the sandy, mottled ground texture, and the changing locations of the stars during turns.

The outbound paths were designed using the Unity Animation toolkit and featured animations of the outbound journey from the first-person perspective. To eliminate potential effects of over-learning or habituation, separate sets of outbound paths were used across the three sessions of practice, in-lab behavioral testing, and fMRI scanning. In the practice session, directional arrows and a virtual traffic cone designating the starting position were presented to familiarize participants with the task demands of the subsequent sessions (see Procedure, for details). During the subsequent sessions of in-lab testing (Experiment 1) and fMRI scanning (Experiment 2), the trials featured eight outbound paths partitioned into two symmetrical sets based on left and right turning directions terminating at two ending points with eccentricities (i.e., bearings with a starting position as the reference point, as termed by Gramann et al., 2005) of $\pm 30^\circ$ and $\pm 45^\circ$ (see Figs. 6C and 6D).³ The allocation of two ending points facilitated the computation of turning and distance errors.⁴

In each test session, there were equal numbers of outbound paths with single turns and double turns (four per each type of path, evenly divided between left and right turns).

² One meter corresponds to a displacement of one virtual unit along the Cartesian planes in the Unity game engine.

³ The positive and negative signs denote clockwise and anticlockwise turning, respectively.

⁴ In programming terms, having two ending points enables the application of the Boolean function in the primary data recording script, which simplifies the computation and recording of the error variables.

The paths in the former set were labeled as “simple paths” whereas the paths in the latter set were labeled as “complex paths.” The presentation of such complex paths was intended to make visual path integration more cognitively demanding (cf. Plank et al., 2010). As such, a subset of complex paths with turns in opposite directions (paths 2c and 2d, see Figs. 6C and 6D) was designed with the purpose of eliminating heuristics that could affect homing performance in simple paths (e.g., rotating in the same direction as that of an observed turn to return to the starting position, see Riecke, 2012). Tables 2 and 3 show the path parameters (i.e., distances and bearings) of all eight outbound paths that were designed for in-lab testing and fMRI scanning, respectively.

In both experiments, the speed of animated translations along each outbound path were maintained at an average speed between 2.0 to 2.5 m/sec — a range that approximates brisk walking speeds in the real world. The implementation of this virtual walking speed followed previous evidence showing that a close correspondence between real world and virtual walking speeds encouraged relatively accurate path integration performance in virtual environments (Ellmore & McNaughton, 2004). Crucially, each turn of the outbound path was programmed to follow a curved path rather than a sharp turn to facilitate a gradual presentation of rotational optic flow. For this purpose, the average speed of rotation along the yaw axis was set between 18° to 20° per second. Based on these speed settings, during both in-lab testing and fMRI scanning, animations of the simple and complex path lasted for eight and 10 seconds, respectively.

To minimize the chances of participants implementing a time- or pace-counting heuristic that could be derived from experiencing relatively consistent movement speeds along the various outbound paths, the homebound translational movement speed was set

at 3.0 m/sec, while the average speed of rotation along the yaw axis was set at 40° per second in all trials. Moreover, to ensure that the two spatial updating strategies are well implemented, “catch” trials, which served the purpose of keeping participants focused on implementing the prescribed strategy, were added to the in-lab test trials (see Procedure, for details).

Table 2

Outbound and Homebound Path Parameters for In-lab Behavioral Testing

Type (ID)	Turning direction	Outbound path					Homebound path		
		Allocentric bearing (°) [first turn]	Allocentric bearing [second turn]	Length of first segment (m)	Total length (m)	Ending point eccentricity (°)	Euclidean distance (m)	Relative bearing (°)	Allocentric bearing (°)
Simple (t1a)	L	-43	–	3.5	12.06	-30	11.20	-167	-210
Simple (t1b)	R	43	–	3.5	12.06	30	11.20	167	210
Simple (t1c)	L	-62	–	3.5	13.21	-45	11.17	-163	-225
Simple (t1d)	R	62	–	3.5	13.21	45	11.17	163	225
Complex (t2a)	L, L	-52	-90	6.25	14.74	-45	11.17	-135	-225
Complex (t2b)	R, R	52	90	6.25	14.74	45	11.17	135	225
Complex (t2c)	L, R	-90	45	6.25	14.26	-45	11.17	-180	-225
Complex (t2d)	R, L	90	-45	6.25	14.26	45	11.17	180	225

Note. “L” denotes a leftward turn whereas “R” denotes a rightward turn. The positive (+) and (-) signs denote clockwise and anti-clockwise rotations, respectively. Homebound allocentric and relative headings specify the orientation of the starting position relative to the ending point of the outbound path with reference to North and the relevant egocentric heading, respectively. Allocentric bearings refer to deviations from the Northward axis whereas relative bearings refer to deviations from egocentric headings at the ending points of outbound paths.

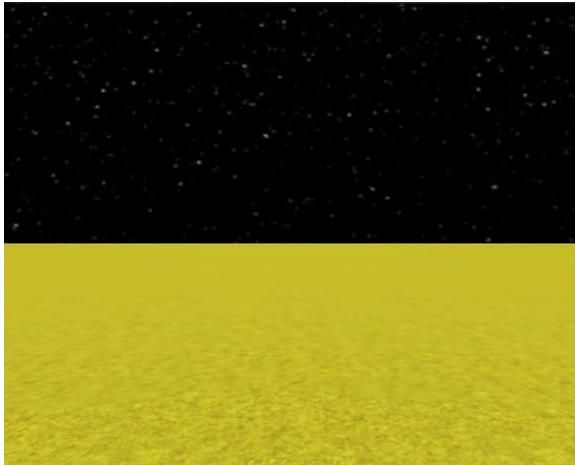
Table 3

Outbound and Homebound Path Parameters for Testing in the MRI Scanner

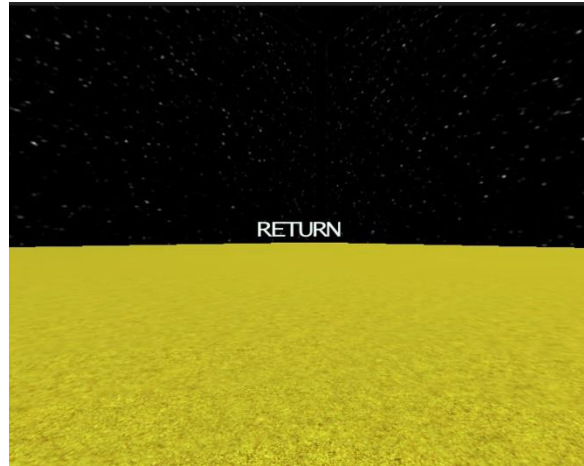
Type (ID)	Turning direction	Outbound path					Homebound path		
		Allocentric bearing (°) [first turn]	Allocentric bearing [second turn]	Length of first segment (m)	Total length (m)	Ending point eccentricity (°)	Euclidean distance (m)	Relative bearing (°)	Allocentric bearing (°)
Simple (1a)	L	-50	–	5.0	12.68	-30	11.20	-160	-210
Simple (1b)	R	50	–	5.0	12.68	30	11.20	160	210
Simple (1c)	L	-70	–	5.0	13.91	-45	11.17	-155	-225
Simple (1d)	R	70	–	5.0	13.91	45	11.17	155	225
Complex (2a)	L, L	-36	-90	5.0	14.40	-45	11.17	-135	-225
Complex (2b)	R, R	36	90	5.0	14.40	45	11.17	135	225
Complex (2c)	L, R	-80	35	5.0	13.87	-45	11.17	-180	-225
Complex (2d)	R, L	80	-35	5.0	13.87	45	11.17	180	225

Note. “L” denotes a leftward turn whereas “R” denotes a rightward turn. The positive (+) and (-) signs denote clockwise and anti-clockwise rotations, respectively. Homebound allocentric and relative headings specify the orientation of the starting position relative to the ending point of the outbound path with reference to North and the relevant egocentric heading, respectively. Allocentric bearings refer to deviations from the Northward axis whereas relative bearings refer to deviations from egocentric headings at the ending points of outbound paths.

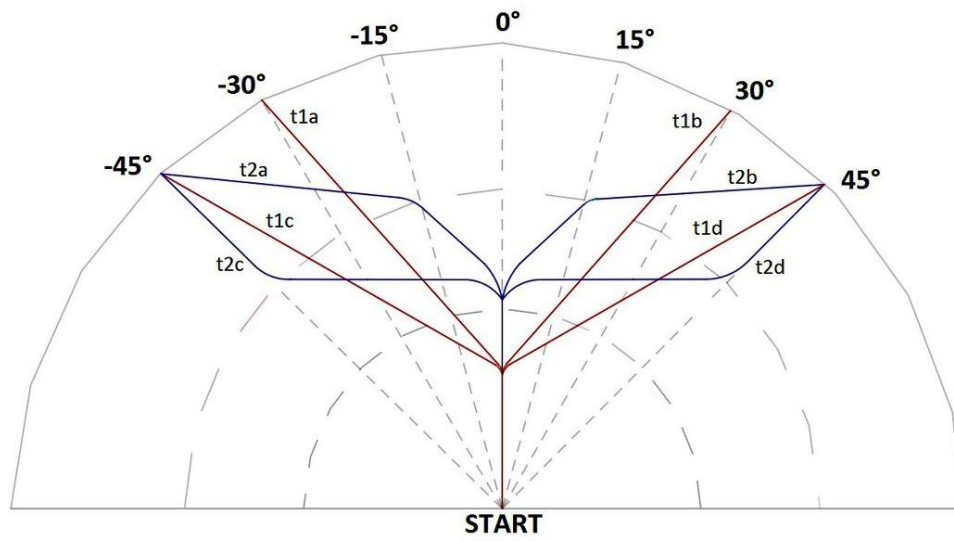
A.



B.



C.



D.

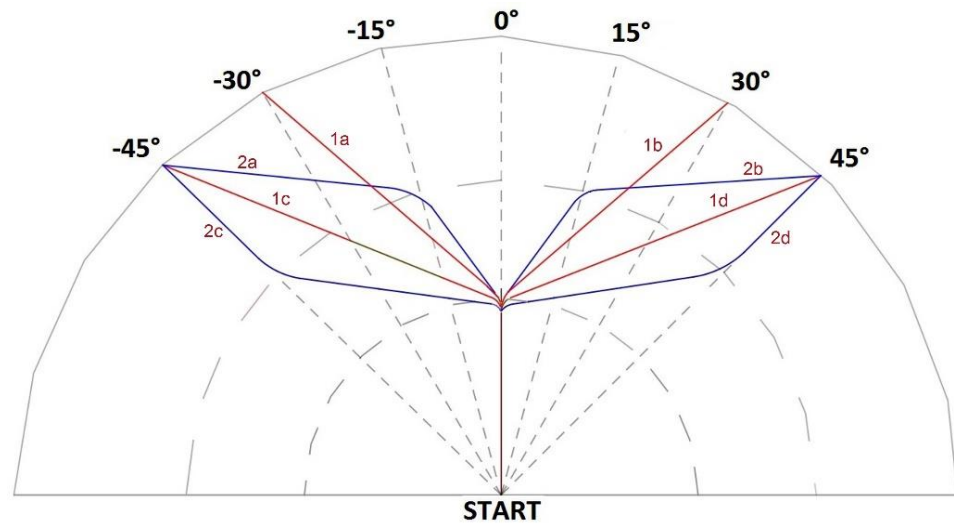


Fig. 6. (A) A scene of the featureless virtual environment designed for path completion, along with (B) the one-second word cue for returning to the starting position at the end of an outbound path. Schematics of the animated outbound paths designed for the path integration trials in the (C) in-lab testing and (D) fMRI sessions. Simple paths (one turn each; 1a to 1d) are colored in red whereas complex paths (two turns each; 2a to 2d) are colored in blue. In both test sessions, paths 2a and 2b represent the unidirectional complex paths (two turns in the same direction) whereas paths 2c and 2d represent the bidirectional complex paths (two turns in opposite directions). In the fMRI scanning session, the first leg of travel was set at a fixed length (5.0 virtual m) for all outbound paths.

2.3.1 Data Recording

In both experiments, the dependent variables representing homing performance were the same as those used by Wiener et al. (2011). Navigational error measures were recorded when participants pressed a joystick button to indicate their perceived starting positions.⁵ Specifically, path integration / homing performance was assessed in terms of five dependent variables: (i) *homing distance error*: the Euclidean distance between the starting and final stopping position in homebound phase (δ , see Fig. 7), (ii) *signed distance error*: signed differences between the linear distance traveled during homing and the correct/pre-computed Euclidean distance back to the starting position from the stopping position at the end of the outbound path ($d_1 - d_0$, see Fig. 7), (iii) *absolute direction error*: absolute angular deviations from the correct bearing of the starting position at the final stopping position in the homebound phase ($|\theta_1 - \theta_0|$, see Fig. 7), (iv) *signed direction error*: signed angular deviations from the correct bearing of the starting position at the final stopping position in the homebound phase ($\theta_1 - \theta_0$), and (v) *homebound response time*: the time taken (recorded to the accuracy of a hundredth of a second) to return to the perceived starting position after the offset of the return cue.

⁵ All mentions of “navigational errors” in the context of this study refer *specifically* to distance and direction errors committed during visual path integration. They do *not* refer to errors committed during any other type of navigational activity, such as wayfinding, for example.

For signed distance error, positive and negative values indicate, respectively, overshoot and undershoot of the most direct path back to the start. Likewise, for signed direction error, positive and negative values indicate, respectively, overshoot and undershoot of the correct angle-of-return to the start. When the overall trajectory of the outbound path faced leftward, instances of undershoot and overshoot were marked, respectively, by under-turning and over-turning of the homing vector (aligned with d_0 in Fig. 7) from the anticlockwise direction. The reverse applied to outbound paths with overall rightward trajectory; instances of undershoot and overshoot were marked, respectively, by under-turning and over-turning of the homing vector from the clockwise direction.

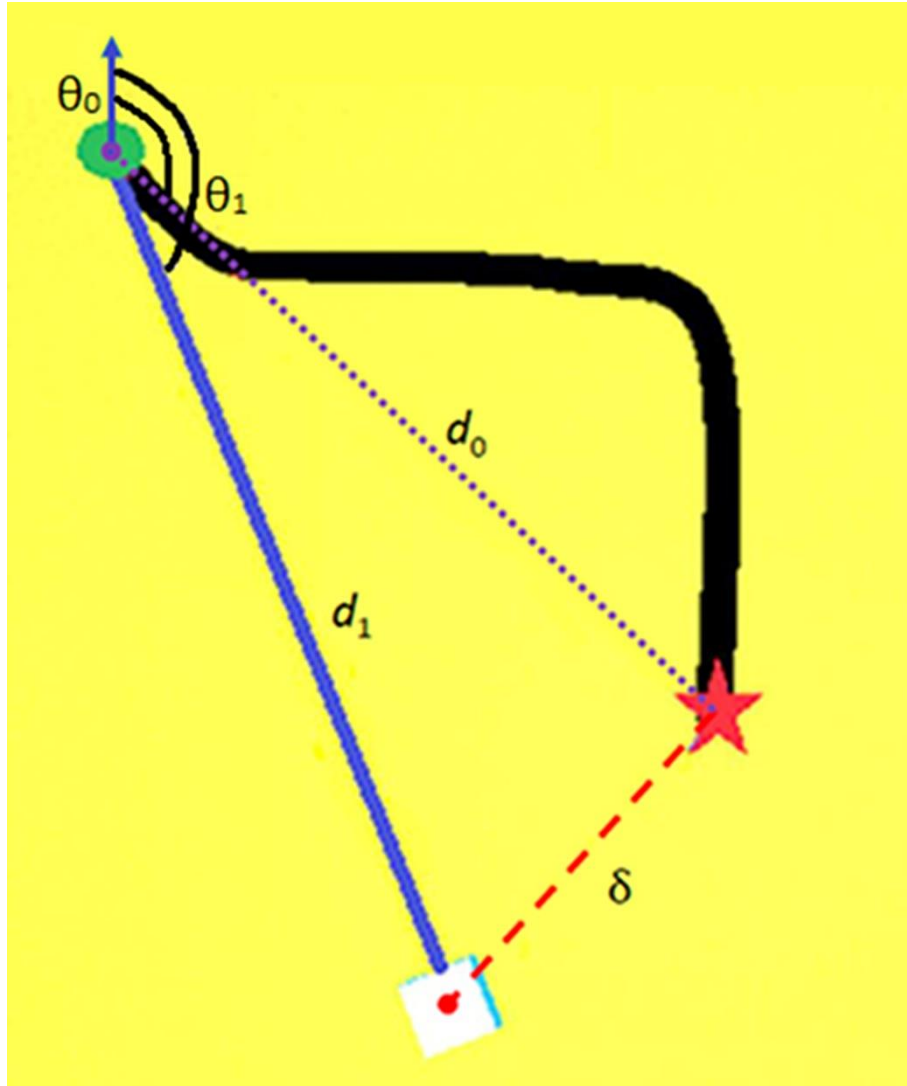


Fig. 7. Schematic showing the computation of the navigational error variables. The outbound path is bolded in black while the homebound path is bolded in purple. The star represents the starting position, the filled circle represents the terminus of the outbound path, and the white cube represents the stopping position. θ_0 (smaller angle) represents the pre-computed / correct bearing relative to the start and θ_1 (bigger angle) represents the bearing relative to the participant's stopping point. $|\theta_1 - \theta_0|$ denotes the absolute direction error. θ are Euler angles ranging from 0° to 360° that registered the moving body (white cube) with respect to the vertical z axis of the xyz Cartesian system. The linear distance of the homebound path traversed by the participant is denoted by d_1 . The deduction of d_0 from d_1 represents the signed distance error. The dashed red line (δ) represents the homing distance error.

2.4 Procedure

2.4.1 *Experiment 1: Strategy Learning and Behavioral Testing*

The participants conducted practice and test sessions in the lab to familiarize themselves with the virtual environment and the task of using a specific strategy.

Throughout the experiment, each participant sat 20 inches in front of a 21-inch LCD monitor and used a joystick to control all virtual movements. The on-screen resolution was set at 1280 x 960.

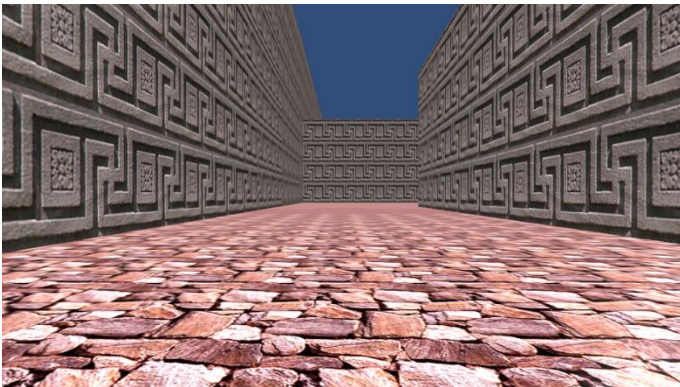
2.4.1.1 Joystick Control Practice and Test

Before commencing the path integration task, each participant practiced controlling a joystick for virtual movements. The joystick was MRI-compatible and was used in both experiments. Under the guidance of the experimenter, the participants first demonstrated competence at using the joystick to control their virtual movements in reaching target objects in a virtual arena (see Fig. 8). After that, they traveled down a winding passageway in a virtual maze (see Fig. 9A) until they reached a treasure chest (see Fig. 9B). They were told to reach and make contact with the treasure chest within two minutes. The application recorded the total time of travel when they made contact with the object. This time was included in the data analysis as “joystick speed test time.” The speed and acceleration settings in the virtual maze were kept similar to those in the path integration trials. The virtual arena and virtual maze were designed using Unreal Engine v3.0 (Epic games, Inc., Cary, NC, USA) and Unity Pro v5.0.2 (Unity Technologies, Inc., San Francisco, CA, USA) respectively.



Fig. 8. A scene from the Unreal virtual arena used for general joystick practice.

A.



B.



Fig. 9. Scenes from the Unity virtual maze used for testing joystick control: **(A)** Opening scene upon maze entry and **(B)** scene upon finding the wooden chest.

2.4.1.2 Strategy Manipulation and Physical Practice

After the joystick practice and control test, the experimenter randomly assigned the participants to receive instructions about the continuous updating and configural updating strategies respectively. 24 participants (11 females) received continuous updating strategy instructions while 26 participants (11 females) received configural updating strategy instructions.⁶ These instructions were analogous to the instructions used by Wiener et al. (2011). The random assignment followed an interleaving pattern whereby switches between strategy assignment readily occurred after testing one or two participants with the same instructions.

Instructions regarding the *continuous updating strategy* were as follows: “*This strategy requires you to monitor your movements with respect to the starting position at all times. When observing the path of travel, please keep constant track of your position relative to the starting point such that at any time, I can stop you and you can point or move directly back to the goal. Do not dwell on any complex homing techniques; just experience the motion and know where you are relative to the starting point at all times.*” The experimenter demonstrated how to implement this strategy by walking forward from a fixed starting point in the lab and pointing his arm and fingers straight to the starting point before and after making a turn. The participants watched this demonstration from the starting point. While traversing the path, the experimenter repeatedly stressed that he visualized the starting point as lying behind him and he was constantly updating its

⁶ To ensure that males and females were not unevenly distributed between the two strategy instruction conditions / groups, a 2 x 2 chi-square test of independence was conducted, showing the non-occurrence of uneven distribution, $\chi^2 = .063, p = .802$.

position as he moved away from it. At the end of this outbound path, the experimenter demonstrated walking back to the starting point in a straight line and told the participants that this is what they must do when using the joystick to return to the start in the upcoming computerized practice.

After this demonstration, the experimenter told each participant to follow closely behind him as he walked out a winding path from the starting point in the experimental lab to the entrance of an adjacent storehouse. The outbound path involved three turns, and the experimenter told the participants to point back to the starting position before every turn, and at the end of the outbound path when the experimental lab was beyond the line of sight. At the end of the path, the experimenter told the participants to guide him directly back to the starting point.

In comparison, instructions regarding the *configural updating strategy* were as follows: “*This strategy requires you to pay close attention to the forward and turning directions of the path traveled. Please visualize and remember the overall shape of the traveled path as if you were viewing it from above — that is, from an aerial perspective. At the same time, try to estimate the magnitudes of the turns you observed. Please use this shape and the turning angles you remembered to estimate the direction and distance back to the start after you reached the end of the traveled path.*” The experimenter demonstrated how to implement this strategy in the lab by traversing two outbound paths (with one and two turns respectively) and drawing out their shapes in sequence on a white board. The participants viewed each demonstration from the starting point and from the *same* viewpoint as that of the experimenter before he moved forward. This ensured that all participants visualized the first path segment in a northbound/upward

direction and that they did have to engage extraneous mental rotations to realign the experimenter's forward movements with a northbound reference direction. While traversing the path, the experimenter turned slowly and told the participants that he was estimating the turning angle and encoding the ensuing shape of the path as he turned and walked forward. The experimenter paused at the end of the outbound path and stressed that he was retrieving the imagined shape of the outbound path, before walking back to the starting point in a straight line. The experimenter also told the participants to continue engaging in this retrieval process when controlling the joystick to return to the start in the upcoming computerized tasks.

After this demonstration, each participant followed the experimenter on two double-turning complex paths (one with turns in the same direction and one with turns in opposite directions) in the lab. Before traversing the paths, the experimenter re-emphasized the need to visualize the shape of the outbound path from an aerial perspective and that they must use this imagined shape to guide their return to the start. At the end of each outbound path, the experimenter told each participant to guide him back to the start in a straight line and to draw the shape of the outbound path on a piece of paper (see Appendix C, for samples). If the participant drew an incorrect shape of any outbound path, the experimenter re-walked that path with the participant and instructed the participant to make another attempt at drawing its shape. The experimenter only continued the experiment when the correct shapes were drawn. Overall, all participants in the configural updating condition were prompt at drawing out the shapes of the paths, and all these drawings were drawn approximately to scale with respect to the distances and turns experienced.

2.4.1.3 Path Integration Practice Task

Upon practicing the strategy in the lab, the participants completed a computerized practice task. This practice task ensured that the participants practiced the strategy further in a virtual environment and they became familiar with the demands of visual path integration before formal testing.

A total of 24 practice trials was presented. Initially, the first four trials presented layouts of the entire path on the floor of the virtual environment from the first-person perspective – as marked out by directional arrows and a traffic cone at the starting position. The participants were moved passively along the outbound path (see Fig. 10A), and upon reaching the end of outbound travel, controlled the joystick to return to the starting position by following the homebound arrows. These practice trials were completed upon contact with the cone (see Fig. 10B). As the participants performed these trials, the experimenter reminded them to keep using the same strategy that they were told during the earlier physical practice. They were also told that the visual aids would disappear gradually with trial progression.

The first four trials featured full availability of visual aids: two simple paths with a right-angled turn each and running symmetrical to each other, and two complex paths, each with an initial right-angled turn, followed by a 45° turn. The two turns of each complex path ran in opposite directions and the two complex paths were symmetrical to each other.

The next four practice trials were the same as the first four practice trials except that the outbound paths were the only paths marked with arrows. The participants

returned to the virtual cone without any arrows marking out the homebound path. In the next eight practice trials, all floor arrows disappeared and only the virtual cone was present at the starting position; the participants were told to continue applying their prescribed strategy when returning to make contact with the cone.

Finally, in the last eight practice trials, the cone was removed, and the participants were told to continue applying their prescribed strategy to return to the starting position. All participants were told explicitly that the starting position was in the same location as that of the previously observed virtual cone and that they must return to where the virtual cone was formerly located in the subsequent practice trials, as well as in the ensuing test trials. In these trials, the participants pressed a joystick button to indicate their stops at where they perceived the starting position to be. The magnitudes and directions of turns in this last block of trials were identical to those in the previous trials but the travelling speed during the outbound journey varied along different straight segments and differed from the travelling speed during the homebound journey. This served to minimize the use of a pace- or time-counting heuristic in the subsequent experimental trials.

When the participants were performing these trials devoid of any object cues, the experimenter paused the task in the middle or after the completion of two randomly chosen trials. For the participants in the continuous updating condition, the experimenter paused two trials at the end of the outbound paths and told them to point with their arms straightened to the perceived starting position. If any pointing response deviated too far from homing vector, the experimenter allowed the participant further attempts on subsequent practice trials until he/she exhibited relatively accurate pointing responses with lower levels of angular deviation. As for the participants in the configural updating

condition, the experimenter paused two trials after completion (i.e., when the fixation cross appeared during the ITI), and told them to draw out the shapes of the outbound paths on a piece of paper.

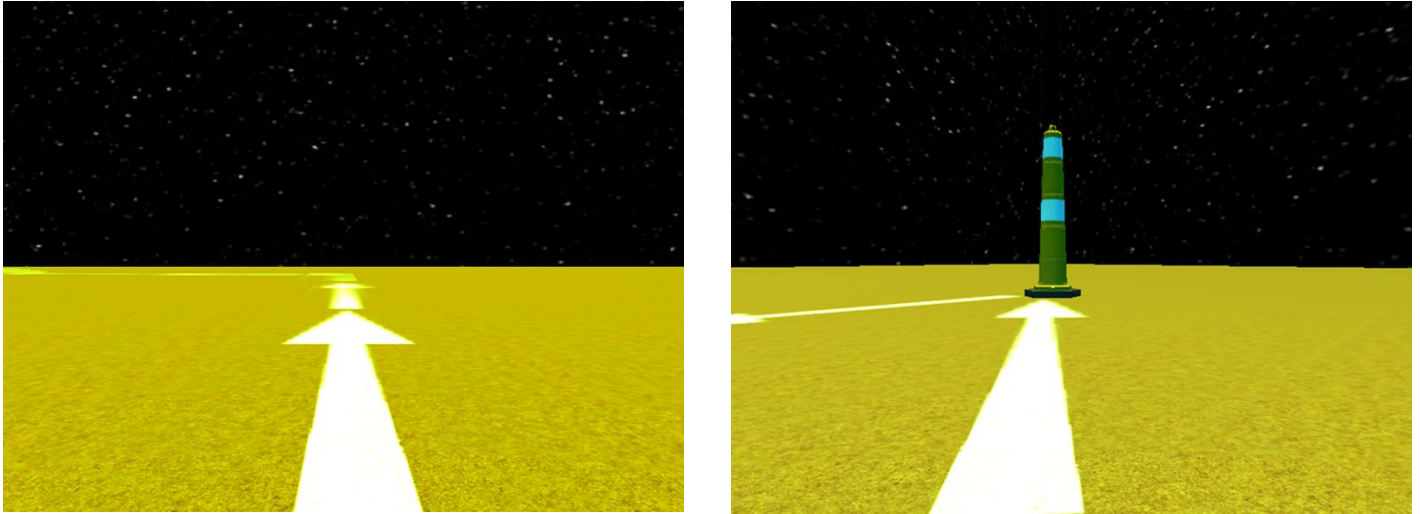


Fig. 10. (A) An opening scene of a rightward turning outbound path marked with directional arrows on the floor. The participants stayed immobile at the start for three seconds before being passively moved forward. **(B)** View of the traffic cone (marking out the start) as one approaches it at the end of the homebound path. Participants made contact with the cone to complete the trial.

2.4.1.4 Post-practice Survey

Upon completion of the practice task, the participants rated their effectiveness of strategy use on a 10-point Likert scale (see Appendix D). This scale was adapted from the *Personal Encoding Preference (PEP) Questionnaire* designed by Powell-Moman and Hertzog (see Hertzog & Dunlosky, 2004). This self-report effectiveness measure was administered in view of the metacognitive impact of personal beliefs or assurances about learning, memory, and strategy use on cognitive task performance (Ariel, Price, & Hertzog, 2015; Hertzog & Dunlosky, 2004), which encompasses spatial navigation (Ariel & Moffat, 2018). To control for the potential effect of personal beliefs about the effectiveness of strategy use on path integration performance, the strategy effectiveness rating was analyzed for consideration as a covariate when comparing the performance of the two strategy groups (see Results, for details).

2.4.1.5 Path Integration Test Session

In the follow-up testing session, the participants were reminded to continue using the strategy that they were instructed on, and that the starting position on all test trials was located at same spot as the virtual cone observed during practice. At the start of the task and before performing the first trial, the participants stayed immobile at the starting position for six seconds with a fixation cross in the middle of the screen.⁷ This initial delay allowed participants to have a quick preliminary assessment of the virtual environment before experiencing animated/passive travel on the first outbound path.

⁷ This equaled the delay required for the MRI scanner to warm up before the commencement of echo planar image (EPI) acquisition, which the participants encountered later in the fMRI session.

Each of the eight outbound paths (see Fig. 6C) in the in-lab test trials were repeated six times to constitute 48 path integration trials. These trials were randomly arranged and evenly divided into two blocks (each with three repetitions of each outbound path) of 24 path integration trials separated by a pause screen during which the participants were given short break of a few minutes. At the end of outbound travel in each trial, the participants controlled the joystick to return perceived starting position within a time-limit of 20 seconds after seeing the one-second “RETURN” cue (see Fig. 6B). After reaching the position of choice, the participants pressed a joystick button. Immediately upon button press, all virtual movements ceased, and an instantaneous recording of homebound response time and homing errors occurred (see Data Recording subsection above).

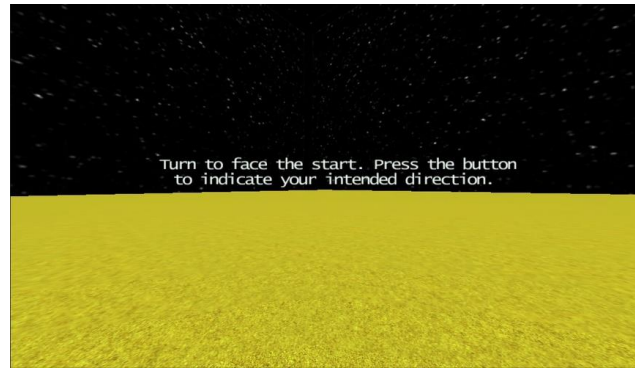
Among the path integration were four “catch” trials – two per block – that contributed to a total of 52 trials. The participants were informed of their inclusion before performing the task. These catch trials ensured that the participants were reminded of the demands of the prescribed strategy and that they were stay consciously aware of it as they performed the path integration trials. In each block, two catch trials appeared at variable positions in the trial sequence (one near the front and the other near the end) with separate on-screen instructions *at the end* of outbound paths to the participants in each strategy group. The outbound paths that were presented in the four catch trials correspond to two simple paths (see Fig. 6C, paths t1b and t1c) and two complex paths (see Fig. 6C, paths t2b and t2c). In the continuous updating strategy condition, the participants were instructed to turn to face the starting position (see Fig. 11A), whereas in the configural updating strategy condition, they were instructed to judge whether or not the nearest

angle-of-return to the start was greater than 135° (see Fig. 11B). Specifically, participants in the configural updating strategy group pressed the joystick button for a “yes” response and waited for the onset of the next trial if they decided on a “no” response. The turning response required by a continuous updating catch trial represented a central characteristic of continuous updating strategy that involves homeward-pointing directional judgements. By contrast, the yes/no response required by the configural updating catch trial recognized the fact that configural updating strategy use requires estimating the homing direction at the end of the outbound path based on its imagined shape.

The maximum duration of each trial (path integration and catch trials alike) averaged 29 seconds [28 seconds (max.) for simple trials and 30 seconds (max.) for complex trials]. The intertrial interval (ITI) was set at two seconds and participants viewed a fixation cross in the middle of the opening scene (at the starting position) with lights dimmed.⁸ No virtual movements could be made with the joystick during the ITI.

⁸ Two seconds correspond to the repetition time (TR) that was implemented in the fMRI experiment.

A.



B.



C.

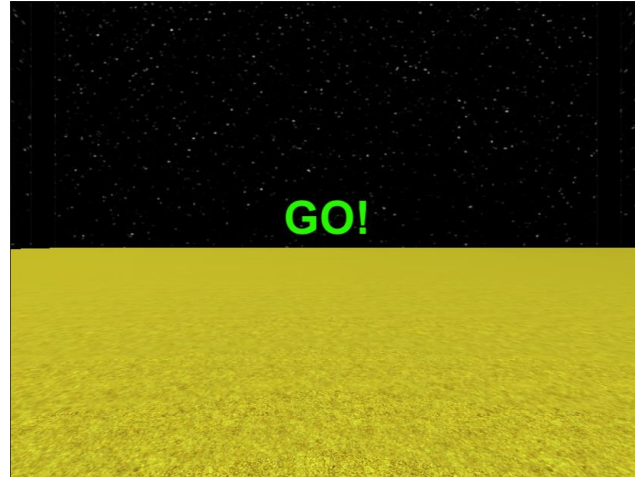


Fig. 11. (A) Messages shown in sample catch trials for participants in the continuous updating strategy condition and (B) configural updating strategy condition. The on-screen instruction for the continuous updating strategy group appeared for five seconds whereas the on-screen instructions for the configural updating strategy group appeared for 10 seconds (due to the lengthier text). (C) A one-second “Go” signal appeared after the offset of the on-screen instructions in both strategy conditions, to which participants made their responses immediately thereafter. This signal served the purpose of disambiguating the latency required for reading and comprehending the on-screen text from the latency involved in making the actual behavioral response.

2.4.1.6 Post-test Survey

At the end of the test session, the one-item survey about strategy effectiveness was re-administered and participants rated how effectively they implemented the prescribed strategy across the second block of trials (see Appendix D). The rating was done with respect to the second block of trials only in order to minimize potential difficulties with recalling the experience of performing the first block of trials on the part of some participants. This rating was combined with the practice-based strategy effectiveness rating to yield a total strategy effectiveness rating (out of 20) for covariate analysis (see Results, for details).

CHAPTER 3

EXPERIMENT 1

RESULTS

The dependent variables took the forms of mean and random errors committed across different outbound path categories. Mean errors referred to the average error values in each outbound path category while random errors referred to the standard deviations (*SDs*) of each error type per outbound path category. Random errors were included in the data analysis because they offered a more specific measure of homing performance by conveying the fluctuations in response consistency across trial repetitions (see Wolbers et al., 2007). These error variables were obtained from each participant across two sets of outbound path categories: (i) *simple paths* [4 paths (see Fig. 6C, paths t1a – t1d,) x 6 repetitions; 24 trials], and (ii) *complex paths* [4 paths (see Fig. 6C, paths t2a - t2b) x 6 repetitions; 24 trials]. Mean and random errors related to (i) homing distance, (ii) signed distance, (iii) absolute direction, and (iv) signed direction were recorded from each participant. This resulted in four sets of mean errors and four sets of random errors per participant. Together with these error measures, the homebound response time was also recorded and analyzed.

These dependent measures were entered independently into three-way mixed ANOVA / ANCOVA models with *strategy group* (2) and *sex* (2) as the between-subjects independent variables and *outbound path category* (2) set as the within-subjects

independent variable.⁹ As numerous studies have shown sex differences in both navigation strategy use (e.g., Cutmore, Hine, Maberly, Langford, & Hawgood, 2000; Dabbs, Chang, Strong, & Milun, 1998; Saucier et al., 2002; Sandstrom, Kaufman, & Huettel, 1998; Silverman et al., 2000; Zhong, 2011, 2013; Zhong & Kozhevnikov, 2016), and navigational performance (e.g., Sandstrom et al., 1998; Silverman et al., 2000; Moffat et al., 1998; Moffat, Zonderman, & Resnick, 2001; Zhong, 2013; Zhong & Moffat, 2016), sex was included to assess and control for any potential effect of sex on performance between the strategy groups.

3.1 Covariate Selection

To determine the covariate(s) that need to be added to the mixed-model ANOVAs, partial correlations – with sex and strategy group effects controlled for – were performed between mean errors, random errors, mean response times, and four survey/pretest variables composing of: (i) spatial anxiety, (ii) computer experience, (iii) joystick speed test time, and (iv) total strategy effectiveness. Table 4 show the partial correlations based on the mean errors and mean response times while Table 5 shows the partial correlations based on the random errors.

For each dependent measure, any survey/pretest variable(s) that correlated with it at a threshold of $p < .05$ gained entry as covariate(s) into the ANOVA model involving

⁹ Within-subjects differences were analyzed in terms of two broad categories of simple and complex paths in order to facilitate the comparisons of behavioral findings between Experiment 1 and 2.

that dependent measure. This resulted in the entry of *joystick speed test time* as a covariate in the analyses of (i) homing distance errors (both mean and random), (ii) absolute direction errors (both mean and random), and (iii) signed direction random error. Along with joystick speed test time, *total strategy effectiveness* was added as a second covariate in the analyses of (i) absolute direction errors (both mean and random) and (ii) signed direction random error.

Table 4

Partial Correlations between Mean Error Measures, Mean Response Time, and Survey/Pretest Measures after controlling for Sex and Strategy Group Effects

	Spatial anxiety	Computer experience	Joystick speed test time (s)	Total strategy effectiveness
Homing distance error (virtual m)	0.06	0.20	0.36*	-0.13
Signed distance error (virtual m)	-0.14	0.05	0.11	0.03
Absolute direction error (°)	0.11	0.13	0.42**	-0.29*
Signed direction error (°)	0.13	0.10	-0.26	-0.06
Response Time (s)	-0.07	-0.12	0.21	0.06

* $p < .05$ (two-tailed)

** $p < .01$ (two-tailed)

Table 5

Partial Correlations between Random Error and Survey/Pretest Measures after controlling for Sex and Strategy Group Effects

	Spatial anxiety	Computer experience	Joystick speed test time (s)	Total strategy effectiveness
Homing distance error (virtual m)	0.01	0.14	0.29*	-0.16
Signed distance error (virtual m)	-0.07	0.27	0.07	0.01
Absolute direction error (°)	0.07	0.17	0.36*	-0.40**
Signed direction error (°)	0.10	0.14	0.43**	-0.35*

* $p < .05$ (two-tailed)

** $p < .01$ (two-tailed)

3.2 Mixed-model ANOVAs / ANCOVAs

Findings from the 2 (sex) x 2 (strategy group) x 2 (outbound path category) mixed-model ANOVAs / ANOCOVAs were reported below in terms of mean and random errors respectively. For ease of discussion, participants instructed on the continuous updating and configural updating strategies were hereafter referred to as *continuous updaters* and *configural updaters*, respectively.

To assess the hypotheses concerning the different patterns of strategy group differences across simple and complex paths, within-subjects effects posed by outbound path category and the interactions between outbound path category, strategy group, and sex were examined first – followed by between-group effects of sex, strategy group, and the interactions between sex and strategy group. All main and interaction effects related to mean and random errors were examined at a Bonferroni-corrected p -threshold of .017. This lower alpha level was set to control for inflated familywise error rates brought about by the analyses of four variables that constituted each error type.¹⁰

3.2.1 Within-subjects Main Effects and Interactions

With regard to all mean and random errors, all within-subjects effects of outbound path category did not reach significance ($ps > .017$). Likewise, there were no significant two-way or three-way interactions of outbound path category with strategy group and/or sex ($ps > .017$).

¹⁰ Due to inconsistent intercorrelations among the mean and random errors, respectively, in which signed errors did not correlate highly or significantly with absolute errors, composite error scores were not computed for the mean and random errors.

There was, however, a significant main effect with respect to response time, $F(1, 46) = 6.04$, $p = .018$, partial $\eta^2 = .116$, with participants taking slightly more time, on average, during homebound travel over simple paths [$M(SE) = 9.88(0.34)$] than over complex paths [$M(SE) = 9.60(0.34)$]. This finding can be explained by the fact that the termini of two simple paths (paths t1a and tb, see Fig. 6C) were positioned further away from the start as compared to the termini of the complex paths.

3.2.2 Between-group Main Effects and Interactions

3.2.2.1 Mean Errors and Response Time

There were significant interactions between strategy group and sex with regard to (i) homing distance, (ii) signed distance, and (iii) absolute direction mean errors ($ps < .017$). There were no significant interactions associated with signed direction mean error and mean response time ($ps > .05$). Similarly, all main effects concerning strategy group and sex were non-significant ($ps > .017$). Table 6 shows a statistical summary of all between-group main and interaction effects derived from mean errors and mean response time after controlling for relevant covariate effects.

3.2.2.2 Random Errors

There was a significant interaction between strategy group and sex with respect to homing distance random error only ($p = .016$). The interaction effects associated with (i) signed distance and (ii) signed direction random errors approximated significance ($p \leq .034$). All remaining interaction and main effects were either non-significant ($ps > .017$) or did not approach significance ($ps > .05$). Table 7 shows a statistical summary of all between-group main and interaction effects derived from random errors after controlling for relevant covariate effects.

Table 6

Main, Interaction, and Covariate Effects derived from the Group Variables of Strategy and Sex in terms of Four Mean Error Measures and Mean Response Time

Mean measure	Strategy	Sex	Sex x Strategy	Joystick speed test time	Total strategy effectiveness
1. Homing distance error (virtual m) ^a					
<i>F</i> (1, 45)	0.37	1.76	10.01**	9.48**	
<i>p</i> -value	.547	.191	.003	.004	
Partial η^2	.008	.038	.183	.182	
2. Signed distance error (virtual m)					
<i>F</i> (1, 46)	2.01	0.02	9.05**		
<i>p</i> -value	.163	.885	.004		
Partial η^2	.042	< .001	.164		
3. Absolute direction error (°) ^b					
<i>F</i> (1, 44)	0.54	3.59	6.86*	10.57**	2.82
<i>p</i> -value	.466	.065	.012	.002	.100
Partial η^2	.012	.075	.135	.194	.060
4. Signed direction error (°)					
<i>F</i> (1, 46)	0.74	0.09	0.90		
<i>p</i> -value	.395	.90	.347		
Partial η^2	.016	.002	.019		
5. Response Time (s)					
<i>F</i> (1, 46)	3.06	0.38	0.99		
<i>p</i> -value	.087	.539	.324		
Partial η^2	.062	.008	.021		

Note. ^a Controlled for the covariate effect of joystick speed test time.

^b Controlled for the covariate effects of joystick speed test time and total strategy effectiveness.

* $01 < p < .05$

** $p < .01$

Table 7

Main, Interaction, and Covariate effects derived from the Group variables of Strategy and Sex in terms of Four Random Error Measures

Mean measure	Strategy	Sex	Sex x Strategy	Joystick speed test time	Total strategy effectiveness
1. Homing distance error (virtual m) ^a					
<i>F</i> (1, 45)	0.15	3.67	6.28**	9.30**	
<i>p</i> -value	.697	.062	.016	.004	
Partial η^2	.003	.075	.122	.171	
2. Signed distance error (virtual m)					
<i>F</i> (1, 46)	1.44	1.29	4.78*		
<i>p</i> -value	.237	.262	.034		
Partial η^2	.030	.027	.094		
3. Absolute direction error (°) ^b					
<i>F</i> (1, 44)	.194	3.80	3.16	7.49**	5.47*
<i>p</i> -value	.662	.058	.083	.009	.024
Partial η^2	.004	.080	.067	.146	.111
4. Signed direction error (°) ^b					
<i>F</i> (1, 44)	0.54	3.02	4.98*	3.44	4.92*
<i>p</i> -value	.468	.089	.031	.070	.032
Partial η^2	.012	.064	.102	.071	.101

Note. ^a Controlled for the covariate effect of joystick speed test time.

^b Controlled for the covariate effects of joystick speed test time and total strategy effectiveness.

* $01 < p < .05$

** $p < .01$

3.2.2.3 Post-hoc Analyses of Strategy x Sex Interactions

Independent t tests were conducted following the significant strategy x group interactions for both mean and random errors. With covariate(s) involved, the group means and standard errors in the pairwise comparisons were adjusted for the covariate effect(s). Alpha was Bonferroni-corrected to .025 when assessing the significance of each simple main effect.

Overall, the t tests showed that all significant findings ($ps \leq .025$) were derived from two types of comparisons – between (i) female continuous updaters and female configural updaters, and between (ii) female configural updaters and male configural updaters. Table 8 shows a statistical summary of these two comparisons in terms of both mean and random error types for each of the four sets of errors.

Among female participants, configural updaters committed significantly larger mean errors than continuous updaters in terms of (i) homing distance ($p = .003$) and (ii) signed distance ($p = .006$) [see Table 8, Figs. 12A and 12B]. The same group difference approached significance with regard to (i) absolute direction mean errors ($p = .035$) [see Fig. 12C] and (ii) signed distance random error ($p = .037$) [see Fig. 13B]. Additional post-hoc testing showed that this simple strategy group effect among female participants was *not* present with any other differences between the same two groups in terms of any survey/pretest variables; these group differences were all non-significant [$ps > .05$].

Between the sexes, female configural updaters committed significantly larger mean errors than male configural updaters in terms of (i) homing distance ($p = .003$) and (ii) absolute direction ($p = .003$) [see Table 8, Figs. 12A and 12C]. The same significant trends were also obtained from the analyses of random errors in terms of (i) homing distance ($p = .003$) and (ii) signed direction ($p = .003$) [see Table 8, Figs. 13A and 13C]. With regard to signed distance

mean and random errors, the performance differences between the sexes were very close to significance ($ps = .027$ for both error types) [see Table 8, Figs. 12B and 13B].

Additional post-hoc testing involving the survey/pretest variables showed that male configural updaters reported higher computer experience [$M (SE) = 17.53 (2.39)$] than female configural updaters [$M (SE) = 13.82 (3.16)$], $t (24) = 3.42$, $p = .004$, $M (SE)_{\text{Difference}} = 3.72 (1.73)$. This difference did not confound the pre-existing group differences in path integration performance as computer experience did *not* correlate significantly with any mean or random error measure among configural updaters [$rs (26) > .16$, $ps > .42$].

3.2.2.4 Catch Trial Performance Difference between Male and Female Configural Updaters

As male and female configural updaters differed significantly in path integration performance, their accuracy scores over the four configural updating catch trials were further examined for potential sex and correlational effects. The catch trial accuracy of male configural updaters [$M (SE) = 3.07 (0.21)$] was found to be higher than that of female configural updaters [$M (SE) = 2.36 (0.31)$], but the difference did not reach significance, $t (24) = 1.97$, $M (SE)_{\text{Difference}} = 0.70 (0.36)$, p (two-tailed) = .061. Female configural updaters performed above the 50 % accuracy mark. Moreover, the mean accuracy scores from all configural updaters did not correlate significantly with any navigational error type (both mean and random), either with or without the effect of sex controlled for ($ps > .05$).

Table 8

Post-hoc Independent t test Statistics comparing Female Configural Updaters with Female Continuous Updaters and Male Configural Updaters

Measure	Error type	Female configural updaters > Female continuous updaters			Female configural updaters > Male configural updaters		
		<i>M</i> (<i>SE</i>) _{Difference}	<i>t</i> (20)	<i>p</i> -value (two-tailed)	<i>M</i> (<i>SE</i>) _{Difference}	<i>t</i> (20)	<i>p</i> -value (two-tailed)
1. Homing distance error (virtual m)	Mean	4.33 (1.73)	2.51**	.003	5.19 (1.60)	3.25**	.003
	Random	1.47 (0.77)	1.93	.068	2.30 (0.72)	3.22**	.004
2. Signed Distance error (virtual m)	Mean	6.67 (2.17)	3.08**	.006	4.75 (2.02)	2.36 [†]	.027
	Random	3.35 (1.48)	2.26 [†]	.035	3.24 (1.38)	2.35 [†]	.027
3. Absolute direction error (°)	Mean	19.48 (2.23)	2.23 [†]	.037	24.69 (8.09)	3.27**	.003
4. Signed direction error (°)	Random	21.08 (10.19)	2.07	.052	27.20 (9.45)	2.88**	.008

Note. Post-hoc *t* tests were performed on the corrected means (*M*) and standard errors (*SEs*) of the dependent measures, whichever relevant.

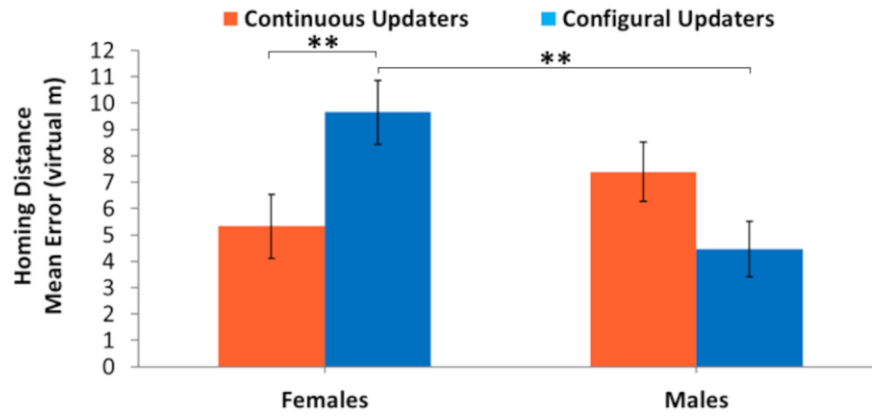
Statistical findings were not presented for absolute direction random error and signed direction mean error due to non-significant strategy x sex interactions (*ps* > .05; as shown in Tables 6 and 7).

[†] .025 < *p* < .05

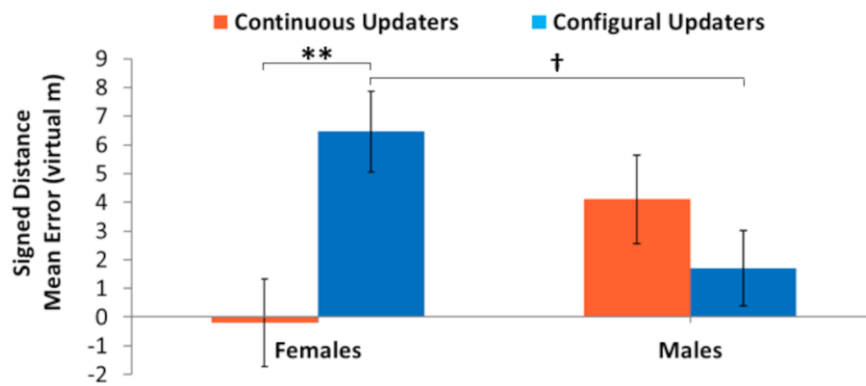
* .01 < *p* < .025

** *p* < .01

A.



B.



C.

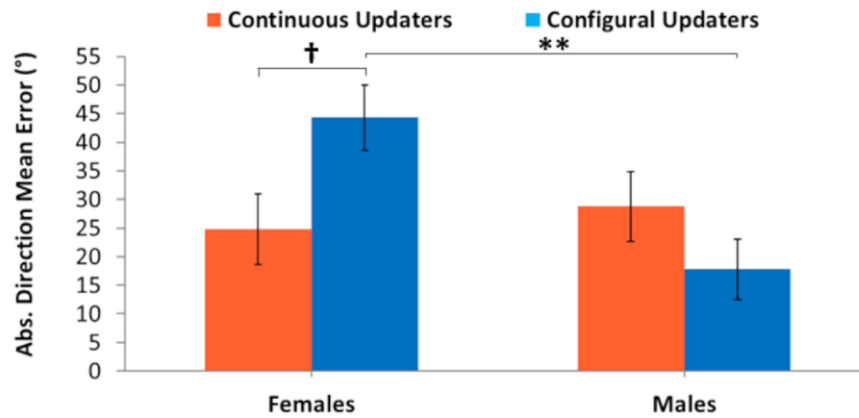
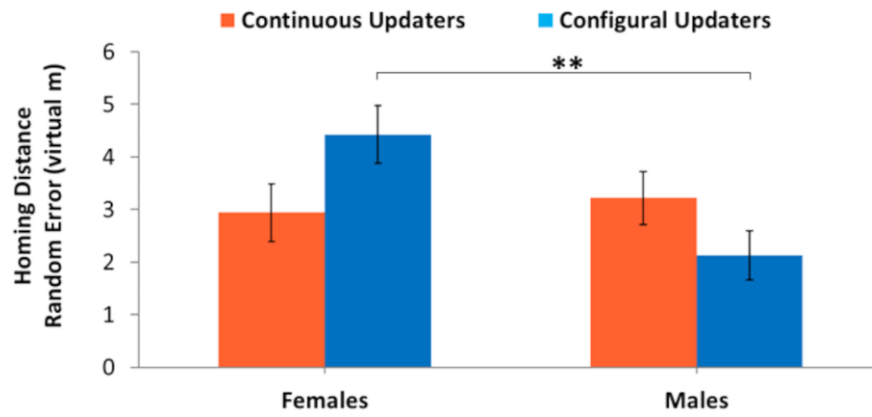


Fig. 12. Comparisons of continuous and configural updaters categorized by sex based on mean errors related to (A) homing distance, (B) signed distance, and (C) absolute direction.

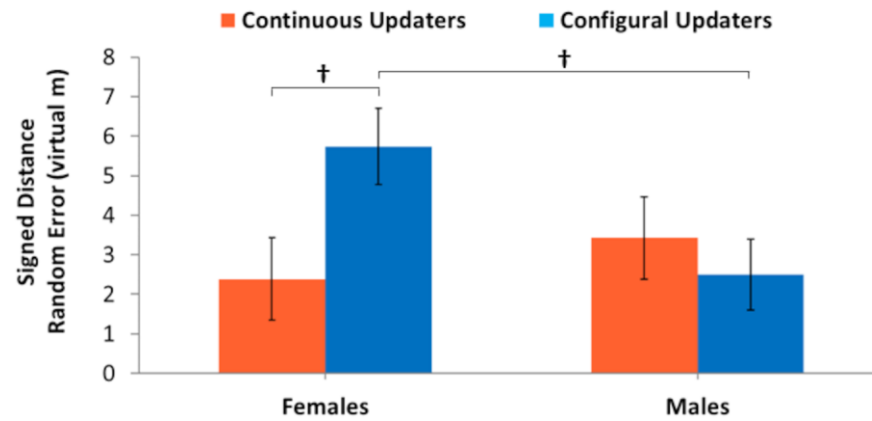
† .025 < p < .05

** p < .01

A.



B.



C.

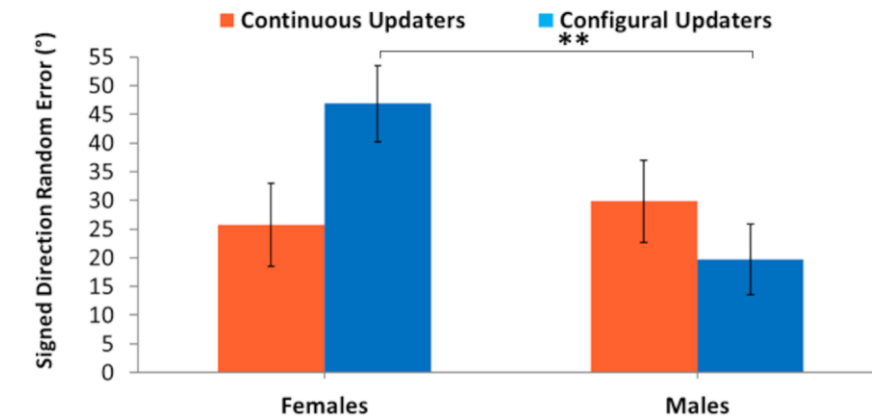


Fig. 13. Comparisons of continuous and configural updaters categorized by sex based on random errors related to (A) homing distance, (B) signed distance, (C) signed direction, Abs. = Absolute.

† .025 < p < .05

** p < .01

CHAPTER 4

EXPERIMENT 1

DISCUSSION

The current experiments investigated differences in visual path integration performance based on two different types of spatial strategies and assessed whether these strategies could be associated with distinct patterns of performance over simple and complex outbound paths. With regard to all mean and random error measures, there were no main effects of strategy group, sex, or outbound category, and neither strategy group nor sex interacted significantly with outbound path category. However, there were significant interactions between strategy group and sex with regard to six error measures: homing and signed distance errors (both mean and random), absolute direction mean error, and signed direction random error. Post-hoc analyses of these six error measures showed that all interactions were mainly characterized by female configural updaters exhibiting significant (or marginally significant) and consistently poorer performance than male configural updaters. Specifically, in terms of mean errors, female configural updaters exhibited larger distance (both homing and signed) and absolute direction errors than male configural updaters. In terms of random errors, female configural updaters exhibited larger distance (both homing and signed) and signed direction errors than male configural updaters. These two sets of findings showed that when compared with male configural updaters, the path integration performance of female configural updaters was not only poorer on average, but also more inconsistent.

It is important to note that these relatively consistent sex differences in path integration performance should *not* be interpreted as an inability or failure on the part of female configural updaters at implementing configural updating, since female configural updaters demonstrated comparable performance as their male counterparts on the catch trials. Instead, these findings could perhaps be best understood with reference to the extant literature on sex differences in spatial abilities, which provides numerous cases of a male advantage in allocentric spatial processing during navigation. For examples, males have been shown to outperform females in finding Euclidean paths or shortcuts to target locations (Boone, Gong, Hegarty, 2018; Rahman, Sharp, McVeigh, & Ho, 2017; Silverman et al., 2000), in utilizing cardinal/compass directions for spatial orientation and wayfinding (Dabbs et al., 1998, Lawton, 1994, 1996; Malinowski & Gillespie, 2001; Ward, Newcombe, & Overton, 1986), and in map reading and terrain visualization (Malinowski & Gillespie, 2001). Within the context of the current path integration task, which presented optic flow in a desert-like virtual environment without any landmarks during behavioral testing, it is highly likely that female configural updaters were challenged by integrating disparate visual information related to different path segments and turns into a coherent allocentric or schematic representation. Notably, this interpretation supports previous findings which showed that sex effects concerning virtual navigational performance were relatively large and robust, with males outperforming females, when there were no landmarks to cue participants about their whereabouts or about the goal location (Andersen, Dahmani, Konishi, & Bohbot, 2012). Recent findings by Harris, Scheuringer, and Pletzer (2019) also support this view that allocentric spatial processing pose challenges for females, such that during wayfinding in

a virtual town, the magnitudes of sex differences were larger, with significantly more accurate performance for males, when participants were instructed to adopt an allocentric Euclidean strategy (i.e., focusing on compass directions and path lengths) as compared to an egocentric landmark strategy (i.e., focusing on body-centered turns and salient distal landmarks).

Furthermore, these challenges associated with allocentric imagery and encoding might have been exacerbated by the lack of proprioceptive and kinesthetic cues that are generally made available through physical locomotion. Such somatosensory information has been shown to contribute to path integration by numerous previous studies (e.g., Adamo et al., 2012; Chance, Gaunet, Beall, & Loomis, 1998, Klatzky et al., 1990, 1998; Kearns, Warren, Duchon, & Tarr, 2002; Loomis et al., 1993, 1999; Philbeck et al., 2001) – specifically by supplementing (Adamo et al., 2012; Klatzky et al., 1998; Philbeck et al., 2001) or dominating over visual information (Kearns et al., 2002) when making homing responses of relatively high accuracy. Critically, a recent study by Coutrot et al. (2019) comparing path integration performances between real-world and virtual environments showed that real-world path integration generated smaller sex effect, supporting the current suggestion that an extra availability of idiothetic self-motion cues may help to minimize sex differences in path integration. To verify this possibility, it may be worthwhile for future studies to expose male and female configural updaters to varying amounts of idiothetic self-motion cues – in addition to visual cues.

In addition to these performance differences between male and female configural updaters, there were significant differences between female continuous and configural updaters with respect to mean distance errors (both homing and signed). However, unlike

the sex differences among the configural updaters, these prominent strategy group differences among the female participants did not extend equally well to mean direction errors and random errors. Consequently, it cannot be confirmed that continuous updating strategy use elicited better performance, in general, than configural updating strategy use in the current sample of female participants.

Nevertheless, it remains possible that continuous updating facilitated the tracking of homebound distances and estimations of the starting location in a way that aligned with a female preference for egocentric strategies. Such strategies incorporate spatial processing from the egocentric (first-person) perspective (Gramann et al., 2005; He & McNamara, 2018; Zhong, 2011, 2013; Zhong & Kozhevnikov, 2016) and generally concern the execution of repetitive navigational responses at familiar places/locations (e.g., Lawton, 1994, 1996; Sandstrom et al., 2002; Zhong, 2011, 2013; Zhong & Kozhevnikov, 2016) and attention to salient or goal-relevant landmark cues [e.g., Lawton, 1994, 1996; Sandstrom et al., 1998; Saucier et al., 2002; Schmitz, 1999; Zhong, 2011, 2013; Zhong & Moffat, 2016). In view of such navigational mechanisms, it seems conceivable that female participants were better at encoding the starting location and initiating repetitive or relatively consistent translational movements back to it from an egocentric perspective that was concomitant with continuous updating than from an allocentric perspective that was concomitant with configural updating.

Lastly, within-subjects analysis showed that all participants, regardless of strategy group, did *not* commit more mean or random errors over complex paths than over simple paths. For both continuous and configural updaters, these findings highlighted that the shape of the outbound path is of minor import in affecting the commission of distance

and direction errors. While these null effects supported the hypothesis that continuous updaters' performance would commit errors of relatively equal proportions across outbound paths of varying complexity (Loomis et al., 1999), they did *not* support the hypothesis that configural updaters would exhibit poorer performance when transitioning from simple paths to complex paths. This suggests that configural updating during visual path integration may not be as context-dependent as it was hypothesized to be – as inferred from real-world path integration studies that gave participants ready access to idiothetic self-motion cues (e.g., Fujita et al., 1993; Klatzky et al., 1990; Loomis et al., 1999; Philbeck et al., 2001; Wiener et al., 2011). As mentioned above, access to such self-motion cues may be a crucial factor that determines how well configural updating is implemented. To my knowledge, it is currently unknown as to how idiothetic self-motion cues can contribute to configural updating strategy use – in addition to visual cues – when traversing paths of varying complexity. Thus, future path integration studies can consider investigating how changes in the types and amounts of idiothetic self-motion cues could facilitate (or hinder) configural updating strategy use across paths of varying complexity.

In summary, findings from this experiment did *not* support previous studies showing that configural updating strategy use contributed to greater performance accuracy over continuous updating strategy use (He & McNamara, 2018; Wiener et al., 2011). However, sex was found to be a significant moderator of strategy use, suggesting that sex differences in egocentric and allocentric spatial information processing are important considerations in the implementation of continuous and configural updating strategies.

CHAPTER 5

EXPERIMENT 2

METHODS

5.1 Participants

38 participants (14 females) who completed Experiment 1 [M (SD) age = 20.78 (3.63); age range: 18 – 38] participated in the fMRI experiment, which occurred *directly* after in-lab testing. There were 19 participants (7 females) in each strategy group. Table 9 shows the demographic details and survey/pretest measures from these returning participants categorized by the two strategy groups they belonged to. The two groups did not differ significantly on any of these measures ($ps > .05$).

Table 9

Descriptive Statistics of the Demographic and Survey/Pretest Variables of Continuous and Configural Updaters who underwent fMRI Scanning

Survey/Pretest variable	Continuous Updaters (<i>n</i> = 19)			Configural Updaters (<i>n</i> =19)			Difference (Continuous – Configural)	
	<i>M</i> (<i>SD</i>)	<i>Min.</i>	<i>Max.</i>	<i>M</i> (<i>SD</i>)	<i>Min.</i>	<i>Max.</i>	<i>M</i> (<i>SE</i>)	95% CI
Age	20.84 (4.40)	18	38	20.74 (2.79)	18	28	0.10 (1.20)	[-2.32, 2.53]
Sex (% females)	37	-	-	37	-	-	-	-
Spatial anxiety	20.53 (6.85)	9	33	18.84 (6.78)	9	29	1.68 (2.21)	[-2.80, 6.17]
Computer experience	15.74 (3.41)	9	21	16.05 (2.74)	11	19	-0.31 (1.00)	[-3.02, 3.44]
Ishihara color blindness	13.61 (1.72)	6.5	14	13.11 (2.69)	5	14	0.50 (0.73)	[-0.98, 1.98]
Mars contrast sensitivity	1.86 (0.05)	1.80	1.92	1.85 (0.05)	1.80	1.92	0.01(0.02)	[-0.02, 0.04]
Joystick speed test (s)	65.89 (4.37)	59	73	65.68 (6.38)	57	78	0.21 (1.59)	[-0.02, 0.04]
Total strategy effectiveness	12.74 (3.60)	3	18	12.95 (2.50)	7	18	-0.21 (1.01)	[-2.25, 1.83]

5.2 Experimental Design

The path integration trials for the fMRI session featured repeated travel over a separate set of eight outbound paths (see Fig. 6D). These new trials were intended to ensure that the patterns of neural activations detected would be strategy-specific in nature and not be attenuated by over-learning or habituation stemming from exposure to a previously learned set of trials.

As for the fMRI experimental protocol, it followed a *compound event-related* paradigm aimed at separating trials incurring two or more distinct processes/responses (e.g., sensory, cognitive, motor) [i.e., *compound trials*] from trials incurring an initial subset of such processes (i.e., *partial trials*) [see Ollinger, Shulman, & Corbetta, 2001a, 2001b]. In the context of this experiment, compound trials pertained to the full path integration trials (as performed in the lab) that involved both outbound and homebound paths, whereas partial trials pertained to the trials that involved the outbound paths only. The delineation of these two types facilitating an assessment of the brain regions involved in visuospatial processing during both phases of outbound and homebound travel.

The time courses of BOLD responses to the outbound and homebound paths were estimated using a General Linear Model (GLM) that made no *a priori* assumption about the shape of the hemodynamic response function (HRF) [Ollinger et al., 2001a, 2001b; Shulman et al., 1999; Wheeler et al., 2006]. This GLM involved: (i) varying lengths of intertrial intervals (ITIs) [i.e., jittering], which increased the level of accuracy in estimating the shape parameters of the HRF through the sampling of more points on the

HRF compared with using a fixed-ITI design (see Dale & Buckner, 1997), and (ii) mixing of partial and compound trials, which ensured that participants were unable to predict the onset of particular trial type.

Specifically, the ITIs were set to vary between 1 to 3 frames of MR acquisition as Monte Carlo simulations performed using measured data from a rapid-event related experiment (Ollinger et al., 2001a) have shown that this range elicited relatively low mean variance, root-mean-squared error of the variance, and root-mean-squared correlations among points in the estimated time courses (Ollinger et al., 2001b). The same pattern of results was produced when the fraction of partial trials was kept between 25% and 40% (Ollinger et al., 2001b). In conjunction, having short ITIs and a moderately low partial trial fraction showed that the time courses of BOLD responses to different cognitive processes could be differentiated from each other. Consequently, the partial trial fraction in this experiment was set at 25%, in consistency with the common practice of previous fMRI studies (e.g., Shulman et al., 1999; Wheeler et al., 2006),

5.3 Procedure

5.3.1 Pre-scan Practice in a Mock fMRI Scanner

Before entering the fMRI scanner proper, the participants were told to continue using the *same* strategy that they applied previously during in-lab practice and testing. They were told that the path integration trials were different from the trials they experienced earlier and that the time-limit for making homebound movements was shortened from 20 to 10 seconds. This served to avoid excessive signal dropouts over

long durations and to insure an acceptable level of signal-to-noise ratio (Murphy, Bodurka, & Bandettini, 2007).

The practice task in the mock scanner featured 16 trials that were mixed based on a randomized sequence. The participants experienced four partial trials that presented the motion of the outbound journey only over two simple paths (paths 1a and 1d, see Fig. 6D) and two complex paths (paths 2a and 2d, see Fig. 6D), and 12 compound trials that involved a threefold repetition of the presentation of the same four paths. These 16 trials were mixed based on a random sequence. The ITIs featured static scenes (each with a fixation cross) identical to those presented during in-lab testing. The ITIs were distributed exponentially such that shorter ITIs occurred more frequently than longer ITIs (Dale, 1999; Wheeler et al., 2006). 60% of ITIs had a delay of one TR, 30% of ITIs had a delay of two TRs, and 10% had a delay of three TRs.

After completing the task, the participants completed a Simulator Sickness Questionnaire (SSQ) [Kennedy, Lane, Berbaum, & Lilienthal, 1993]. This served to identify any participants who felt dizzy or nauseous following mock scanning and who did not want to proceed with fMRI scanning. All participants gave ratings that approximated zero on average, indicating the absence of any discomforts, and went on to complete their assessment in the fMRI scanner.

5.3.2 *fMRI Scanning Session*

Before entering the fMRI scanner, the participants were reminded to keep on applying the same strategy they applied thus far. In the scanner, they performed two runs of 32 path integration trials, each with six partial trials, which made up 25% of the total number of trials. During the break between the two runs, the participants were reminded again (through the microphone) to consistently apply the same strategy in all trials. In each run, the eight partial trials presented passive travel on all the eight outbound paths (Fig. 6D) while the remaining 24 compound trials presented each outbound path three times, along with the homebound phase. A different random sequence was applied to these 32 trials in each run. In total, each participant performed 64 trials: 16 partial trials and 48 compound trials.¹¹ The exponential distribution of the ITIs, as well as the durations of outbound and homebound travel, were identical to those implemented in the mock scanner.

5.3.2.1 Image Acquisition

Brain images were collected at the Georgia State / Georgia Tech Center for Advanced Brain Imaging (CABI) by a 3 Tesla Siemens TIM Trio Magnetic Resonance Imaging system (Siemens Medical Solutions, Erlangen, Germany) with a 12-channel head coil. Whole-brain structural images were acquired in the sagittal plane using a T1-weighted multi-echo magnetization-prepared rapid gradient-echo (ME-MPRAGE) sequence (TR = 2530 ms, TE₁₋₄ = 1.76 ms - 7.32ms, field of view = 256 mm, voxel size =

¹¹ Note that the number of compound trials matched the number of path integration trials experienced in-Experiment 1.

1.0 mm x 1.0 mm x 1.0 mm, flip angle = 7° , slice no. = 176; slice thickness = 1.00 mm).

Whole-brain multiband accelerated echo planar imaging (EPI) with BOLD contrast was used to collect functional data in the transverse plane. Images were acquired in 60 interleaved oblique slices based on a multiband acceleration factor of 2 over two 11.5 min runs (TR = 2000 ms, TE = 30.0 ms, field of view = 256 mm, voxel size = 2.0 mm x 2.0 mm x 2.0 mm, flip angle = 77° , slice thickness = 1.00 mm).

CHAPTER 6

EXPERIMENT 2

RESULTS

Experiment 2 aimed at differentiating the patterns of brain activations between 19 continuous updaters and 19 configural updaters who completed Experiment 1. No participant reported any nausea or dizziness after fMRI scanning and hence data from all participants were retained for analyses. As examining sex differences in brain activations was not an *a priori* aim, the behavioral and fMRI analyses below focused on comparing the two strategy groups and the two types of path categories (simple versus complex). Nevertheless, sex differences among configural updaters, and strategy group differences among female participants, were analyzed in order to supplement the corresponding significant findings derived from Experiment 1 (see subsection 5.1.3).

6.1 Behavioral Data Analysis

Behavioral performance between continuous updaters and configural updaters over simple and complex outbound paths were analyzed in terms of all mean and random error types, as well as mean response time. Mixed-model ANOVAs / ANCOVAs were conducted with the independent variables set as strategy group (2) and outbound path category (2). Behavioral data from equal numbers of simple and complex path trials ($n = 32$ per path category) were recorded from participants across both fMRI runs.

6.1.1 Covariate Selection

Similar to Experiment 1, an assessment of potential covariates was performed before conducting the mixed-model analysis. After controlling for the effect of strategy group, *total strategy effectiveness* emerged as the only variable exhibiting significant and negative partial correlations with the navigational error measures ($ps < .05$). Specifically, it correlated significantly with four error measures: [(i) homing distance mean error [$r(35) = -.47, p = .004$]; (ii) absolute direction mean error [$r(35) = -.43, p = .008$]; (iii) absolute direction random error [$r(35) = -.39, p = .018$]; and (iv) signed direction random error [$r(35) = -.40, p = .014$]. Consequently, total strategy effectiveness was entered as a covariate into the ANOVA models that contained these four error measures as dependent variables.

6.1.2 Main Effects of Strategy Group and Path Category

With alpha set at .017 after Bonferroni-correction for each set of mean and random errors, there was a marginally significant strategy group effect with respect to signed distance mean error only, $F(1, 36) = 4.20, p = .048$, partial $\eta^2 = .104$, with continuous updaters [$M(SE) = 1.99(0.64)$] committing larger errors than configural updaters [$M(SE) = 0.13(0.64)$]. As for within-subjects main effects, they were significant – with relatively larger errors committed over complex paths – in terms of (i) homing distance and (ii) signed distance mean errors [$ps < .017$ (Bonferroni-corrected)]. There was also a marginally significant effect with respect to absolute direction mean error, with larger errors committed over complex paths. ($p = .027$) [see Table 10]. All

remaining main and interaction effects related to signed direction mean error, and all four random error measures, were not significant ($ps > .05$).

Moreover, with alpha set at the default of .05 in the analysis of mean response time, there was also a marginally significant strategy group effect, $F(1, 36) = 3.30$, $p = .077$, partial $\eta^2 = .084$, with configural updaters [$M(SE) = 9.10(0.34)$] taking more time than continuous updaters [$M(SE) = 8.23(0.34)$] during homebound travel.

Furthermore, with regard to the ANCOVAs of homing distance and absolute direction mean errors that showed significant within-subjects main effects, ANOVAs were performed to examine whether these effects remained significant after excluding total strategy effectiveness as covariate. These ANOVAs showed that the within-subjects effects involving homing distance and absolute direction mean errors remained significant ($ps < .05$) [see Table 10]. These additional statistical tests served the purpose of complementing the analysis of fMRI data, which was done without the inclusion of any covariates.

6.1.3 Sex Differences in Performance among Configural Updaters

As male and female configural updaters differed significantly in path integration performance in Experiment 1, the performance differences between them were re-examined in Experiment 2 with regard to all mean and random error measures after controlling for the relevant covariate effect of total strategy effectiveness.

With alpha set at .025 (Bonferroni-corrected), signed distance random error emerged as the only measure that yielded a significant performance difference. Specifically, female configural updaters exhibited larger signed distance random errors

[$M (SE) = 2.85 (1.05)$] than male configural updaters [$M (SE) = 2.19 (0.61)$], $F (1, 17) = 8.89$, $p = .008$, partial $\eta^2 = .343$.

The same trend was observed, albeit marginally significant, among configural updaters with regard to homing distance random error [females: $M (SE) = 2.58 (1.13)$, males; $M (SE) = 1.65 (0.49)$; $F (1, 16) = 4.57$, $p = .048$, partial $\eta^2 = .222$], and absolute direction random error [females: $M (SE) = 24.19 (15.56)$, males; $M (SE) = 11.25 (5.96)$; $F (1, 16) = 4.97$, $p = .041$, partial $\eta^2 = .237$].

Sex differences between male and female configural updaters in terms of the remaining error types (i.e., all mean errors and signed direction random errors) were all non-significant ($ps > .05$). It is important to note that the null effects derived from mean errors could be attributed to low statistical power stemming from a small number of returning female configural updaters ($n = 7$).

6.1.4 Strategy Group Differences in Performance among Female Participants

Among female participants, with alpha set at .025, continuous and configural updaters did not differ significantly with regard to any mean or random error measures ($ps > .025$). The same trends applied to male participants ($ps > .025$). Once more, it is worth considering that the non-significant strategy group differences among female participants could be related to low statistical power associated with the small sample of returning female participants ($n = 7$ in each strategy group).

Table 10

Significant Within-subjects Effects derived from Outbound Path Category in terms of Mean Navigational Errors

	Measure	Error type	Covariate(s)	Simple <i>M (SE)</i>	Complex <i>M (SE)</i>	<i>M (SE)</i> Difference	<i>F</i> -value	<i>df</i> _{error}	<i>p</i> -value	Partial η^2
1.	Homing distance error (virtual m)	Mean ^a	-	4.92 (0.27)	5.47 (0.31)	0.55 (0.19)	8.67	35	.006	.198
			Total strategy effectiveness	-	-	-	10.20	35	.003	.226
		Mean ^b	-	4.92 (0.30)	5.47 (0.36)	0.55 (0.19)	8.89	36	.005	.198
2.	Signed distance error (virtual m)	Mean	-	0.82 (0.44)	1.30 (0.49)	0.48 (0.20)	5.82	36	.021	.139
3.	Absolute direction error (°)	Mean ^c	-	23.92 (2.21)	27.35 (2.79)	3.43 (1.49)	5.30	35	.027	.131
			Total strategy effectiveness	-	-	-	6.73	35	.014	.161
		Mean ^b	-	23.92 (2.49)	27.35 (2.98)	3.43 (1.47)	5.44	36	.025	.131

Note. ^a Controlled for the covariate effects of total strategy effectiveness.

^b Covariate(s) excluded from analysis.

^c Controlled for the covariate effect of total strategy effectiveness.

6.2 fMRI Data Analysis

6.2.1 Preprocessing of Single-subject Data

fMRI data for all participants were processed and analyzed using the *Analysis of Functional Neuroimages (AFNI)* software package [National Institute of Mental Health, National Institutes of Health; available at: <https://afni.nimh.nih.gov/download>]. The acquired brain images/volumes were first corrected for slice timing correction and realigned to the first image. Motion correction then followed by registering (i.e., realigning and unwrapping) the BOLD images to the average time-shifted image/volume in each run to correct for image distortions caused by susceptibility-by-movement interactions (Andersson et al., 2001). Fourier interpolation was applied to the heptic degree over two passes to reduce the voxel intensity differences between images to the smallest extent. Subsequently, the high-resolution T1 structural image from each participant was co-registered to the mean BOLD image created from slice timing correction and motion correction using AFNI's "align_epi_anat.py" script. These co-registered structural and BOLD images were then spatially normalized into standard Montreal Neurological (MNI) space and resampled during normalization to resolutions of 1 mm³ and 2 mm³ isotropic voxels, respectively, using AFNI's "@auto_tlrc" program. A resolution of 1 mm³ isotropic voxels was set for the structural images to ensure a high-resolution display of the anatomical regions. The structural images of participants from the two strategy groups were averaged, respectively, after normalization to act as underlays for displaying overlays of functional images collected from each group.

To identify task-related changes in the BOLD signal, the time courses of all trials were examined in a whole-brain analysis based on a within-trial model / GLM (Shulman et al., 1999) factored by navigational / path integration phase (*outbound* versus *homebound*) and path complexity (*simple* versus *complex*). This engendered four within-subjects conditions or navigational phases: (i) simple outbound (32 trials), (ii) complex outbound (32 trials); (iii) simple homebound (24 trials); and (iv) complex homebound (24 trials). The delineation of these four phases served the purpose of a fine-grained examination of the brain activations unique to each phase.

More importantly, as the compound/partial trial paradigm makes no *a priori* assumption about the shape of the HRF (Ollinger et al., 2001a, 2001b; Shulman et al., 1999), the recorded hemodynamic responses were modeled based on tent functions specified by AFNI's "3dDeconvolve" program. Before modelling began, the slice timing and motion corrected data was smoothed with a 6 mm FWHM Gaussian kernel. Upon executing the tent functions, the HRF shape and magnitude were computed, after stimulus onset, through the linear interpolation of hemodynamic responses at arbitrary timepoints separated by regular two-second intervals. Each interval spanned one TR.

From each participant, four sets of stimulus onset times, each referring to the start of one of the four navigational phases (as aforementioned), were entered as task regressors into the ANOVA model. These temporal regressors were accompanied by six motion regressors-of-no-interest that registered noise emanating from excessive head motion along the three axes/planes (xyz) of rotation and translation, respectively.

In addition, there were two general linear tests (GLTs), each under the outbound and homebound conditions, respectively, that subtracted simple path parameter estimates

from complex path parameter estimates (complex > simple). These GLTs generated contrast maps that conveyed the average BOLD signal change occurring within the outbound and homebound phases when switching from navigating simple paths to navigating complex paths (i.e., when path complexity increased).¹² For each participant, parameter estimates representing average signal change in each within-subjects condition, and from each GLT (i.e., difference scores of parameter estimates), were computed. All parameter estimates were converted to percent signal change (PSC) values to ensure standardized comparisons at the group level. These PSC values were corrected for the extraneous effect posed by the autocorrelation of temporal residuals from regression models via AFNI's "3dREML" program.

6.2.2 Group-level Random Effects Analysis

6.2.2.1 Whole-brain Analysis

AFNI's "3dttest++" program was used to examine BOLD signal changes during each navigational phase within each strategy group, as well as to compare such signal changes between the groups. To correct for multiple comparisons of activated voxels across the entire brain volume, cluster thresholding was conducted using AFNI's "3dClustSim" program based on a 10,000 iteration Monte Carlo simulation analysis on voxels within the group-level functional brain space (234,146 voxels). AFNI's

¹² The same type of contrast of activation patterns between outbound and homebound phases (of either simple or complex paths) was not performed because the within-trial analysis precludes a contrast of such qualitatively different events.

“3dFWHMx” program was used to compute the spatial autocorrelation function (ACF) parameters (representing the smoothness of the time series noise from all participants) for generating the random noise cluster fields spanning across the entire brain volume in the Monte Carlo simulation. Based on the analysis, the minimum number of voxels fulfilling a voxel-wise/height threshold of 0.01 and a cluster-level/extent threshold of 0.05 was found to be 343. This cluster size threshold was applied to all within- and between-subjects analyses at the whole-brain level.

6.2.2.2 Region-of-interest Analysis

In addition to the whole-brain analysis, a region-of-interest (ROI) analysis centered on the hippocampus proper and the entorhinal cortex was also performed with regard to the *a priori* expectations that the configural updaters and continuous updaters would differentially engage these two regions during the homebound phase. The Eickhoff-Zilles cytoarchitectonic probability maps/atlas (Eickhoff, Heim, Zilles, & Amunts, 2006; Eickhoff et al., 2005), supplied by AFNI’s “whereami” program, was used to specify two anatomical regions that circumscribed the hippocampus proper and the entorhinal cortex, respectively. The anatomical coordinates of these two ROIs were resampled to align with the coordinates of MNI functional space, which were standardized across participants. At the group level, whole-brain functional data from each participant (normalized into MNI space) were averaged and then circumscribed within the anatomical boundaries of these resampled ROIs to allow a close examination of activations in the entorhinal cortex and hippocampus.

To correct for multiple comparisons, the functional data circumscribed within both ROIs from all participants were combined, and cluster thresholded with AFNI's "3dClustSim" program based on a 10,000 iteration Monte Carlo simulation analysis on the total number of voxels within the combined ROI volume (1129 voxels). AFNI's "3dFWHMx" program was used to compute the spatial ACF parameters for generating the random noise cluster fields specific to the total ROI volume in the Monte Carlo simulation. Based on the analysis, the minimum number of voxels fulfilling a voxel-wise threshold of $p = .01$ and a cluster-wise threshold of $p = .05$ was found to be 23. This cluster size threshold was applied to all within- and between-subjects analyses encompassing the hippocampus and entorhinal cortex.

6.2.3 Whole-brain and ROI-based Activations and Deactivations in Configural and Continuous Updaters

6.2.3.1 Phase-specific Activations and Deactivations (Non-contrast-related)

Brain activations in each of the four navigational phases and the contrasts between complex and simple paths [complex > simple] during the outbound and homebound phases, respectively, were examined for each strategy group. The BOLD signal derived from each phase pertained to the average signal computed – via linear interpolation – after stimulus onset from all signals at regularly spaced timepoints (by one TR) spanning across the entire stimulus duration. In each phase, significant brain activations and deactivations were determined in relation to a functional baseline that was

modeled based on the entire time series, which comprised the onsets and durations of all phases (as derived from the temporal regressors).

As shown in Table 11, there were distinctive phase-specific regions of activation and deactivation in each strategy group. Figure 14 shows the sagittal views of some key brain regions (mainly in the prefrontal and parietal cortices) that were activated or deactivated during the outbound and homebound phases in each group. In both groups, the homebound journey experienced after traversing simple outbound paths yielded the highest number of activated / deactivated clusters.

During this simple homebound phase, configural updaters exhibited activations in the precuneus (BA 7) [see Fig. 14D] and postcentral gyrus (BA 3) – and deactivations in the middle temporal gyrus (BA 21) and inferior medial frontal gyrus (BA 11) [see Fig. 14C]. Continuous updaters exhibited activation in the inferior parietal lobule (BA 40) [see Fig. 14F] and deactivations in the superior temporal gyrus (BA 38; close to the temporal pole) and medial frontal gyrus (BA 10) [see Fig. 14E]. The activated and deactivated regions during this phase were lateralized to the left and right hemispheres, respectively, in both groups.

In the remaining three phases (i.e., simple outbound, complex outbound, complex homebound), only configural updaters exhibited activation in the left temporo-parietal junction (TPJ) – located at the posterior end of the middle temporal gyrus (BA 39 / 21) – during the outbound phases of both simple and complex paths [see Figs. 14A and 14B]. Continuous updaters did not exhibit any significant activations or deactivations in any of these three phases in both simple and complex paths.

6.2.3.2 Phase-specific Activations (Contrast-related)

As within-subjects differences in path integration performance were found in relation to path complexity, activation patterns from simple paths were contrasted against corresponding patterns from complex paths in the outbound and homebound phases, respectively, to examine if such behavioral differences were related to differences in the magnitudes of brain activations associated with each path type. An examination of these [complex > simple] contrasts showed significant activations during the homebound phase only (see Table 11). Configural updaters exhibited activation in the right inferior medial frontal gyrus (BA 11) [see Fig. 14G] whereas continuous updaters exhibited activation in the left entorhinal cortex (BA 28) [see Fig. 14H; see also Fig. 15, for a magnified view]. Significant entorhinal activation was found with reference to the minimum ROI cluster extent (23 voxels) satisfying the cluster-level threshold.

Both strategy groups further exhibited activations in the left hippocampus with clusters (one per group) that approached the minimum ROI cluster extent (see Fig. 16). These ROI-based hippocampal activations reached cluster-level significance (corrected $p \leq .05$) with the height threshold readjusted to a more liberal level of $p = .014$: 25 voxels for configural updaters and 23 voxels for continuous updaters.

To ensure that the peak voxels of activations observed at the group level resided within the anatomical boundaries of the entorhinal cortex and hippocampus in each participant, the group-averaged ROI functional data was further overlaid on the normalized structural image of each participant. The coordinates of these peak voxels were found to fall within the image space of the entorhinal cortex and hippocampus in each participant.

6.2.3.3 Between-group Comparisons of Whole-brain and ROI-based Activations (Non-contrast-related)

Between-group comparisons were performed to examine the extend to magnitudes of differences in brain activations between the two strategy groups. For this purpose, non-contrast-related PSC values representing the average BOLD signal specific to each of the four navigational phases were compared between the two strategy groups. At both the whole-brain and ROI levels of analyses, the comparison of configural updaters against continuous updaters in terms of these standardized parameter estimates did *not* reveal any cluster with significant higher (or lower) degrees of activation in the navigational phase of both simple and complex paths.

6.2.3.4 Between-group Comparisons of Whole-brain and ROI-based Activations (Contrast-related)

In addition to the between-group comparisons of phase-specific, non-contrast-related activations, PSC difference scores representing contrast-related activations [complex > simple] from both outbound and homebound phase were compared between the two strategy groups. At both the whole-brain and ROI levels of analyses, the comparison of configural updaters against continuous updaters in terms of these standardized difference scores did *not* reveal any cluster with significant higher (or lower) degrees of activation during either the outbound or homebound phase.

Table 11

Brain Activations / Deactivations in Configural and Continuous Updaters during each Navigational Phase

Path type / contrast	Phase	Region	BA	Side	Cluster size (voxels)	x	y	z	T
Configural Updaters									
Simple	Outbound	TPJ	39	L	516	-34	-60	24	5.40
	Homebound	Precuneus	7	L	786	-26	-62	34	5.76
		Middle temporal gyrus	21	R	738	66	-38	-8	-5.45
		Medial frontal gyrus	11	R	586	18	60	-10	-6.84
		Postcentral gyrus	3	L	545	-34	-30	54	5.47
Complex	Outbound	TPJ	39	L	363	-38	-62	28	5.00
Complex > Simple	Homebound	Medial frontal gyrus	11	R	347	4	50	-18	4.62
		Hippocampus ^a		L	18	-30	-12	-14	3.89 (n.s.)
Continuous Updaters									
Simple	Homebound	Medial frontal gyrus	10	R	1811	3	56	18	-6.10
		Inferior parietal lobule	40	L	636	-46	-36	40	5.40
		Superior temporal gyrus (near pole)	38	R	548	42	20	-18	-7.66
Complex > Simple	Homebound	Entorhinal Cortex	28	L	27	-18	-18	-26	4.22
		Hippocampus ^a		L	17	-24	-12	-20	3.83 (n.s.)

Note. TPJ = Temporo-parietal junction; n.s. = non-significant at a voxel-wise threshold of .01 and a cluster-wise threshold of .05.

^a Cluster-level significance reached with voxel-wise/uncorrected *p*-value readjusted to .014.

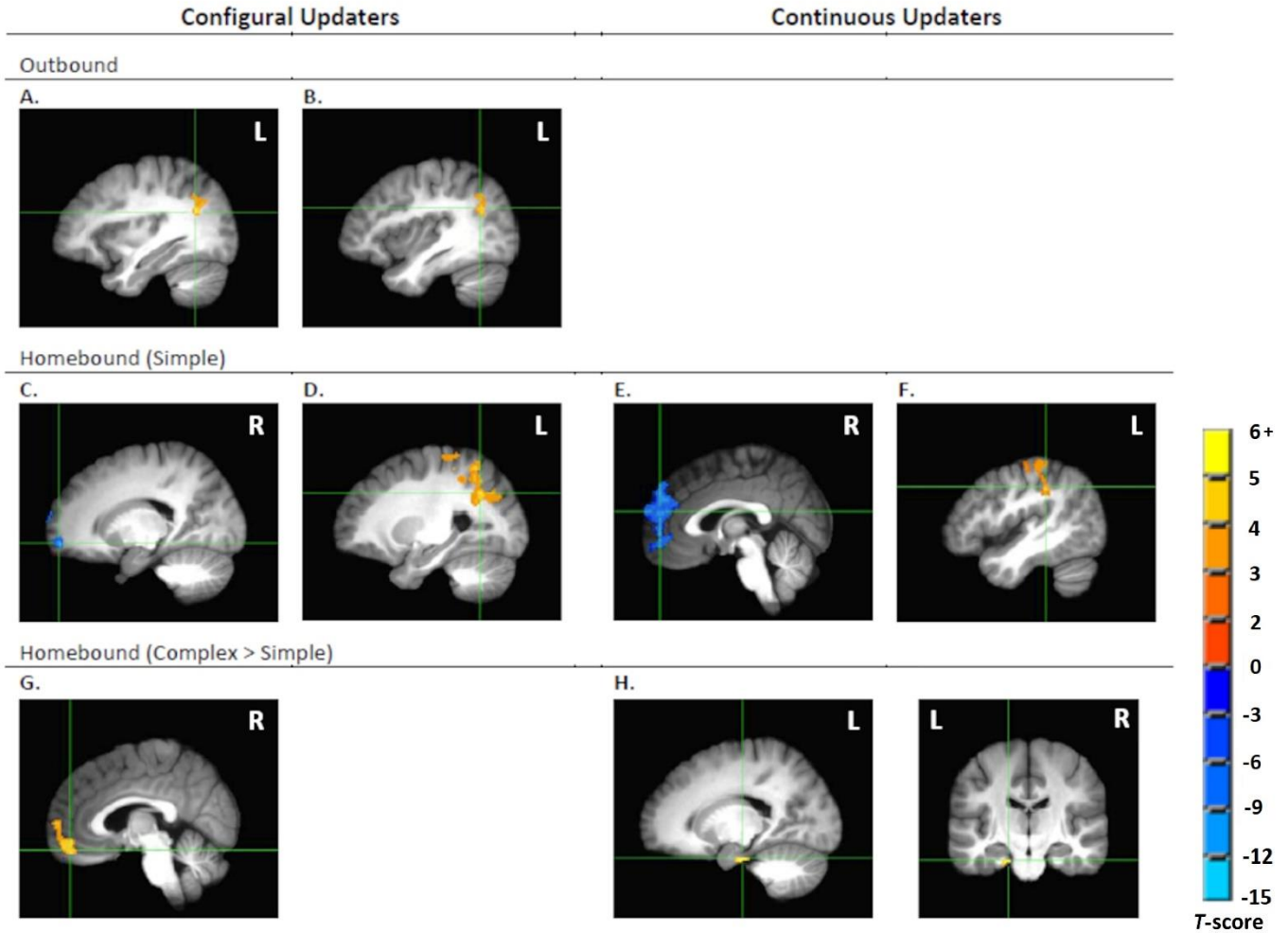


Fig. 14. Regions of activation and deactivation in configural and continuous updaters during the outbound and homebound phases. In each strategy group, activation images were superimposed on spatially normalized high-resolution T1-weighted image averaged across all group members. Configural updaters exhibited activations in the temporo-parietal junction during the simple (A) and complex (B) outbound phases. During the simple homebound phase, both groups exhibited deactivations in the medial frontal gyrus: (C) BA 11 (configural updaters) and (E) BA 10 (continuous updaters). As regards to activations in the same phase, they occurred in (D) the precuneus (BA 7) among configural updaters and in (F) the inferior parietal lobule (BA 40) among continuous updaters. When activations from the simple homebound phase were contrasted against activations from the complex homebound phase, (G) configural updaters exhibited activation in the inferior medial frontal gyrus (BA 11) while (H) continuous updaters exhibited activation in the entorhinal cortex (showing both sagittal and coronal sections). Cross hairs were centered on the peak voxel of activation / deactivation in each specified region. L = left hemisphere; R = right hemisphere.

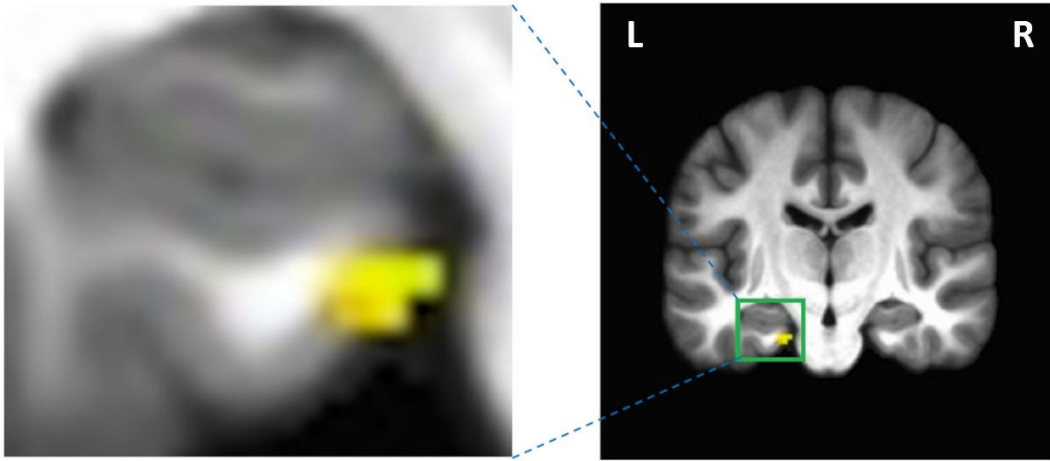
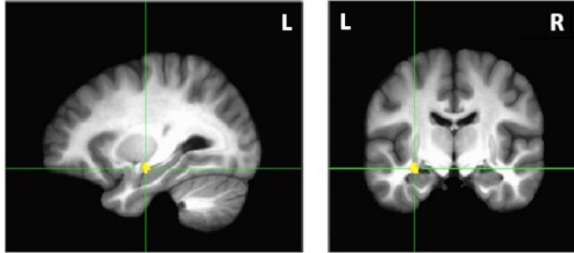


Fig. 15. Magnified coronal view of left entorhinal activation in continuous updaters derived from the contrast of activations between simple and complex homebound phases [complex > simple]. L = left hemisphere; R = right hemisphere.

Configural Updaters

A.



Continuous Updaters

B.

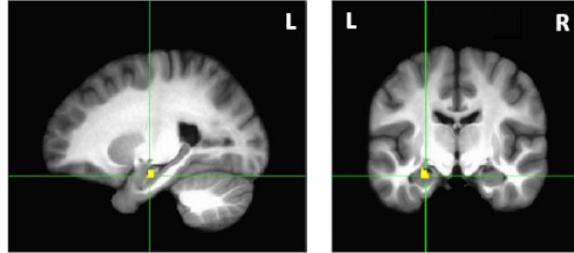


Fig. 16. Marginally significant clusters of activation in the left hippocampus in configural (18 voxels; **A**) and continuous (17 voxels; **B**) updaters derived from the contrast of activations between simple and complex homebound phases [complex > simple]. In each strategy group, activation images were superimposed on spatially normalized high-resolution T1-weighted image averaged across all group members. Both sagittal and coronal views are shown for each group. Cross hairs were centered on the peak voxel of activation in each specified region. L = left hemisphere; R = right hemisphere.

6.2.4 Brain-behavior Correlations

In addition to the within- and between-subjects analyses, the patterns of brain activations during the simple and complex homebound phases – from all participants ($n = 38$) and each strategy group ($n = 19$ per group) – were regressed against the navigational errors committed during the respective phases. Brain-behavior correlations were analyzed separately for simple and complex paths in view of significant within-subjects differences in homebound performance between these two path types (see behavioral findings above). The full set of eight error variables – homing distance, signed distance, absolute direction, and signed direction errors; incorporating both mean and random measures for each error type – were applied as parametric regressors.

In all correlational analyses at both whole-brain and ROI levels, the voxel-wise threshold was set at .01. The cluster-level threshold remained at 218 for the whole-brain analysis and 23 for the ROI analysis. Tables 12 and 13 list the relevant error measures that correlated significantly with the brain regions of concern according to simple and complex paths; Table 12 presents all positive correlations while Table 13 presents all negative correlations. Figures 17 and 18 show the regions that correlated significantly with these navigational error measures during the simple and complex homebound phases respectively.

Across all participants, during the simple homebound phase, larger homing distance mean errors were associated with higher activation in the left cuneus (see Fig. 17A) while larger signed distance random errors were associated with lower activations in the right precuneus (see Fig. 17B). During the complex homebound phase, larger signed direction random errors were associated with higher activations in the right

inferior frontal gyrus (BA 45 / 46) [see Figs. 18C and 18D] while larger absolute direction errors were associated with lower activations in the right anterior cingulate (see Fig. 18A) and left cuneus (see Fig. 18B).

Among configural updaters, during the simple homebound phase, larger signed direction mean errors were associated with higher activation in the right paracentral lobule (BA 4) [see Fig. 17C]. During the complex homebound phase, larger homing distance mean errors were associated with lower activation in the left inferior frontal gyrus (BA 47) [see Fig. 18E].

Among continuous updaters, during the simple homebound phase, larger signed distance random errors were associated with lower activation in the right precuneus (see Fig. 17D). During the complex homebound phase, larger signed direction mean errors were associated with lower activation in the left cuneus (see 18F).

Table 12

Positive Brain-behavior Correlations during the Homebound Phases of Simple and Complex Paths

Path type	Performance Measure	Region	BA	Side	Cluster size (voxels)	x	y	z	<i>T</i>
<i>All Participants</i>									
Simple	Homing distance mean error	Cuneus	18	L	383	-2	-78	20	3.89
Complex	Signed direction random error	Inferior frontal gyrus	46	R	650	48	40	6	5.53
			45	R	447	40	20	4	4.61
<i>Configural Updaters</i>									
Simple	Signed direction mean error	Paracentral lobule	4	R	349	2	-30	68	7.55

Note. There were no significant regions of activation that correlated positively with any error measures during the complex homebound phase among configural updaters and during both simple and complex homebound phases among continuous updaters.

Table 13

Negative Brain-behavior Correlations during the Homebound Phases of Simple and Complex Paths

Path type	Performance Measure	Region	BA	Side	Cluster size (voxels)	x	y	z	<i>T</i>
<i>All Participants</i>									
Simple	Signed distance random error	Precuneus	7	R	414	14	-48	38	-5.10
Complex	Absolute direction mean error	Anterior cingulate	32	R	519	4	38	-4	-4.39
		Cuneus	18	L	429	-10	-82	12	-4.55
<i>Configural Updaters</i>									
Complex	Homing distance mean error	Inferior frontal gyrus	47	L	757	-32	30	-2	-6.67
<i>Continuous Updaters</i>									
Simple	Signed distance random error	Precuneus	7	R	387	18	-52	46	-10.55
Complex	Signed direction mean error	Cuneus	18	L	752	-10	-86	16	-6.68

Note. There were no significant regions of activation that correlated negatively with any error measures during the simple homebound phase among configural updaters.

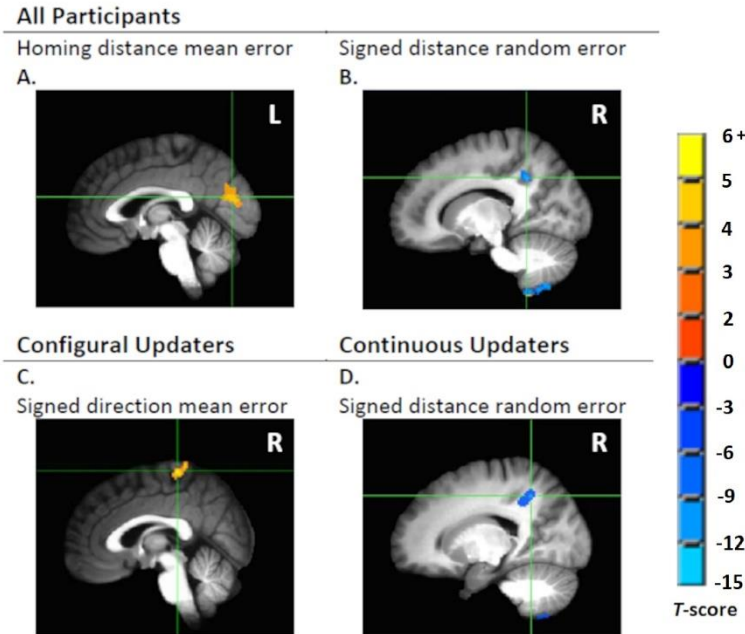


Fig. 17. Significant correlations between different types of navigational errors and the activation patterns from all participants, configural updaters, and continuous updaters during the simple homebound phase. In each of these three groups, activation images were superimposed on spatially normalized high-resolution T1-weighted images averaged across all group members. In all participants, **(A)** homing distance mean error correlated positively with activation in the cuneus (BA 18) while **(B)** signed distance random error correlated negatively with activation in the precuneus (BA 7). **(C)** In configural updaters, signed direction mean error correlated positively with activation in the paracentral lobule. **(D)** In continuous updaters, signed distance random error correlated negatively with activation in the precuneus (BA 7). Cross hairs were centered on the peak voxel of correlational strength in each specified region. L = left hemisphere; R = right hemisphere.

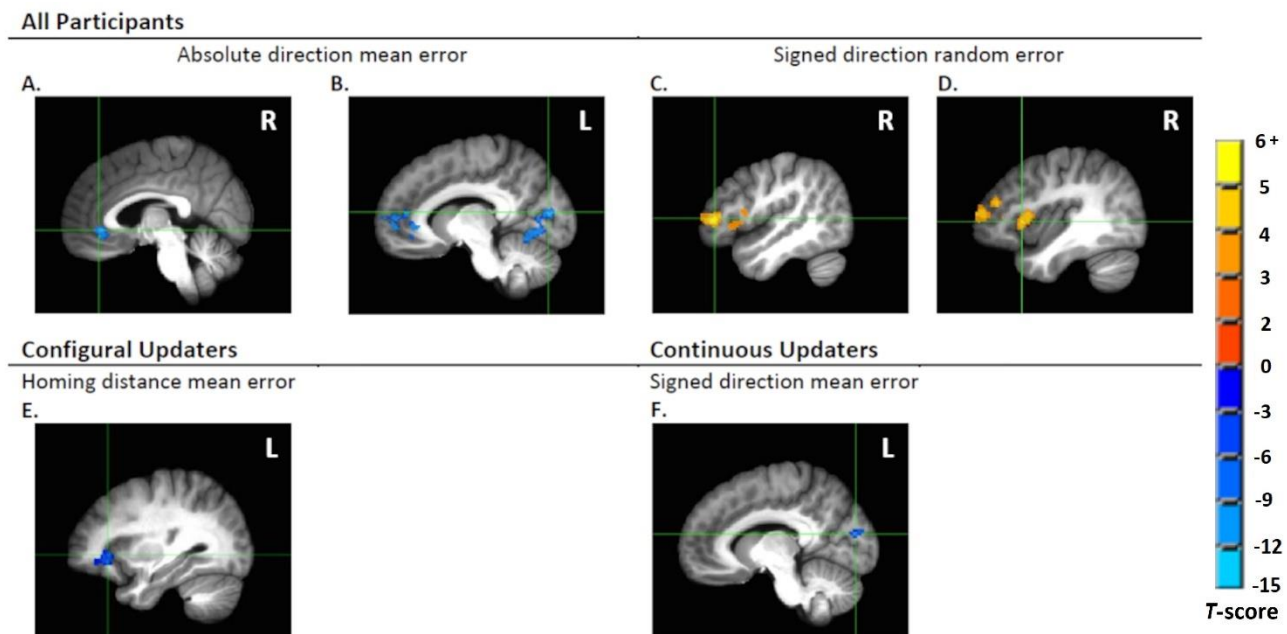


Fig. 18. Significant correlations between different types of navigational errors and the activation patterns from all participants, configural updaters, and continuous updaters during the complex homebound phase. In each of these three groups, activation images were superimposed on spatially normalized high-resolution T1-weighted images averaged across all group members. In all participants, absolute direction mean error correlated negatively with activations in the (A) anterior cingulate and (B) cuneus, while signed direction random error correlated positively with activations in the inferior frontal gyrus [(C) BA 46; (D) BA 45]. (E) In configural updaters, homing distance mean error correlated negatively with activation in the inferior frontal gyrus (BA 47). (G) In continuous updaters, signed direction mean error correlated negatively with activation in the cuneus (BA 18). Cross hairs were centered on the peak voxel of correlational strength in each specified region. L = left hemisphere; R = right hemisphere.

CHAPTER 7

EXPERIMENT 2

DISCUSSION

The current experiment investigated the extent to which the hippocampus and the entorhinal cortex were involved in the implementation of configural and continuous updating strategies, respectively, during visual path integration. Specifically, it was hypothesized that configural updating use would engage the hippocampus proper during the homebound phase while continuous updating use would engage the entorhinal cortex during the same phase. Based on within-trial analysis that examined brain activations in specific navigational phases relative to a functional baseline encompassing the entire time series, no significant activation (or deactivation) in either the hippocampus or the entorhinal cortex was found during the homebound phase, as well as during the outbound phase, in either strategy group. There were also no significant correlations between the activity in either region and any type of navigational error committed during simple and homebound travels in the entire sample, as well as in each strategy group. Between-group comparisons of activation patterns (both contrast- and non-contrast-related) further showed that there were no overall differences in functional activity between the strategy groups. This supported the non-significant behavioral performance differences between them and suggested that neither strategy evoked more neural resources than the other.

Notwithstanding these non-significant findings, there was significant activation in the entorhinal cortex among continuous updaters based on a linear contrast of activation patterns from simple and complex paths [complex > simple] during the homebound

phase. The same contrast also yielded marginally significant hippocampal activations in both strategy groups. Notably, this pattern of hippocampal activation in continuous updaters partially supported the hypothesis of coincidental entorhinal and hippocampal involvement, which stipulated that hippocampal place cell activity might be modulated by efferent entorhinal signals entering through the perforant pathway (Moser et al., 2015; Savelli et al., 2008; Solstad et al., 2008). More importantly, the observed pattern of entorhinal activation in continuous updaters suggests that the entorhinal cortex was actively involved in making homing decisions or responses *after* detecting changes in outbound travel between simple and complex paths. This pattern of entorhinal activation could perhaps be best explained by underlying changes in the firing patterns of entorhinal grid cells in response to an alteration of homing responses between simple and complex paths. Specifically, different outbound trajectories of simple and complex paths might have induced a rescaling of the firing fields (or phases) of grid cells, a physiological change which manifested itself metabolically as different levels of entorhinal BOLD responses during the simple and complex homebound phases (cf. Barry, Hayman, Burgess, & Jeffery, 2007; Chen et al., 2015; Fiete, Burak, & Brookings, 2008). Critically, this upscaling of homebound-based entorhinal activity when switching from simple to complex paths might have also arose from specific attentional demands incurred by the instructions on continuous updating strategy use (see General Discussion, for more details).

With these findings in mind, it should be noted that the main differences in brain activation patterns between configural and continuous updaters were found *not* in the hippocampal formation but in extrahippocampal regions. When examining the phase-

specific, non-contrast-related brain activations and deactivations in each strategy group, they were found to encompass the medial prefrontal, lateral temporal, and parietal cortices. In particular, activations specific to the outbound phase were found in configural updaters only and were localized to the left TPJ for both simple and complex paths. It is critical to note that the TPJ is a key component of the frontoparietal control network that was posited to be centrally involved in the allocation of attentional resources (see, e.g., Corbetta & Shulman, 2002; Vincent, Kahn, Snyder, Raichle, & Buckner, 2008; Vossel, Geng, & Fink, 2014). This network has been shown to be activated during the navigational activities of path integration (Arnold et al., 2004; Izen, Chrastil, & Stern, 2018) and wayfinding (Spreng, Mar, & Kim, 2009), as well as during autobiographical and visuospatial planning (Spreng et al., 2009; Spreng, Stevens, Chamberlain, Gilmore, & Schacter, 2010). Most probably, TPJ activation in configural updaters during outbound travel represented focused attention to salient optic flow information (e.g., rapid changes in texture-density gradient of the mottled ground during self-motion) [cf. Cabeza, Ciaramelli, Olson, & Moscovitch, 2008; Ciaramelli, Grady, & Moscovitch, 2008] for the purpose of integrating such sensory information into a conceivable shape of the outbound path.

Further examination of other parietal regions revealed activations in the precuneus among configural updaters and in the inferior parietal lobule among continuous updaters during the simple homebound phase. These two parietal regions, like the TPJ, are part of the frontoparietal network, with the precuneus being part of a dorsal attention network and the inferior parietal lobule being part of a ventral attention network, which also comprises the TPJ (Cabeza et al., 2008; Corbetta & Shulman, 2002). Critically, there are

functional differences between these two attention networks in relation to the control and allocation of attention. Specifically, the dorsal network was proposed to be associated with top-down attention driven by self-preparatory goals whereas the ventral network was proposed to be associated with bottom-up attention guided by external sensory stimuli or retrieved memories of such stimuli/cues (Cabeza et al., 2008; Corbetta & Shulman, 2002; Vossel et al., 2014). In lieu of these proposed functions, it is possible that precuneus activation in configural updaters reflected some form of top-down attentional control concomitant with the central goal of configural strategy use – that is, to return to the start with referral to an internal allocentric image of the outbound path. By contrast, inferior parietal activation in continuous updaters suggests that they were involved in bottom-up attentional processing during the homebound phase – ostensibly guided by egocentric perceptual representations of external stimuli observed during outbound travel. Conceptually, this interpretation aligns well with the notion of continuous strategy use as a dynamic navigational process that requires *constant* monitoring of ego-motion information (Wiener et al., 2011; He & McNamara, 2018).

Moreover, at the perceptual level, it is worth considering that precuneus activation in configural updaters during simple homebound travel might have also represented: (i) increased egocentric reference frame use (Chiu et al., 2012; Gramann et al., 2006; Lin et al., 2015; Plank et al., 2010; Wolbers, Hegarty, & Loomis, 2008) – putatively directed toward encoding multiple egocentric viewpoints or scenes relevant for approximating the starting position – or (ii) increased attempts at converting ego-motion information experienced during homebound travel into an allocentric format for long-term storage and retrieval (Lin et al., 2015; Gramann et al., 2010). Furthermore, with respect to brain-

behavior correlations, the relevance of the precuneus for making homing decisions and responses in continuous updaters could not be eschewed as precuneus activation in continuous updaters was found to be negatively associated with individual differences in signed distance random error during the simple homebound phase. This negative relationship shows that higher precuneus engagement among continuous updaters facilitated their consistency of homebound travel over simple paths. Interestingly, it suggests that top-performing continuous updaters directed top-down attention toward maintaining the consistency of their translational virtual movements when navigating simple homebound paths.

These different group- and individual-based observations of parietal activations in the simple homebound phase were accompanied by common patterns of deactivations in the medial prefrontal cortex (mPFC) and the lateral temporal lobe in both groups. These regions, together with the hippocampus, TPJ / angular gyrus, and the precuneus / posterior parietal cortex, constitute key components of the default mode network (DMN), which is a set of interconnected brain regions that are *suppressed* in activity during tasks that demand bottom-up attention (see, e.g., Buckner, Andrews-Hanna, & Schacter, 2008; Laird et al., 2009; Raichle et al., 2001; Shulman et al., 1997). Deactivations in the mPFC and lateral temporal lobe have been previously documented to occur when activation patterns elicited by active (i.e., attention-demanding) tasks were compared against those elicited by passive control tasks (e.g., viewing a stimulus array without any response) [see Shulman et al., 1997]. As the current within-trial analysis presented the activation pattern of each navigational phase against the backdrop of a common functional baseline that applied to all phases, deactivations in the mPFC and lateral temporal lobe might have

occurred as a consequence of (i) attention-demanding processes that were *commonly* engaged by both strategy groups during the simple homebound phase (e.g., attention to the magnitudes of turns for estimating the shortest path back to the start), and/or (ii) a suspension or attenuation of activity devoted to the processing of redundant visual information (e.g., immobile stars in the night sky) during the simple homebound phase (cf. Raichle et al., 2001; Shulman et al., 1997; see also, Raichle & Snyder, 2007, for similar views). Notably, these two possibilities hint at the potential involvement of strategy-invariant processes that could be engaged to similar degrees regardless of the strategy-at-hand.

Thus far, there were no other findings on brain deactivations that paralleled the existing findings, and thus it could not be determined as to which of the two possibilities was more plausible. Crucially, given the absence of corresponding findings, any valid explanation(s) of functional activity changes derived from linear contrasts involving these deactivations – which in this experiment, occurred in the form of mPFC activation in configural updaters – should also be forestalled. To fully address the implications of these patterns of deactivations currently observed, more work on clarifying the relationships between deactivations in DMN regions and goal-oriented attention and behavior during path integration is definitely needed (see General Discussion, for more details).

Further examination of the prefrontal activity showed that regions constituting the inferior / ventrolateral prefrontal cortex (vIPFC) correlated both positively and negatively with navigational errors committed during homebound travel over complex paths. Specifically, higher activation in the left vIPFC (BA 47) was associated with improved homing performance among configural updaters (i.e., closer proximity to the start) but

higher activation in the right vIPFC was associated with poorer homing performance in all participants (i.e., greater inconsistency in turning). Previous studies which investigated the hemispheric lateralization of vIPFC proposed that the left vIPFC was involved in the controlled access to memory and retrieval of contextual details from past events (see Badre & Wagner, 2007; Levy & Wagner, 2011, for reviews; see also Cona & Scarpezza, 2019, for a meta-analysis) and that the right vIPFC was engaged during (i) motor inhibition (Aron, Robbins, & Poldrack, 2004), (ii) reflexive reorienting of attention (Corbetta & Shulman, 2002; Corbetta, Patel, & Shulman 2008), and (iii) presence of response uncertainty (Levy & Wagner, 2011). With reference to these extant views, increased left vIPFC activation in configural updaters most probably reflected certain intentional efforts at homing vector computation, ostensibly after access to mental images that captured the contextual elements (i.e., segments and turns) of complex outbound paths (cf. Badre & Wagner, 2007). Increased right vIPFC activation in all participants, on the other hand, most probably reflected heightened response uncertainty (Levy & Wagner, 2011) in the form of inconsistent homebound heading responses that persisted across complex paths – even after repeated exposures to the same paths. Moreover, this response uncertainty might have applied only to the complex homebound phase due to the perceived difficulty of complex homebound travel.

In addition, it is worth noting that activations in the anterior cingulate cortex (ACC) and cuneus in all participants decreased with increased commission of absolute direction mean errors over complex homebound paths. Activations in these two regions have been shown to be largely present during attention-demanding path integration events involving turning movements (Chiu et al., 2012; Gramann et al., 2006, 2010; Lin

et al., 2015; Plank et al., 2010). In view of these previous observations, the current findings of increased activation in the ACC and cuneus might have reflected an increased expenditure of attentional and working memory resources in a controlled processing of rotational optic flow signals (Gramann et al., 2010; Plank et al., 2010), such that all rotations made did not deviate drastically from the homebound orientation of an estimated homing vector. Lastly, it is important to note that increased cuneus activation may not always facilitate homing performance, since it co-occurred with increased commission of homing distance mean errors (denoting decreased proximity to the start) over simple homebound paths. In the simplest sense, elevated cuneus activation during simple homebound travel could represent increased bottom-up attention to optic flow information with further displacement from the start. Alternatively, the same increases in cuneus activation could be influenced by simultaneous activity changes in other regions that were involved in the computation of homebound distances (e.g., left vIPFC and right precuneus, as currently observed). To clarify these possibilities, future path integration studies can consider investigating the functional connectivity of the cuneus with other neocortical regions that have been shown to be associated with distance-related responses.

CHAPTER 8

SUMMARY OF MAJOR FINDINGS

The current study acknowledged previous neuroimaging and neuropsychological findings showing the inconsistent involvement of the hippocampal formation in visual path integration and was conducted with the central aim of clarifying hippocampal involvement in visual path integration based on continuous and configural updating strategy use. The findings from in-lab testing (Experiment 1) did not support previous studies that showed configural updaters to exhibit more accurate path integration (Wiener et al., 2011) and target-pointing (He & McNamara, 2018) performance than continuous updaters. What Experiment 1 did demonstrate, however, was that the sex of the participant moderated strategy use after controlling for all relevant covariate effects. This led to two sets of major findings: (i) configural updating led to males outperforming females with regard to almost all error types (signed direction mean errors and absolute direction random errors excluded), and (ii) continuous updating, *not* configural updating, led to more accurate performance among females. These findings were discussed with respect to challenges faced by female configural updaters in abstracting out the shape of outbound from access to optical flow alone and potentially better encoding, on the part of female continuous updaters, of the starting location and homebound translational movements from an egocentric perspective.

Experiment 2 involved the fMRI scanning of a subsample of the participants who completed Experiment 1. Its main aim was to compare the activation patterns between the two strategy groups in both hippocampal and extrahippocampal regions. To that end, both

whole-brain and ROI (centering on the hippocampus and entorhinal cortex) analyses were conducted. An examination of activation patterns unique to the outbound and homebound phases of both simple and complex paths revealed three sets of major findings: (i) entorhinal activation in continuous updaters based on a contrast of activations from the simple and complex homebound phases [complex > simple], (ii) relatively distinct non-contrast-related activations in the left parietal cortex in each group during outbound and simple homebound travel, and (iii) non-contrast-related deactivations in the mPFC and lateral temporal lobe, common to both groups, during the simple homebound phase.

In sequence, these fMRI findings were suggested to reflect: (i) altered grid cell firing patterns corresponding with different homing responses associated with simple and complex homebound travel (ii) differential allocation of attention through top-down and bottom-up mechanisms; (iii) an expenditure of a common pool of attentional resources or a temporary suspension of general information processing. Supplementary findings from brain-behavior correlations did not show any significant relationships between navigational errors (all types) and functional activity changes in the hippocampus or entorhinal cortex. Instead, they showed that increased activity in regions involved in attending to rotational visual signals (ACC, cuneus) and egocentric spatial processing (precuneus) were associated with lower magnitudes of absolute direction mean errors in all participants. A hemispheric lateralization of functions in the vIPFC was also suggested to explain the varying patterns of path integration accuracy observed between all participants and configural updaters.

CHAPTER 9

GENERAL DISCUSSION

In conjunction, the two experiments in the current study were novel for exhibiting findings that contradicted expectations. This final chapter shall focus on addressing the broader impact of these findings, limitations of the current methodology, and ideas for further investigations.

In both experiments, despite differences in sex ratio, outbound path configuration, and time-limit for homebound travel, female configural updaters were found to be less consistent in path integration performance than male configural updaters and that the self-report measure of total strategy effectiveness covaried significantly with direction errors (absolute and signed random errors in Experiment 1; absolute mean errors in Experiment 2). The former findings reinforced the argument that females were less proficient at implementing configural updating than males while the latter findings suggest that there is a metacognitive component in path integration. In particular, the significant covariate effects posed by total strategy effectiveness show that self-perceived strategy effectiveness can mediate the effects of learned strategies on direction- or orientation-related performance during path integration, regardless of the shapes of outbound paths. Critically, these findings support the notion that personal beliefs about cognitive performance contribute to strategy implementation (Hertzog & Dunlosky, 2004), as well as supplemented recent findings showing positive association between confidence of

one's spatial memory and a preference for allocentric navigation strategy (Ariel & Moffat, 2018).¹³ Due to the absence of additional cognitive or metacognitive assessments, it is currently unknown as to the exact mechanisms/processes that mediate the associations between self-perceived strategy effectiveness and path integration directional/orientation performance, and further investigations – involving both quantitative/psychometric and qualitative (e.g., interview-based) components – can be performed.

In addition, it is worth noting that the comparisons of the behavioral findings from both experiments showed inconsistent patterns of within-subjects effects posed by outbound path category. There was a commission of larger distance (both homing and signed) and absolute direction mean errors over complex paths than over simple paths in Experiment 2 but not in Experiment 1. These differences in behavioral performance between the two experiments must be considered in the context of stimuli changes in Experiment 2 related to (i) fixing the length of the first path segment, (ii) altering the turning angles of the outbound paths, and (iii) truncating the maximum duration for response-making from 20 seconds to 10 seconds. Most probably, variations in these spatiotemporal factors affected path integration over paths of varying complexity. For example, halving the period for response-making might have compelled participants to respond faster than usual due to time pressure (Edland & Svenson, 1993), which in turn

¹³ Note that the assessment of strategy effectiveness measured in this study should *not* be seen as equivalent to an assessment of *confidence of strategy use*, owing to the subjective/inferential nature of the strategy effectiveness survey.

reduced their capacity for efficient attentional control and spatial information processing over complex paths (cf. Brunyé, Wood, Houck, & Taylor, 2017).

Turning to the activation profiles of each strategy groups, the current findings showed both similar and different patterns of activations in each group. Particularly interesting were the findings on parietal activations during both outbound (in configural updaters) and homebound (in both groups) travel, which implicated the dual involvement of top-down and bottom-up attention mechanisms in the implementation of each strategy. More importantly, these findings suggest that it might have been the specific demands evoked by each set of strategy instructions that induced differential attentional processing in each strategy group (cf. Berger & Bühlhoff, 2009). Based on this notion, it is possible that significant activation in the entorhinal cortex [complex > simple] during the homebound phase also reflected different levels of attentional processing or control, ostensibly with more attentional resources allocated to virtual movements over complex homebound paths than over simple homebound paths. At the cellular level, it is unknown, however, as to whether these proposed changes in attentional control during continuous updating relate to entorhinal grid cell activities coding for real-time changes in position and orientation (Barry et al., 2007; Hafting et al., 2005; Gil et al., 2018; Jacobs et al., 2013; Jacob et al., 2017; Stangl et al., 2018). Thus, further investigations aiming at clarifying the nature of such psychophysiological relationships are required.

Given this potential close coupling of attention and strategy use, it seems reasonable to argue that strategy use in the current path integration task largely engaged attentional or perceptual processes without an explicit need for hippocampus-dependent processes. This interpretation supports similar views endorsed by previous researchers

who did not regard hippocampal involvement as necessary for successful path integration (Arnold et al., 2014; Kim et al., 2013; Shrager et al., 2008). However, a simplistic notion of the hippocampus as being *totally* irrelevant for path integration must be caveated in view of the currently observed hippocampal activations [complex > simple] that approximated significance in both strategy groups during the homebound phase. Even though these findings were not significant, they showed that hippocampal involvement was not confined to the implementation of one spatial updating strategy only. Critically, they suggest that the hippocampus has the *potential* of being involved in an online planning or detection of variations in homing responses between simple and complex paths. This interpretation supports accumulating evidence proposing that the hippocampus was highly involved in the prospective thinking or simulation of goal-directed behaviors during spatial navigation (see, e.g., Brown, Hasselmo, & Stern, 2014; Brown et al., 2016; Spiers, Olafsdottir, & Lever, 2018). Consequently, future studies aiming to clarify the connection between the hippocampus and path complexity should consider assessing the extent to which hippocampal activity can be parametrically modulated by paths of increasing complexity. To ensure a detailed inspection of such functional changes, more outbound paths that vary systematically (i.e., on a continuous scale) with regard to path segments, lengths, and turn values, would need to be designed.

Taken together, the fMRI findings from this study suggest that extrahippocampal processes related to attention and perception overshadowed hippocampus-dependent processes in yielding successful visual path integration performance. Significant patterns of activations and deactivations in the association cortex were largely found during the simple homebound phase and proposed to represent the attentional and perceptual

processes directed to the implementation of each strategy. As these regions constituted key components of the default mode and frontoparietal networks, the interaction of the functional or neural dynamics between these two networks can be investigated further. This recommendation is made with reference to posterior regions constituting both networks that are commonly activated during spatial navigation (e.g., precuneus, TPJ, as currently observed) [see Spreng et al., 2009]. Alternatively, interconnections between the hippocampus and the default mode and frontoparietal networks can also be investigated, given recent findings showing that hippocampal activity is modulated by variations in the functional activity of the default mode and frontoparietal networks during visual path integration (see Izen et al., 2018). For instance, functional connectivity between hippocampal and the neocortical regions of these two networks can be examined in the context of systematic variation in outbound path complexity, as mentioned above.

Overall, these recommendations are specified with the intention of rendering a better picture of how visual path integration operates, particularly when influenced by different strategies. An interactionist account is missing based on the current practice of examining brain activations localized to distinct regions, and thus, it is hoped that future path integration studies adopting a connectionist approach will be better positioned to uncover the intricacies of strategy-specific brain functions.

APPENDIX A

Computer Experience Questionnaire (Moffat, Hampson, & Hatzipantelis, 1998)

Online instructions:

The following statements concern your experience with using computers and virtual environments. For each statement, choose the best option that is specified by the header.

1	2	3	4	5	6	7
<i>I have never used a computer before</i>	<i>A few times in my life</i>	<i>A few times per year</i>	<i>Several times per year</i>	<i>A few times per month</i>	<i>A few times per week</i>	<i>Almost everyday</i>

1. Please rate the amount of experience you have with using a computer.
2. Please rate the amount of experience you have at playing computer or video games.
3. Please rate the amount of experience you have at playing computer or video games that specifically involve navigating through 3D mazes or other 3D environments (e.g., driving and flight simulators, Doom, Duke Nukem 3D, Quake, Unreal tournament, etc.)

APPENDIX B

Spatial Anxiety Scale [Lawton, 1994] {Source: Table 2, Lawton (1994)}.

Online instructions (Note: The scale for each item was represented by five stars):

This survey concerns the level of anxiety you feel when moving about in your everyday environment.

For each item:

A solitary star = not anxious;

Two stars = slightly anxious;

Three stars = moderately anxious;

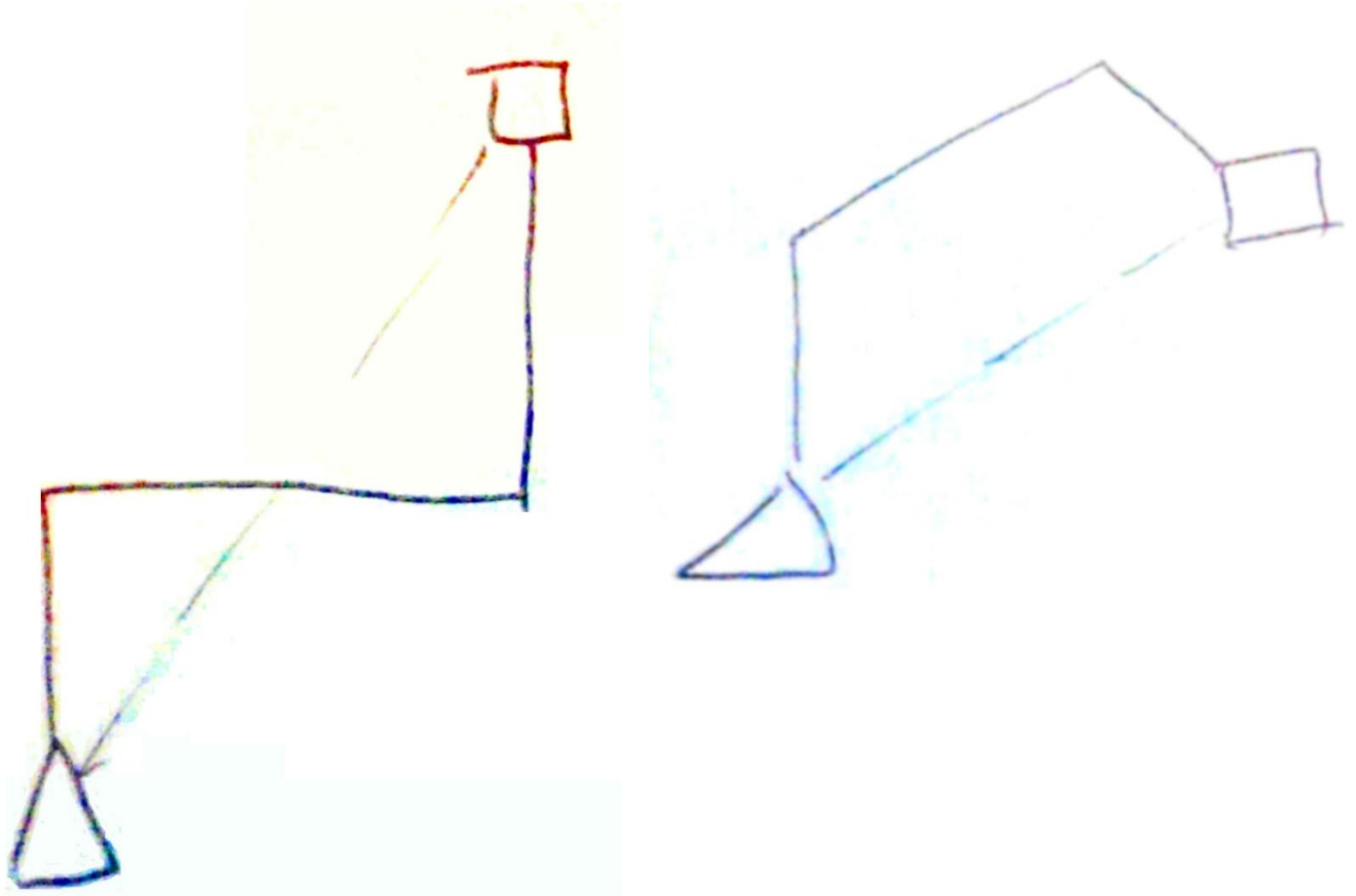
Four stars = anxious

Five stars = very anxious.

-
1. Leaving a store that you have been to for the first time and deciding which way to turn to get to a destination.
 2. Finding your way out of a complex arrangement of offices that you have visited for the first time.
 3. Pointing in the direction of a place outside that someone wants to get to and has asked you for directions, when you are in a windowless room.
 4. Locating your car in a very large parking lot or parking garage.
 5. Trying a new route that you think will be a shortcut without the benefit of a map.
 6. Finding your way back to a familiar area after realizing you have made a wrong turn and become lost while driving.
 7. Finding your way around in an unfamiliar mall.
 8. Finding your way to an appointment in an area of a city or town with which you are not familiar.
-

APPENDIX C

Exemplary sketches of two outbound paths walked out physically by a randomly selected participant during the practice session. The triangle marks the starting position. The square marks the ending position of the outbound journey. Intact lines represent the outbound path while dashed lines represent the homebound path.



APPENDIX D

Post-practice Survey on the Effectiveness of Strategy Use

Regardless of how accurately you got back to the start, please rate how effectively you applied the strategy-at-hand toward successful performance in the practice trials.

1	2	3	4	5	6	7	8	9	10
<i>Least effective</i>				<i>Moderately effective</i>				<i>Most effective</i>	

Post-test Survey on the Effectiveness of Strategy Use

Regardless of how accurately you got back to the start, please rate how effectively you applied the strategy-at-hand toward successful performance in the second set of test trials after the break.

1	2	3	4	5	6	7	8	9	10
<i>Least effective</i>				<i>Moderately effective</i>				<i>Most effective</i>	

REFERENCES

- Adamo, D. E., Briceño, E. M., Sindone, J. A., Alexander, N. B., & Moffat, S. D. (2012). Age differences in virtual environment and real world path integration. *Frontiers in Aging Neuroscience*, 4, 1-9. doi: 10.3389/fnagi.2012.00026
- Andersen, N. E., Dahmani, L., Konishi, K., & Bohbot, V. D. (2012). Eye tracking, strategies, and sex differences in virtual navigation. *Neurobiology of learning and memory*, 97(1), 81-89. doi: 10.1016/j.nlm.2011.09.007
- Andersson, J. L., Hutton, C., Ashburner, J., Turner, R., & Friston, K. (2001). Modeling geometric deformations in EPI time series. *NeuroImage*, 13, 903-919. doi: 10.1006/nimg.2001.0746
- Andersen, P., Morris, R., Amaral, D. Bliss, T., & O'Keefe, J. (Eds.). (2007). *The hippocampus book*. New York: Oxford University Press.
- Alyan, S., & McNaughton, B. L. (1999). Hippocampectomized rats are capable of homing by path integration. *Behavioral Neuroscience*, 113, 19-31. doi: 10.1037/0735-7044.113.1.19
- Ariel, R., & Moffat, S. D. (2018). Age-related similarities and differences in monitoring spatial cognition. *Aging, Neuropsychology, and Cognition*, 25, 351-377. doi: 10.1080/13825585.2017.1305086
- Ariel, R., Price, J., & Hertzog, C. (2015). Age-related associative memory deficits in value-based remembering: The contribution of agenda-based regulation and strategy use. *Psychology and aging*, 30, 795-808. doi: 10.1037/a0039818
- Arnold, A. E. G. F., Burles, F., Bray, S., Levy, R. M., & Iaria, G. (2014). Differential neural network configuration during human path integration. *Frontiers in Human Neuroscience*, 8, 1-12. doi: 10.3389/fnhum.2014.00263
- Aron, A. R., Robbins, T. W., & Poldrack, R. A. (2004). Inhibition and the right inferior frontal cortex. *Trends in Cognitive Sciences*, 8, 170-177. doi: 10.1016/j.tics.2004.02.010

- Badre, D., & Wagner, A. D. (2007). Left ventrolateral prefrontal cortex and the cognitive control of memory. *Neuropsychologia*, *45*, 2883-2901. doi: 10.1016/j.neuropsychologia.2007.06.015
- Barry, C., Hayman, R., Burgess, N., & Jeffery, K. J. (2007). Experience-dependent rescaling of entorhinal grids. *Nature Neuroscience*, *10*, 682-684. doi: 10.1038/nn1905
- Bassett, D. S., & Sporns, O. (2017). Network neuroscience. *Nature Neuroscience*, *20*, 353-364. doi: 10.1038/nn.4502
- Berger, D. R., & Bühlhoff, H. H. (2009). The role of attention on the integration of visual and inertial cues. *Experimental brain research*, *198*, 287-300. doi: 10.1007/s00221-009-1767-8
- Blajenkova, O., Motes, M. A., & Kozhevnikov, M. (2005). Individual differences in the representations of novel environments. *Journal of Environmental Psychology*, *25*, 97-109. doi: 10.1016/j.jenvp.2004.12.003
- Bohbot, V. D., Iaria, G., & Petrides, M. (2004). Hippocampal function and spatial memory: evidence from functional neuroimaging in healthy participants and performance of patients with medial temporal lobe resections. *Neuropsychology*, *18*, 418-425. doi: 10.1037/0894-4105.18.3.418
- Boone, A. P., Gong, X., & Hegarty, M. (2018). Sex differences in navigation strategy and efficiency. *Memory & Cognition*, 1-14. doi: 10.3758/s13421-018-0811-y
- Brown, T. I., Carr, V. A., LaRocque, K. F., Favila, S. E., Gordon, A. M., Bowles, B., ... & Wagner, A. D. (2016). Prospective representation of navigational goals in the human hippocampus. *Science*, *352*, 1323-1326. doi: 10.1126/science.aaf0784
- Brown, T. I., Hasselmo, M. E., & Stern, C. E. (2014). A high-resolution study of hippocampal and medial temporal lobe correlates of spatial context and prospective overlapping route memory. *Hippocampus*, *24*, 819-839. doi: 10.1002/hipo.22273
- Brown, T. I., Ross, R. S., Tobyne, S. M., & Stern, C. E. (2012). Cooperative interactions between hippocampal and striatal systems support flexible navigation. *NeuroImage*, *60*, 1316-1330. doi: 10.1016/j.neuroimage.2012.01.046

- Brunyé, T. T., Wood, M. D., Houck, L. A., & Taylor, H. A. (2017). The path more travelled: Time pressure increases reliance on familiar route-based strategies during navigation. *The Quarterly Journal of Experimental Psychology*, 70, 1439-1452. doi: 10.1080/17470218.2016.1187637
- Buckner, R. L., Andrews-Hanna, J. R., & Schacter, D. L. (2008). The brain's default network. *Annals of the New York Academy of Sciences*, 1124, 1-38. doi: 10.1196/annals.1440.011
- Burgess, N. (2014). The 2014 Nobel Prize in Physiology or Medicine: A spatial model for Cognitive Neuroscience. *Neuron*, 84, 1120-1125. doi: 10.1016/j.neuron.2014.12.009
- Cabeza, R., Ciaramelli, E., Olson, I. R., & Moscovitch, M. (2008). The parietal cortex and episodic memory: an attentional account. *Nature Reviews Neuroscience*, 9, 613-625. doi: 10.1038/nrn2459
- Canto, C. B., Wouterlood, F. G., & Witter, M. P. (2008). What does the anatomical organization of the entorhinal cortex tell us? *Neural Plasticity*, 2008, 1-18. <http://dx.doi.org/10.1155/2008/381243>
- Chadwick, M. J., Jolly, A. E., Amos, D. P., Hassabis, D., & Spiers, H. J. (2015). A goal direction signal in the human entorhinal/subicular region. *Current Biology*, 25, 87-92. doi: 10.1016/j.cub.2014.11.001
- Chance, S. S., Gaunet, F., Beall, A. C., & Loomis, J. M. (1998). Locomotion mode affects the updating of objects encountered during travel: The contribution of vestibular and proprioceptive inputs to path integration. *Presence*, 7, 168-178. doi: 10.1162/105474698565659
- Chen, X., He, Q., Kelly, J. W., Fiete, I. R., & McNamara, T. P. (2015). Bias in human path integration is predicted by properties of grid cells. *Current Biology*, 25, 1771-1776. doi: 10.1016/j.cub.2015.05.031
- Chiu, T. C., Gramann, K., Ko, L. W., Duann, J. R., Jung, T. P., & Lin, C. T. (2012). Alpha modulation in parietal and retrosplenial cortex correlates with navigation performance. *Psychophysiology*, 49, 43-55. doi: 10.1111/j.1469-8986.2011.01270.x

- Chrastil, E. R., Sherrill, K. R., Hasselmo, M. E., & Stern, C. E. (2016). Which way and how far? Tracking of translation and rotation information for human path integration. *Human Brain Mapping*, 37, 3636-3655. doi: 10.1002/hbm.23265
- Ciaramelli, E., Grady, C. L., & Moscovitch, M. (2008). Top-down and bottom-up attention to memory: a hypothesis (AtoM) on the role of the posterior parietal cortex in memory retrieval. *Neuropsychologia*, 46, 1828-1851. doi: 10.1016/j.neuropsychologia.2008.03.022
- Cona, G., & Scarpazza, C. (2019). Where is the “where” in the brain? A meta-analysis of neuroimaging studies on spatial cognition. *Human brain mapping*, 1-20. doi: 10.1002/hbm.24496
- Corbetta, M., & Shulman, G. L. (2002). Control of goal-directed and stimulus-driven attention in the brain. *Nature Reviews Neuroscience*, 3, 201-215. doi: 10.1038/nrn755
- Corbetta, M., Patel, G., & Shulman, G. L. (2008). The reorienting system of the human brain: from environment to theory of mind. *Neuron*, 58, 306-324. doi: 10.1016/j.neuron.2008.04.017
- Coutrot, A., Schmidt, S., Coutrot, L., Pittman, J., Hong, L., Wiener, J. M., ... & Spiers, H. J. (2019). Virtual navigation tested on a mobile app is predictive of real-world wayfinding navigation performance. *PloS ONE*, 14, e0213272. doi: 10.1371/journal.pone.0213272
- Cutmore, T. R., Hine, T. J., Maberly, K. J., Langford, N. M., & Hawgood, G. (2000). Cognitive and gender factors influencing navigation in a virtual environment. *International Journal of Human-Computer Studies*, 53, 223-249. doi: 10.1006/ijhc.2000.0389
- Dabbs Jr, J. M., Chang, E. L., Strong, R. A., & Milun, R. (1998). Spatial ability, navigation strategy, and geographic knowledge among men and women. *Evolution and Human Behavior*, 19, 89-98. doi: 10.1016/S1090-5138(97)00107-4
- Dale, A. M. (1999). Optimal experimental design for event-related fMRI. *Human Brain Mapping*, 8, 109-114. doi: 10.1002/(SICI)1097-0193(1999)8:2/3<109::AID-HBM7>3.0.CO;2-W

- Dale, A. M., & Buckner, R. L. (1997). Selective averaging of rapidly presented individual trials using fMRI. *Human Brain Mapping*, 5, 329-340. 10.1002/(SICI)1097-0193(1997)5:5<329::AID-HBM1>3.0
- Darwin, C. (1873). Origin of certain instincts. *Nature*, 7, 417-418.
- Doeller, C. F., Barry, C., & Burgess, N. (2010). Evidence for grid cells in a human memory network. *Nature*, 463, 657-661. doi: 10.1038/nature08704
- Edland, A., & Svenson, O. (1993). Judgment and decision making under time pressure Studies and findings. In O. Svenson & A. J. Maule (Eds.), *Time pressure and stress in human judgment and decision making* (pp. 27-40). New York: Springer.
- Eickhoff, S. B., Heim, S., Zilles, K., & Amunts, K. (2006). Testing anatomically specified hypotheses in functional imaging using cytoarchitectonic maps. *NeuroImage*, 32, 570-582. doi: 10.1016/j.neuroimage.2006.04.204
- Eickhoff, S. B., Stephan, K. E., Mohlberg, H., Grefkes, C., Fink, G. R., Amunts, K., & Zilles, K. (2005). A new SPM toolbox for combining probabilistic cytoarchitectonic maps and functional imaging data. *NeuroImage*, 25, 1325-1335. doi: 10.1016/j.neuroimage.2004.12.034
- Ellmore, T. M., & McNaughton, B. L. (2004). Human path integration by optic flow. *Spatial Cognition and Computation*, 4, 255-272. doi: 10.1207/s15427633scc0403_3
- Etienne, A. S., & Jeffery, K. J. (2004). Path integration in mammals. *Hippocampus*, 14, 180-192. doi: 10.1002/hipo.10173
- Fiete, I. R., Burak, Y., & Brookings, T. (2008). What grid cells convey about rat location. *Journal of Neuroscience*, 28, 6858-6871.
- Fujita, N., Klatzky, R. L., Loomis, J. M., & Golledge, R. G. (1993). The Encoding-Error Model of Pathway Completion without Vision. *Geographical Analysis*, 25, 295-314. doi: 10.1111/j.1538-4632.1993.tb00300.x
- Fukushima, S. S., Loomis, J. M., & Da Silva, J. A. (1997). Visual perception of egocentric distance as assessed by triangulation. *Journal of Experimental Psychology*:

Human Perception and Performance, 23, 86-100. doi: 10.1111/1467-8721.ep10772783

Fyhn, M., Molden, S., Witter, M. P., Moser, E. I., & Moser, M. B. (2004). Spatial representation in the entorhinal cortex. *Science*, 305, 1258–1264. doi: 10.1126/science.1099901

Gallistel, C. R. (1990). *The organization of learning*. Cambridge, MA: Bradford Books/MIT Press.

Golledge, R. G. (1999). *Wayfinding behavior: Cognitive mapping and other spatial processes*. Baltimore: Johns Hopkins University Press.

Gramann, K., Müller, H. J., Eick, E. M., & Schönebeck, B. (2005). Evidence of separable spatial representations in a virtual navigation task. *Journal of Experimental Psychology: Human Perception and Performance*, 31, 1199-1223. doi: 10.1037/0096-1523.31.6.1199

Gramann, K., Müller, H. J., Schönebeck, B., & Debus, G. (2006). The neural basis of ego-and allocentric reference frames in spatial navigation: Evidence from spatio-temporal coupled current density reconstruction. *Brain Research*, 1118, 116-129. doi: 10.1016/j.brainres.2006.08.005

Gramann, K., Onton, J., Riccobon, D., Mueller, H. J., Bardins, S., & Makeig, S. (2010). Human brain dynamics accompanying use of egocentric and allocentric reference frames during navigation. *Journal of Cognitive Neuroscience*, 22, 2836-2849. doi: 10.1162/jocn.2009.21369

Grieves, R. M., & Jeffery, K. J. (2017). The representation of space in the brain. *Behavioural Processes*, 135, 113-131. doi: 10.1016/j.beproc.2016.12.012.

Gil, M., Ancau, M., Schlesiger, M. I., Neitz, A., Allen, K., De Marco, R. J., and Monyer, H. (2018). Impaired path integration in mice with disrupted grid cell firing. *Nature Neuroscience*, 21, 81-91. doi:10.1038/s41593-017-0039-3

Harris, M. A., & Wolbers T. (2012). Ageing effects on path integration and landmark navigation. *Hippocampus*, 22, 1770-1780. doi: 10.1002/hipo.22011

- Harris, M. A., & Wolbers, T. (2014). How age-related strategy switching deficits affect wayfinding in complex environments. *Neurobiology of Aging*, *35*, 1095-1102. doi: 10.1016/j.neurobiolaging.2013.10.086
- Harris, T., Scheuringer, A., & Pletzer, B. (2019). Perspective and strategy interactively modulate sex differences in a 3D navigation task. *Biology of Sex Differences*, *10*, 1-12. doi: 10.1186/s13293-019-0232-z
- Hafting, T., Fyhn, M., Molden, S., Moser, M. B., & Moser, E. I. (2005). Microstructure of a spatial map in the entorhinal cortex. *Nature*, *436*, 801-806. doi: 10.1038/nature03721
- Hertzog, C., & Dunlosky, J. (2004). Aging, metacognition, and cognitive control. In B. H. Ross (Ed.), *Psychology of learning and motivation*. San Diego, CA: Academic Press, 215-251.
- He, Q., & McNamara, T. P. (2018). Spatial updating strategy affects the reference frame in path integration. *Psychonomic Bulletin & Review*, *25*, 1073-1079.
- Howard, L. R., Javadi, A. H., Yu, Y., Mill, R. D., Morrison, L. C., Knight, R., ... & Spiers, H. J. (2014). The hippocampus and entorhinal cortex encode the path and Euclidean distances to goals during navigation. *Current Biology*, *24*, 1331-1340. doi: 10.1016/j.cub.2014.05.001
- Iaria, G., Chen, J. K., Guariglia, C., Ptito, A., & Petrides, M. (2007). Retrosplenial and hippocampal brain regions in human navigation: Complementary functional contributions to the formation and use of cognitive maps. *European Journal of Neuroscience*, *25*, 890-899. doi: 10.1111/j.1460-9568.2007.05371.x
- Izen, S., Chrastil, E. R., & Stern, C. E. (2018). Resting State Connectivity Between Medial Temporal Lobe Regions and Intrinsic Cortical Networks Predicts Performance in a Path Integration Task. *Frontiers in Human Neuroscience*, *12*, 1-12. doi:10.3389/fnhum.2018.00415
- Jacob, P. Y., Gordillo-Salas, M., Facchini, J., Poucet, B., Save, E., & Sargolini, F. (2017). Medial entorhinal cortex and medial septum contribute to self-motion-based linear distance estimation. *Brain Structure and Function*, 1-16. doi: 10.1007/s00429-017-1368-4

- Jacobs, J., Weidemann, C. T., Miller, J. F., Solway, A., Burke, J. F., Wei, X. X., ... & Kahana, M. J. (2013). Direct recordings of grid-like neuronal activity in human spatial navigation. *Nature Neuroscience*, *16*, 1188-1190. doi: 10.1038/nn.3466
- Kearns, M. J., Warren, W. H., Duchon, A. P., & Tarr, M. J. (2002). Path integration from optic flow and body senses in a homing task. *Perception*, *31*, 349-374. doi: 10.1068/p3311
- Kennedy, R. S., Lane, N. E., Berbaum, K. S., & Lilienthal, M. G. (1993). Simulator sickness questionnaire: An enhanced method for quantifying simulator sickness. *The International Journal of Aviation Psychology*, *3*, 203-220. doi: 10.1207/s15327108ijap0303_3
- Kim, S., Sapiurka, M., Clark, R. E., and Squire, L. R. (2013). Contrasting effects on path integration after hippocampal damage in humans and rats. *Proceedings of the National Academy of Sciences, USA*, *110*, 4732-4737. doi: 10.1073/pnas.1300869110
- Klatzky, R. L., Loomis, J. M., Beall, A. C., Chance, S. S., & Golledge, R. G. (1998). Spatial updating of self-position and orientation during real, imagined, and virtual locomotion. *Psychological Science*, *9*, 293-298. doi: 10.1111/1467-9280.00058
- Klatzky, R. L., Loomis, J. M., Golledge, R. G., Cicinelli, J. G., Doherty, S., & Pellegrino, J. W. (1990). Acquisition of route and survey knowledge in the absence of vision. *Journal of Motor Behavior*, *22*, 19-43. doi:10.1080/00222895.1990.10735500
- Laird, A. R., Eickhoff, S. B., Li, K., Robin, D. A., Glahn, D. C., & Fox, P. T. (2009). Investigating the functional heterogeneity of the default mode network using coordinate-based meta-analytic modeling. *Journal of Neuroscience*, *29*, 14496-14505. doi: 10.1523/JNEUROSCI.4004-09.2009
- Lappe, M., & Frenz, H. (2009). Visual estimation of travel distance during walking. *Experimental Brain Research*, *199*, 369-375. doi: 10.1007/s00221-009-1890-6
- Lappe, M., Jenkin, M., & Harris, L. R. (2007). Travel distance estimation from visual motion by leaky path integration. *Experimental Brain Research*, *180*, 35-48. doi: 10.1007/s00221-006-0835-6

- Lappe, M., Stiels, M., Frenz, H., & Loomis, J. M. (2011). Keeping track of the distance from home by leaky integration along veering paths. *Experimental Brain Research*, 212, 81-89. doi: 10.1007/s00221-011-2696-x
- Lawton, C. A. (1994). Gender differences in way-finding strategies: Relationship to spatial ability and spatial anxiety. *Sex Roles*, 30, 765-779. doi: 10.1023/A:1021668724970
- Lawton, C. A. (1996). Strategies for indoor wayfinding: the role of orientation. *Journal of Environmental Psychology*, 16, 137-145. doi: 10.1006/jevp.1996.0011
- Levy, B. J., & Wagner, A. D. (2011). Cognitive control and right ventrolateral prefrontal cortex: reflexive reorienting, motor inhibition, and action updating. *Annals of the New York Academy of Sciences*, 1224, 40-62. doi: 10.1111/j.1749-6632.2011.05958.x
- Lin, C. T., Chiu, T. C., & Gramann, K. (2015). EEG correlates of spatial orientation in the human retrosplenial complex. *NeuroImage*, 120, 123-132. doi: 0.1016/j.neuroimage.2015.07.009
- Loomis, J. M., Klatzky, R. L., & Golledge, R. G. (2001). Navigating without vision: Basic and applied research. *Optometry & Vision Science*, 78, 282-289. doi: 10.1097/00006324-200105000-00011
- Loomis, J. M., Klatzky, R. L., Golledge, R. G., Cicinelli, J. G., Pellegrino, J. W., & Fry, P. A. (1993). Nonvisual navigation by blind and sighted: assessment of path integration ability. *Journal of Experimental Psychology: General*, 122, 73-91. doi: 10.1037/0096-3445.122.1.73
- Loomis, J. M., Klatzky, R. L., Golledge, R. G., & Philbeck, J. W. (1999). Human navigation by path integration. In Golledge, R. G. (Ed.), *Wayfinding behavior: Cognitive mapping and other spatial processes* (pp. 125-151). Baltimore: Johns Hopkins University Press.
- Mahmood, O., Adamo, D., Briceno, E., & Moffat, S. D. (2009). Age differences in visual path integration. *Behavioural Brain Research*, 205, 88-95. doi: 10.1016/j.bbr.2009.08.001

- Makeig, S., Bell, A. J., Jung, T. P., & Sejnowski, T. J. (1996). Independent component analysis of electroencephalographic data. *Advances in Neural Information Processing Systems*, 8, 145-151.
- Malinowski, J. C., & Gillespie, W. T. (2001). Individual differences in performance on a large-scale, real-world wayfinding task. *Journal of Environmental Psychology*, 21, 73-82. doi: 10.1006/jevp.2000.0183
- McNaughton, B. L., Barnes, C. A., Gerrard, J. L., Gothard, K., Jung, M. W., Knierim, J. J., ... & Weaver, K. L. (1996). Deciphering the hippocampal polyglot: The hippocampus as a path integration system. *Journal of Experimental Biology*, 199, 173-185.
- McNaughton, B. L., Battaglia, F. P., Jensen, O., Moser, E. I., & Moser, M. B. (2006). Path integration and the neural basis of the 'cognitive map'. *Nature Reviews Neuroscience*, 7, 663–678. doi: 10.1038/nrn1932
- Mittelstaedt, M. L., & Mittelstaedt, H. (1980). Homing by path integration in a mammal. *Naturwissenschaften*, 67, 566-567. doi:10.1007/BF00450672
- Mittelstaedt, H., & Mittelstaedt, M. L. (1982). Homing by path integration. In F. Papi & H. G. Wallraff (Eds.), *Avian navigation* (pp. 290-297). Berlin Heidelberg: Springer-Verlag.
- Moffat, S. D., Hampson, E., & Hatzipantelis, M. (1998). Navigation in a “virtual” maze: Sex differences and correlation with psychometric measures of spatial ability in humans. *Evolution and Human Behavior*, 19, 73-87. doi: 10.1016/S1090-5138(97)00104-9
- Moffat, S. D., Zonderman, A. B., & Resnick, S. M. (2001). Age differences in spatial memory in a virtual environment navigation task. *Neurobiology of Aging*, 22, 787-796. doi: 10.1016/S0197-4580(01)00251-2
- Moser, E. I., Kropff, E., & Moser, M. B. (2008). Place cells, grid cells, and the brain's spatial representation system. *Annual Review of Neuroscience*, 31, 69-89. doi: 10.1146/annurev.neuro.31.061307.090723.
- Moser, M. B., Rowland, D. C., & Moser, E. I. (2015). Place cells, grid cells, and memory. *Cold Spring Harbor Perspectives in Biology*, 7, a021808. doi: 10.1101/cshperspect.a021808

- Müller, M., & Wehner, R. (1988). Path integration in desert ants, *Cataglyphis fortis*. *Proceedings of the National Academy of Sciences of the United States of America*, 85, 5287-5290. doi: 10.1098/rspb.2004.2749
- Murphy, K., Bodurka, J., & Bandettini, P. A. (2007). How long to scan? The relationship between fMRI temporal signal to noise ratio and necessary scan duration. *NeuroImage*, 34, 565-574.
- O'Keefe, J., & Nadel, L. (1978). *The Hippocampus as a Cognitive Map*. Vol. 3. Oxford: Clarendon Press.
- Oldfield, R. C. (1971). The assessment and analysis of handedness: The Edinburgh inventory. *Neuropsychologia*, 9, 97-113. doi: 10.1016/0028-3932(71)90067-4
- Ollinger, J. M., Shulman, G. L., & Corbetta, M. (2001a). Separating processes within a trial in event-related functional MRI: I. The method. *NeuroImage*, 13, 210-217. doi: 10.1006/nimg.2000.0710
- Ollinger, J. M., Corbetta, M., & Shulman, G. L. (2001b). Separating processes within a trial in event-related functional MRI: II. Analysis. *NeuroImage*, 13, 218-229. doi: 10.1006/nimg.2000.0711
- Onton, J., & Makeig, S. (2006). Information-based modeling of event-related brain dynamics. In C. Neuper, E. Klimesch (Eds.), *Progress in Brain Research*, Vol. 159, pp. 99-120. doi: 10.1016/S0079-6123(06)59007-7
- Onton, J., Westerfield, M., Townsend, J., & Makeig, S. (2006) Imaging human EEG dynamics using independent component analysis. *Neuroscience and Biobehavioral Reviews*, 30, 808-822. doi: 10.1016/j.neubiorev.2006.06.007
- Philbeck, J. W., Behrmann, M., Levy, L., Potolicchio, S. J., and Caputy, A. J. (2004). Path integration deficits during linear locomotion after human medial temporal lobectomy. *Journal of Cognitive Neuroscience*, 16, 510-520. doi: 10.1162/089892904323057254
- Philbeck, J. W., Klatzky, R. L., Behrmann, M., Loomis, J. M., & Goodridge, J. (2001). Active control of locomotion facilitates nonvisual navigation. *Journal of Experimental Psychology: Human Perception and Performance*, 27, 141-153. doi: 10.1037/0096-1523.27.1.141

- Plank, M., Müller, H. J., Onton, J., Makeig, S., & Gramann, K. (2010). Human EEG correlates of spatial navigation within egocentric and allocentric reference frames. In C. Hölscher, T. Shipley, M. O. Belardinelli, J. Bateman, & N. Newcombe (Eds.). *Spatial Cognition VII* (vol. 6222, pp. 191-206). Berlin Heidelberg: Springer.
- Rahman, Q., Sharp, J., McVeigh, M., & Ho, M. L. (2017). Sexual orientation-related differences in virtual spatial navigation and spatial search strategies. *Archives of Sexual Behavior*, 46, 1279-1294. doi: 10.1007/s10508-017-0986-5
- Raichle, M. E., MacLeod, A. M., Snyder, A. Z., Powers, W. J., Gusnard, D. A., & Shulman, G. L. (2001). A default mode of brain function. *Proceedings of the National Academy of Sciences*, 98, 676-682. doi: 10.1073/pnas.98.2.676
- Raichle, M. E., & Snyder, A. Z. (2007). A default mode of brain function: a brief history of an evolving idea. *NeuroImage*, 37, 1083-1090. doi: 10.1016/j.neuroimage.2007.02.041
- Riecke, B. (2012). Are left-right hemisphere errors in point-to-origin tasks in VR caused by failure to incorporate heading changes? In C. Stachniss, K. Schill, & D. Uttal (Eds.), *Spatial Cognition VIII: Proceedings of the international conference in spatial cognition, LNAI 7463* (pp. 143–162). Berlin Heidelberg: Springer-Verlag.
- Remondes, M., & Schuman, E. M. (2004). Role for a cortical input to hippocampal area CA1 in the consolidation of a long-term memory. *Nature*, 431, 699-703. doi: 10.1038/nature02965
- Sandstrom, N. J., Kaufman, J., & Huettel, S. A. (1998). Males and females use different distal cues in a virtual environment navigation task1. *Cognitive brain research*, 6, 351-360. doi: 10.1016/S0926-6410(98)00002-0
- Saucier, D. M., Green, S. M., Leason, J., MacFadden, A., Bell, S., & Elias, L. J. (2002). Are sex differences in navigation caused by sexually dimorphic strategies or by differences in the ability to use the strategies?. *Behavioral neuroscience*, 116, 403-410. doi: 10.1037/0735-7044.116.3.403
- Savelli, F., Yoganarasimha, D., & Knierim, J. J. (2008). Influence of boundary removal on the spatial representations of the medial entorhinal cortex. *Hippocampus*, 18, 1270-1282. doi: 10.1002/hipo.20511

- Schinazi, V. R., Nardi, D., Newcombe, N. S., Shipley, T. F., & Epstein, R. A. (2013). Hippocampal size predicts rapid learning of a cognitive map in humans. *Hippocampus*, 23, 515-528. doi: 10.1002/hipo.22111
- Schmitz, S. (1999). Gender differences in acquisition of environmental knowledge related to wayfinding behavior, spatial anxiety and self-estimated environmental competencies. *Sex Roles*, 41, 71-93. doi: 10.1023/A:1018837808724
- Sherrill, K. R., Chrastil, E. R., Ross, R. S., Erdem, U. M., Hasselmo, M. E., & Stern, C. E. (2015). Functional connections between optic flow areas and navigationally responsive brain regions during goal-directed navigation. *NeuroImage*, 118, 386-396. doi: 10.1016/j.neuroimage.2015.06.009
- Sherrill, K. R., Erdem, U. M., Ross, R. S., Brown, T. I., Hasselmo, M. E., & Stern, C. E. (2013). Hippocampus and retrosplenial cortex combine path integration signals for successful navigation. *The Journal of Neuroscience*, 33, 19304-19313. doi: 10.1523/JNEUROSCI.1825-13.2013
- Sholl, M. J. (1989). The relation between horizontality and rod-and-frame and vestibular navigational performance. *Journal of Experimental Psychology: Learning, Memory, and Cognition*, 15, 110-125. doi: 10.1037/0278-7393.15.1.110
- Shrager, Y., Kirwan, C. B., & Squire, L. R. (2008). Neural basis of the cognitive map: Path integration does not require hippocampus or entorhinal cortex. *Proceedings of the National Academy of Sciences, USA*, 105, 12034-12038. doi: 10.1073/pnas.0805414105
- Shulman, G. L., Fiez, J. A., Corbetta, M., Buckner, R. L., Miezin, F. M., Raichle, M. E., & Petersen, S. E. (1997). Common blood flow changes across visual tasks: II. Decreases in cerebral cortex. *Journal of Cognitive Neuroscience*, 9, 648-663. doi: 10.1162/jocn.1997.9.5.648
- Shulman, G. L., Ollinger, J. M., Akbudak, E., Conturo, T. E., Snyder, A. Z., Petersen, S. E., & Corbetta, M. (1999). Areas involved in encoding and applying directional expectations to moving objects. *The Journal of Neuroscience*, 19, 9480-9496. doi: 10.1162/jocn.1997.9.5.648
- Silverman, I., Choi, J., Mackewn, A., Fisher, M., Moro, J., & Olshansky, E. (2000). Evolved mechanisms underlying wayfinding: Further studies on the hunter-gatherer theory of spatial sex differences. *Evolution and Human Behavior*, 21, 201-213. doi: 10.1016/S1090-5138(00)00036-2

- Solstad, T., Boccara, C. N., Kropff, E., Moser, M. B., & Moser, E. I. (2008). Representation of geometric borders in the entorhinal cortex. *Science*, 322, 1865-1868. doi: 0.1126/science.1166466
- Spiers, H. J., & Maguire, E. A. (2006). Thoughts, behaviour, and brain dynamics during navigation in the real world. *NeuroImage*, 31, 1826-1840. doi: 10.1016/j.neuroimage.2006.01.037
- Spiers, H. J., & Maguire, E. A. (2007). A navigational guidance system in the human brain. *Hippocampus*, 17, 618-626. doi: 10.1002/hipo.20298
- Spiers, H. J., Olafsdottir, H. F., & Lever, C. (2018). Hippocampal CA1 activity correlated with the distance to the goal and navigation performance. *Hippocampus*, 28, 644-658. doi: 10.1002/hipo.22813
- Spreng, R. N., Mar, R. A., & Kim, A. S. (2009). The common neural basis of autobiographical memory, prospection, navigation, theory of mind, and the default mode: a quantitative meta-analysis. *Journal of Cognitive Neuroscience*, 21, 489-510. doi: 10.1162/jocn.2008.21029
- Spreng, R. N., Stevens, W. D., Chamberlain, J. P., Gilmore, A. W., & Schacter, D. L. (2010). Default network activity, coupled with the frontoparietal control network, supports goal-directed cognition. *NeuroImage*, 53, 303-317. doi: 10.1016/j.neuroimage.2010.06.016
- Srinivasan, M. V. (2015). Where paths meet and cross: Navigation by path integration in the desert ant and the honeybee. *Journal of Comparative Physiology A*, 201, 533-546. doi: 10.1007/s00359-015-1000-0
- Stangl, M., Achtzehn, J., Huber, K., Dietrich, C., Tempelmann, C., & Wolbers, T. (2018). Compromised Grid-Cell-like Representations in Old Age as a Key Mechanism to Explain Age-Related Navigational Deficits. *Current Biology*, 28, 1108-1115. doi:10.1016/j.cub.2018.02.038
- Steffenach, H. A., Witter, M., Moser, M. B., & Moser, E. I. (2005). Spatial memory in the rat requires the dorsolateral band of the entorhinal cortex. *Neuron*, 45, 301-313. doi: 10.1016/j.neuron.2004.12.044
- Taylor, H. A., & Tversky, B. (1996). Perspective in spatial descriptions. *Journal of Memory and Language*, 35, 371-391. doi: 10.1006/jmla.1996.0021

- Vago, D. R., & Kesner, R. P. (2008). Disruption of the direct perforant path input to the CA1 subregion of the dorsal hippocampus interferes with spatial working memory and novelty detection. *Behavioural Brain Research*, 189, 273-283. doi: 10.1016/j.bbr.2008.01.002
- Vincent, J. L., Kahn, I., Snyder, A. Z., Raichle, M. E., & Buckner, R. L. (2008). Evidence for a frontoparietal control system revealed by intrinsic functional connectivity. *Journal of Neurophysiology*, 100, 3328-3342. doi: 10.1152/jn.90355.2008
- Vossel, S., Geng, J. J., & Fink, G. R. (2014). Dorsal and ventral attention systems: distinct neural circuits but collaborative roles. *The Neuroscientist*, 20, 150-159. doi: 10.1177/1073858413494269
- Ward, S. L., Newcombe, N., & Overton, W. F. (1986). Turn left at the church, or three miles north: A study of direction giving and sex differences. *Environment and Behavior*, 18, 192-213. doi: 10.1177/0013916586182003
- Wheeler, M. E., Shulman, G. L., Buckner, R. L., Miezin, F. M., Velanova, K., & Petersen, S. E. (2006). Evidence for separate perceptual reactivation and search processes during remembering. *Cerebral Cortex*, 16, 949-959. doi: 10.1093/cercor/bhj037
- Whishaw, I. Q., & Gorny, B. (1999). Path integration absent in scent-tracking fimbria-fornix rats: Evidence for hippocampal involvement in “sense of direction” and “sense of distance” using self-movement cues. *The Journal of Neuroscience*, 19, 4662-4673.
- Whishaw, I. Q., Hines, D. J., & Wallace, D. G. (2001). Dead reckoning (path integration) requires the hippocampal formation: Evidence from spontaneous exploration and spatial learning tasks in light (allothetic) and dark (idiothetic) tests. *Behavioural Brain Research*, 127, 49-69. doi: 10.1016/S0166-4328(01)00359-X
- Whishaw, I. Q., & Maaswinkel, H. (1998). Rats with fimbria-fornix lesions are impaired in path integration: A role for the hippocampus in “sense of direction”. *The Journal of Neuroscience*, 18, 3050-3058.
- Whishaw, I. Q., McKenna, J. E., & Maaswinkel, H. (1997). Hippocampal lesions and path integration. *Current Opinion in Neurobiology*, 7, 228-234. 10.1016/S0959-4388(97)80011-6

- Whishaw, I. Q., & Tomie, J. A. (1996). Of mice and mazes: Similarities between mice and rats on dry land but not water mazes. *Physiology & Behavior*, 60, 1191-1197. doi: 10.1016/S0031-9384(96)00176-X
- Wiener, J. M., Berthoz, A., & Wolbers, T. (2011). Dissociable cognitive mechanisms underlying human path integration. *Experimental Brain Research*, 208, 61-71. doi: 10.1007/s00221-010-2460-7
- Wiener, S. I., Korshunov, V. A., Garcia, R., & Berthoz, A. (1995). Inertial, substratal and landmark cue control of hippocampal CA1 place cell activity. *European Journal of Neuroscience*, 7, 2206-2219. 10.1016/S0031-9384(96)00176-X
- Witter, M. P., Naber, P. A., van Haeften, T., Machielsen, W. C., Rombouts, S. A., Barkhof, F., ... & Lopes da Silva, F. H. (2000). Cortico-hippocampal communication by way of parallel parahippocampal-subicular pathways. *Hippocampus*, 10, 398-410. 10.1002/1098-1063(2000)10:4<398::AID-HIPO6>3.0.CO;2-K
- Wolbers, T., Hegarty, M., Büchel, C., & Loomis, J. M. (2008). Spatial updating: how the brain keeps track of changing object locations during observer motion. *Nature Neuroscience*, 11, 1223-1230. doi: 10.1038/nn.2189
- Wolbers, T., & Wiener, J. M. (2014). Challenges for identifying the neural mechanisms that support spatial navigation: The impact of spatial scale. *Frontiers in Human Neuroscience*, 8, 1-12. doi: 10.3389/fnhum.2014.00571
- Wolbers, T., Wiener, J. M., Mallot, H. A., & Büchel, C. (2007). Differential recruitment of the hippocampus, medial prefrontal cortex, and the human motion complex during path integration in humans. *The Journal of Neuroscience*, 27, 9408-9416. doi: 10.1523/JNEUROSCI.2146-07.2007
- Worsley, C. L., Recce, M., Spiers, H. J., Marley, J., Polkey, C. E., & Morris, R. G. (2001). Path integration following temporal lobectomy in humans. *Neuropsychologia*, 39, 452-464. doi: 10.1016/S0028-3932(00)00140-8
- Zhong, J. Y. (2011). *Individual differences in navigational strategies and mental representations of large scale environments*. Unpublished Honors Thesis. National University of Singapore, Singapore. Retrieved from <http://dx.doi.org/10.13140/RG.2.1.3948.6322/3>

- Zhong, J. Y. (2013). *Three types of environmental representations and individual differences in spatial navigation*. Unpublished Master's Thesis, National University of Singapore, Singapore. Retrieved from <http://scholarbank.nus.edu.sg/handle/10635/47243>.
- Zhong, J. Y., & Kozhevnikov, M. (2016). Relating allocentric and egocentric survey-based representations to the self-reported use of a navigation strategy of egocentric spatial updating. *Journal of Environmental Psychology*, 46, 154-175. doi: 10.1016/j.jenvp.2016.04.007
- Zhong, J. Y., & Moffat, S. D. (2016). Age-related differences in associative learning of landmarks and heading directions in a virtual navigation task. *Frontiers in Aging Neuroscience*, 8, 1-11. doi: 10.3389/fnagi.2016.00122